This Dissertation Committee for Runhua Guo certifies that this is the approved version of the following dissertation:

PREDICTING IN-SERVICE FATIGUE LIFE OF FLEXIBLE PAVEMENTS BASED ON ACCELERATED PAVEMENT TESTING

Committee:

_____
Jorge A. Prozzi, Supervisor

_____
Randy B. Machemehl

_____
C. Michael Walton

_____
Kevin J. Folliard

_____
Harovel G. Wheat

PREDICTING IN-SERVICE FATIGUE LIFE OF FLEXIBLE PAVEMENTS BASED ON ACCELERATED PAVEMENT TESTING

by

Runhua Guo, B.S., M.S.

Dissertation

Presented to the Faculty of the Graduate School of

The University of Texas at Austin

in Partial Fulfillment

of the Requirements

for the Degree of

Doctor of Philosophy

The University of Texas at Austin

December 2007

To my family for their unconditional love and support,

To my Xiao-tu-di and Zao-zao

ACKNOWLEDGEMENTS

I wish to express my deepest appreciation to my dissertation supervisor, Dr. Jorge A. Prozzi and Ms. Jolanda Prozzi, for all of the support and mentorship that they have provided me during my time here at the University of Texas at Austin. It has been an honor, a pleasure, and a blessing to have the opportunity to work with them.

I would like to thank my committee member Randy B. Machemehl, Kevin J. Folliard, C. Michael Walton, and Harovel G. Wheat for their insights and valuable suggestions to this work. The author also is very grateful to Darhao Chen for his provision of data and other support. My special thanks go to Janet A Slack for all of the assistance she provided during these years.

The discussions with Feng Hong, Feng Wang, Zhong Wang, Bin Zhou, Jianming Ma, Zheng Li, Xiaokun Wang, Lu Gao, Hui Wu, Jessica Y. Guo, Isabel Victoria and Jose Pablo Aguiar-Moya are helpful and should be credited. My special thanks also go to Huimin Zhao and Yong Zhao for the precious friendship and for their sincere and generous support.

Last but not least, I am indebted to my wife Hangwen Liang, my parents Zhonghe Guo and Shifeng Yang, my parents-in-law Xueti Liang and Xiafang Yu, my brother Yaping Guo, my brother Yaqun Guo, my sister Yali Guo, my brother-in-law Tinghui Xu, my sister-in-law Xuemei Li, and my sister-in-law Chunxia Wang. Without their support and encouragement, I would never finish this work. I shall make it up to them during my lifetime.

PREDICTING IN-SERVICE FATIGUE LIFE OF FLEXIBLE PAVEMENTS BASED ON ACCELERATED PAVEMENT TESTING

Publication No._____

Runhua Guo, Ph.D.

The University of Texas at Austin, 2007

Supervisor: Jorge A. Prozzi

Pavement performance prediction in terms of fatigue cracking and surface rutting are essential for any mechanistically-based pavement design method. Traditionally, the estimation of the expected fatigue field performance has been based on the laboratory bending beam test. Full-scale Accelerated Pavement Testing (APT) is an alternative to laboratory testing leading to advances in practice and economic savings for the evaluation of new pavement configurations, stress level related factors, new materials and design improvements. This type of testing closely simulates field conditions; however, it does not capture actual performance because of the limited ability to address long-term phenomena. The same pavement structure may exhibit different response and performance under APT than when in-service. Actual field performance is better captured by experiments such as Federal Highway Administration's Long-Term Pavement

Performance (LTPP) studies. Therefore, to fully utilize the benefits of APT, there is a need for a methodology to predict the long-term performance of in-service pavement structures from the results of APT tests that will account for such differences. Three models are generally suggested to account for the difference: shift factors, statistical and mechanistic approaches.

A reliability based methodology for fatigue cracking prediction is proposed in this research, through which the three models suggested previously are combined into one general approach that builds on their individual strengths to overcome some of the shortcomings when the models are applied individually. The Bias Correction Factor (BCF) should account for all quantifiable differences between the fatigue life of the pavement site under APT and in-service conditions. In addition to the Bias Correction Factor, a marginal shift factor, M, should be included to account for the unquantifiable differences when predicting the in-service pavement fatigue life from APT.

The Bias Correction Factor represents an improvement of the currently used "shift factors" since they are more general and based on laboratory testing or computer simulation. By applying the proposed methodology, APT performance results from a structure similar to an in-service structure can be used to perform four-point bending beam tests and structural analysis to obtain an accurate estimate of the necessary Bias Correction Factor to estimate in-service performance.

Table of Contents

List of Figures

List of Tables

Chapter 1: Introduction

1.1 Background

Pavement performance prediction in terms of fatigue cracking and surface rutting is essential for any mechanistically-based pavement design method (NCHRP, 2006). The estimation of the expected fatigue performance of a flexible pavement in the field is based on the estimation of the maximum tensile strain at the bottom of the asphalt layers and its correlation to the performance of the same mix in the laboratory under bending beam test. This laboratory-based estimation is further calibrated to better predict actual field performance by means of shift factors (Al-Qadi and Nassar, 2003). But none of these shift factors have been comprehensive and often are limited to assessing the effect of one variable at a time.

Full-scale Accelerated Pavement Testing (APT) is a supplement to laboratory testing. It is defined as the controlled application of a prototype wheel loading, at or above loads representative of field traffic loads to a prototype or actual, layered, structural pavement system to determine pavement response and performance under a controlled, accelerated accumulation of damage in a compressed time period (Metcalf, 1996). There are a wide variety of APT programs in operation today. Metcalf indicated that 35 full scale APT facilities existed worldwide in 1996, of which 19 had active research programs. By 2004, 28 such programs were reported as being active, among which more than half are in the

United States (Hugo and Epps, 2004). Therefore, a globally scaled knowledge exists in the field of APT. As a facet of pavement engineering, APT generates knowledge over a wide spectrum and broad basis. Figure 1.1 locates the APT technology in context to computer simulation, engineering judgment, field testing, laboratory testing, test roads, and pavement performance studies. Both laboratory testing and APT are necessary to provide fast and accurate answers to engineering concerns, and the Long-Term Pavement Performance (LTPP) studies could be used to calibrate these two results. None of the methods could provide a complete solution individually, so the methods should all supplement each other (Hugo et al., 1991). Full-scale APT has become a powerful technique for collecting information for optimum pavement design to reduce life cycle costs and for assisting with understanding pavement deterioration under realistic conditions. It forms an essential bridge between laboratory testing and LTPP studies.

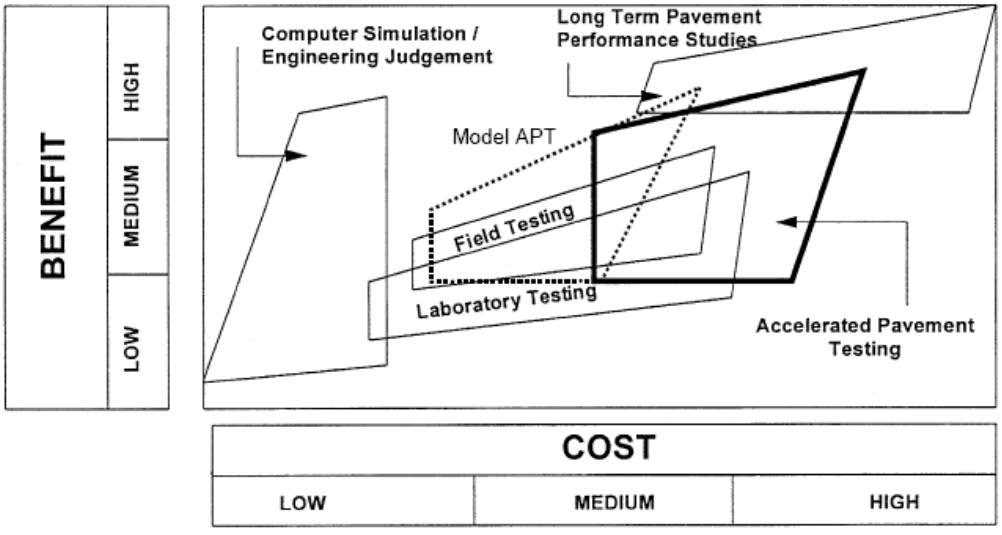

Figure 1.1 Interrelationship between pavement engineering facets (Hugo et al., 1991)

1.2 Problem Statement

To date, the main factors that differentiate APT and in-field pavement performance can be summarized as follows: (1) traffic: loading time (speed), loading ratio (rest periods over loading time), and traffic distribution (wandering), (2) environmental conditions: moisture, temperature , and (3) other long term effects such as climate and age hardening of asphalt.

Traffic loading

The effect of truck speed on the response of asphalt concrete (AC) pavements is significant. Increasing truck speed will greatly reduce the peak longitudinal strain while the effect on transverse strain is less pronounced (Chatti et al., 1996). The loading speed also greatly influences the behavior of viscoelastic and viscoelastoplastic materials, drainable materials, slow setting stabilized materials, and materials that age with time. The majority of APT facilities use loading speeds between 5 and 25 km/h, much lower than typical highway speeds (70 to 120 km/h).

Loading ratio (LR) is defined as the ratio of rest period over loading time. Loading ratios in APT experiments are much lower than those in actual highways, and result in shorter fatigue life. This can primarily be explained by the rate of healing. Although damage caused by repeated traffic loading accumulates in asphalt pavements, it heals during rest periods (time between traffic loadings), which enhances the fatigue life of the

pavement (Kim and Roque, 2006; Al-Balbissi and Little, 1990). The interval of APT loading cycles varies between 2 and 15 seconds. In an in-service pavement, the time spacing between the two heavy vehicles passing in the same location varies from 5 seconds to several hours.

Channelized instead of wandering lateral traffic distribution has been used for studies where the comparative performance of several materials or construction procedures is investigated. The most commonly used method is to reduce or eliminate the lateral wandering of the loading wheel. This will greatly accelerate the development of rutting and fatigue cracking in asphalt pavements, as well as rutting in granular pavements.

Environmental conditions

The moisture and temperature condition of APT and in-service pavement differs from each other significantly. APT always results in controlled, accelerated accumulation of damage in a compressed time period. From a fatigue perspective, the effect of differential moisture condition between APT and in-service pavements relates primarily to the loss of support of the asphalt concrete layer and the consequential increase in tensile strains for the same applied wheel loads. Pavement temperature contributes significantly to the difference in performance because of the temperature susceptibility of asphalt binder. Asphalt concrete with a softer binder has been proven to result in longer fatigue life; therefore, the temperature has a pronounced effect on the fatigue life of asphalt concrete mixtures.

Exclusion of long term effects (climate and age hardening of asphalt)

Since APT is carried out in a compressed time period, it does not capture actual performance because of the limited ability to address long-term phenomena. This is primarily because of material aging properties over a long time period. Asphalt materials harden with loss of volatile components, which is mainly due to volatilization during mix production and construction and oxidation in the field. Both factors result in an increase in viscosity of the asphalt, and consequently the asphalt mixture becomes hard and brittle and susceptible to cracking failure.

All the factors mentioned above have restricted APT practitioners and researchers from developing an accurate methodology for estimating the performance of the APT pavements they tested if subjected to in-service conditions.

1.3 Research Objective

The objectives of this research are to: (1) establish a database of APT and in-service pavement performance data in terms of fatigue cracking, (2) quantify and analyze the difference between APT results and in-service pavement fatigue performance, (3) find a means of accounting for the difference between APT and in-service performance, and (4) quantify uncertainties and develop a methodology for the prediction of pavement performance.

The Bias Correction Factor and Bias Correction Functions should account for all quantifiable differences between the performance of the pavement section under APT and in-service conditions. Laboratory tests are carried out, as required, to evaluate specific quantifiable and measurable differences. To account for the unquantifiable differences, a margin of shift factor, M, is also included and calibrated by combining data sets.

1.4 Organization of this Dissertation

Chapter 2 contains the literature review, including fatigue testing of asphalt mixtures and fatigue performance prediction, with particular emphasis on fatigue characteristics of asphalt mixtures. Finally, previous work involving the application of APT is reviewed.

Chapter 3 proposes a methodology to calibrate the performance difference between APT and in-service pavement sections. First, the methodology principles are introduced, followed by the supplemental laboratory testing programs to gain full benefit. The detailed methods and procedures are also presented. Thereafter, a reliability based method for fatigue performance prediction is introduced.

Chapter 4 reviews the data used in this research, which include 1) Accelerated Pavement Testing in California; 2) Federal Highway Administration's Accelerated Loading Facility; and 3) performance data for in-service flexible pavement from LTPP.

Chapter 5 focuses on the formulation of the Bias Correction Functions. Experimental results are arranged according to frequency, temperature and strain level considerations. This is followed by laboratory test results analysis and, based on the analysis, the development of the Bias Correction Functions for temperature and frequency is described. The development of the Bias Correction Functions and calibration for moisture and wandering are also included. Chapter 5 concludes with the sensitivity analysis of the Bias Correction Functions on pavement fatigue performance.

Chapter 6 focuses on the specification of Bias Correction Functions (BCFs) based on LTPP, FHWA/ALF and CAL/APT data sets. The main characteristics of the LTPP and CAL/APT data sets are discussed and described first. Thereafter, the basic specification of the BCFs is given. This is followed by another component of the model: marginal shift consideration. Based on that consideration, this chapter concludes with the reliability based fatigue life prediction.

Chapter 7 is the validation of the fatigue life prediction. Chapter 8 summarizes this dissertation with conclusions and identifies methodology limitations and further research needs.

Chapter 2: Literature Review

2.1 Overview

The concept of fatigue failure was first introduced into asphalt pavement design in the United States in 1948 by Hveem and Carmany to recognize pavement distress from repeated bending (Hveem and Carmany, 1948), and in Europe in 1953 by Nijboer and van der Poel, who investigated the problem with road vibration equipment (Nijboer and Van der Poel, 1953). Since that time, fatigue distress has been a major consideration for researchers and designers.

The fatigue behavior of asphalt pavements had been intensively studied through the phenomenological approach in the 1960s and 1970s (Deacon, 1965; Monismith and Deacon, 1969; Epps and Monismith, 1972; Pell and Cooper, 1975). A large number of laboratory fatigue tests on asphalt mixtures were conducted to characterize asphalt pavement fatigue response. With this phenomenological approach, the fatigue life of asphalt concrete mixtures was related to stress or strain levels and other material constants. The fatigue properties of asphalt concrete were expressed by a relationship between repetitive loading applications and the tensile stress or strain repeatedly applied. Later-developed design procedures such as the Asphalt Institute and the Shell asphalt pavement design guide make use of these principles. Attempts have also been made to

determine the mode of loading that best simulates actual pavement conditions (Monismith and Deacon, 1969).

Early in the 1970s, other two alternative approaches were studied: (1) dissipated energy and (2) fracture mechanics methods. In the dissipated energy approach, credited to Chomton and Valayer (1972) and van Dijk (1975), cumulative dissipated energy was recognized as the only factor used to predict fatigue life, and this energy seemed to be independent of the mix formulation and testing type, which meant that the fatigue life could be predicted if only the dissipated energy was measured. Later work (Van Dijk and Vesser, 1977) suggested that the relationship between cumulative dissipated energy and the number of cycles is not independent of the mix formulation and other characteristics of the test methods, such as temperature, modes of loading, and frequency. Recent work by Daniel et al. (2004) presented a comparison of the viscoelastic, continuum damage (VECD) and dissipated energy (DE) using uniaxial direct tension fatigue tests on WestTrack mixtures. Although the DE approach does not show agreement with observed field performance, it is highly correlated and similar with VECD if the DE failure criterion is modified. The major problem of the DE approach is that it is not valid for crack propagation. Furthermore, the basic assumption of current application that all of the dissipated energy goes into damaging the material is not flawless. Despite these disappointments, dissipated energy remains a useful concept in fatigue investigation and is highly correlated with stiffness reduction during fatigue testing and helps explain the effects of mode of loading on mix behavior.

In the early 1970s, Ohio State University researchers considered fatigue as a process of damage and utilized fracture mechanics principles to investigate cracking of paving mixtures (Majidzadeh et al., 1972). As a conclusion, they presented a method to determine crack growth with considerations for foundation modulus and material characteristics. The major shortcoming of this approach is that uncertain determination of the initial crack size and only a type-I cracking is included. Extensive literature on the application of fracture mechanics to modeling crack propagation on asphalt concrete existed during the 1970s (Paris and Erdogan, 1963; Cook and Erdogan, 1972; Majidzadeh et al., 1976).

It was the Strategic Highway Research Program (SHRP) that first promoted a combined method to take advantage of different approaches (Tangella et al., 1990; Tayebali et al., 1994). Phenomenological approach and fracture mechanics methods were separately used to take care of different stages of the fatigue process: a fatigue model based on beam fatigue tests conducted under both stress controlled and strain controlled loading conditions was established for the crack initiation stage, while crack propagation was described by a model based on a stress intensity factor and Paris's law. Note that Paris' Law is used to relate the stress intensity factor to subcritical crack growth under a fatigue stress regime. Although this method stood for the state-of-the-art, it still had many shortcomings because of the inherent flaws: it is only inclusive of bottom-up and type-I cracking. In the real world, the crack initiation may occur anywhere within the layer due to tensile stress concentration at one point. If the surface layer is in two lifts

constructed, the crack initiation will occur even in the middle of the layer (Harvey et al., 1999).

Similar to the currently used method for modeling in-service pavement fatigue performance based on laboratory testing, the approach for predicting in-service flexible pavement fatigue performance from APT was intensively applied over the past decade. Hugo and Epps in their recent NCHRP Synthesis 325 summarized the state of the art and the attempts to model the asphalt fatigue and cracking performance of APT sections (Hugo and Epps, 2004). FHWA's Turner Fairbanks Research Center made use of the Accelerated Loading Facility (ALF) to evaluate the fatigue performance of a relatively thin asphalt pavement surface layer on top of a granular base (Tayebali et al., 1994). The observed field performance was correlated with third-point bending fatigue testing of rectangular beams cut out of the test sections. Similar approaches have been followed by other research groups such as the Minnesota Road Research Center (MnRoad) (Newcomb et al., 1999) and the circular APT facility at the Laboratoire Central des Ponts et Chaussees in Nantes (France) (Gramsammer et al., 1999). The relationship between observed field performance and laboratory testing was developed with regression analysis. Unfortunately, except for the last facility mentioned herein, very few pairs of APT and in-service sections have been found that can provide adequate data to validate and calibrate the various individual models, i.e. shift factors, statistical and mechanistic. Therefore, the current prediction model based on APT needs to be improved on a number of aspects.

2.2 Fatigue Test of Asphalt Mixtures

2.2.1 Fatigue failure criteria

Before discussing the fatigue life of asphalt mixtures, it is necessary to clarify the definition of fatigue failure. Different testing methods or research approaches have different failure criterion according to the performance or mechanism. The time of failure is given by the time at which an unacceptable level of service is reached by the pavement structure or when the extent of cracking is such that further delaying of repair work (maintenance or rehabilitation) would increase the cost of the repair work to an unacceptably high level. Thus, failure should always be determined from an economic point of view. In the first case, the level of service is such that user costs (such as operating costs and delay costs) are higher than the cost necessary to repair the road. In the second case, if maintenance and rehabilitation work is delayed, the marginal costs of such delay would surpass the marginal benefit of the savings (Prozzi et al., 2005).

It should be noted that in most cases, the number of repetitions to fatigue failure in controlled strain is considered as the number of repetitions that cause a 50 % drop in the calculated beam stiffness or, traditionally, failure has been defined as a 50 % reduction in initial stiffness (Pronk and Hopman, 1990; Tayebali et al., 1992). This aspect was questioned in The Netherlands where it is believed that after the distresses that produce a drop in the original stiffness take place, there is still life remaining in the pavement (Molenaar et al., 1999). In controlled-stress testing the failure was defined as the

complete fracture of the sample (Bazin and Saunier 1967; Pell and Cooper 1975). From the mechanics viewpoint (Majidzadeh et al., 1972), it was assumed that failure occurs by brittle fracture at a critical crack depth or until the crack grows to almost the full depth of the specimen. After comparing with other existing failure criterion, Al-Khateeb et al. (2004) presented a distinctive fatigue failure criterion at a point where stress and strain are no longer correlated, instead of using the arbitrary 50 % reduction in stiffness. This failure criterion still needs to be verified not only in the fatigue test but also in the pavement performance. In the dissipated energy approach, Ghuzlan and Carpenter defined the failure point as *"… the number of load cycles at which the percentage change of dissipated energy begins to increase rapidly, indicating instability"* (Ghuzlan and Carpenter, 2006).

Prior to Al-Khateeb's achievement, Prozzi and Madanat (2000) presented a survival model to better analyze the American Association of State Highway Officials (AASHO) road test data, which is more appealing than the original AASHO formulation. More recently, survival models have been used to predict in situ pavement fatigue performance from laboratory fatigue test results (Tsai et al. 2003). The Weibull distribution was used to model fatigue failures (Prozzi and Madanat, 2000; Tsai et al., 2003) for its natural properties of extreme value data and its capability to model failure times for mechanisms (random failure processes exist).

Researchers recently defined a fatigue failure threshold based on the fact that most of the LTPP fatigue cracking in the wheel path did not appear for several years and when the cracks did appear they soon propagated to a significant level. According to this definition, 20 m^2 of fatigue cracking of different severity level was selected as the failure threshold for each LTPP section (500 ft length ×12 ft width), i.e. 3.6 % of each LTPP section. If different threshold values are used, the fatigue life of these pavement sections may change accordingly.

2.2.2 Fatigue test methods

There are seven main categories of methodologies for measuring the fatigue behavior and response of asphalt concrete, which include (Porter and Kennedy, 1975; Tayebali et al., 1994):

(1). *Simple flexure with a direct relationship between fatigue life and stress/strain developed by subjecting beams to pulsating or sinusoidal loads in either a third- or center-point configuration; rotating cantilever beams; and trapezoidal cantilever beams subjected to sinusoidal loading.* The center-point, third-point loading and cantilever loading all fall into this category. Deacon developed a controlled stress flexure apparatus with two-point systematical loading (Deacon, 1965). Kallas and Puzinauskas (1972) used different specimens and loading system from Deacon's, while Pell (1962) used the rotating cantilever testing apparatus. This basic technique measures a fundamental property and the results can be directly used in the structural design of pavement. The

main limitations of this methodology are the validation of laboratory results when comparing with in-situ pavement performance; furthermore, the state of stress is essentially uniaxial and its elastic theory assumption.

(2). *Supported flexure with a direct relationship between fatigue life and stress/strain developed by loading beams or slabs that are supported in various ways to directly simulate in-situ modes of loading and sometimes to simulate a more representative stress state.* Although this method better simulates the field conditions, the state of stress is predominantly uniaxial and depends on how the specimen is "clamped" in the test apparatus; it may not be subjected to stress reversals (Barksdale, 1977).

(3). *Direct axial with a direct relationship between fatigue life and stress/strain developed by applying pulsating or sinusoidal loads, uniaxially, with or without stress reversal.* Direct axial method includes tension only and tension/compression. Except for the ability to simulate the loading pulse observed in the field, this test does not well represent field conditions. Raithby and Ramshaw (1972) used a direct tension and compression axial load on specimens, while Kallas (1970) applied tension, compression, and the combination of both with several loading frequencies.

(4). *Diametral with a direct relationship between fatigue life and stress/strain developed by applying pulsating loads to cylindrical specimens in the diametral direction.* Most of the repeated-load indirect tensile tests have been conducted at the Center for Highway

Research at the University of Texas at Austin (Moore and Kennedy, 1971; Navarro and Kennedy, 1975; Cowher, 1975; Kennedy, 1977). The diametral test offers a biaxial state of stress, which is possibly of a type that better represents field conditions. A key problem with this method is that it will significantly underestimate fatigue life if the principal tensile stress is used as the damage determinant.

(5). *Triaxial with a direct relationship between fatigue life and stress/strain developed by testing similar to direct axial testing but with confinement.* Several agencies such as the University of Nottingham (Pell and Brown, 1972; Pell and Cooper, 1975) and the University of California, Berkeley (McLean, 1974; Sousa, 1986) developed this type of device to best represent the state of stress in situ. The only concern about this kind of test is that the shear strains must be well controlled; otherwise the predicted fatigue lives could be considerably different than the field results.

(6). *Fracture tests and the use of fracture mechanics principles to predict fatigue life.* According to this method, fatigue consists of three main phases: crack initiation, stable crack growth, and unstable crack propagation. The second phase is assumed to consume most of the fatigue life. Consequently, the quantitative fatigue models based on fracture mechanics have been proposed in this phase (Majidzadeh et al., 1971; Salam, 1971; Monismith et al., 1973). Although the need for conducting fatigue testing is eliminated and this theory well explains the low temperature crack propagation, its applicability is

not good because of the need for a considerable amount of currently unavailable experimental data. In other words, this method is not valid.

(7). *Wheel-tracking tests, including both laboratory and full-scale arrangements, with a direct relationship between the amount of cracking, the number of load applications, and the measured and/or computed stress/strain. For full-scale tests, both linear and circular track configurations have been used.* To better simulate the effects of a rolling wheel on the pavement and to better understand the pattern of crack initiation and propagation, van Dijk (1975) developed a wheel tracking machine to study fatigue characteristics of asphalt slabs. The problem with the wheel tracking machine is the speed limitation, as well as being disadvantageous for full-scale testing due to centrifugal forces. Currently there are a large number of active full-scale testing facilities around the world. NCHRP syntheses 235 and 325 (Metcalf, 1996; Hugo and Epps, 2004) summarized the state of the art.

Large differences exist among fatigue lives obtained in different studies (Porter and Kennedy, 1975), mainly because of the differences in test methods, loading conditions, material properties, and environmental testing conditions. The mechanics of different test methods also differ from each other on loading configuration, stress distribution, load waveform, loading frequency, permanent deformation, and the state of stress.

2.2.3 Factors affecting fatigue response of asphalt mixtures

Many factors have been identified that affect the fatigue response of asphalt paving mixtures, and are classified into three main categories: load variables, environmental variables, and mixture variables.

Load variables

The fatigue behavior of asphalt mixtures is affected by the characteristics of the applied load, such as loading mode, loading waveform, rest period and loading frequency. These characteristics are summarized next.

Attempts have been made to determine the mode of loading that best simulates actual pavement conditions (Monismith and Deacon 1969; Monismith et al., 1977). The type of loading is expressed by means of a mode factor (MF) defined in Equation 2.1:

$$MF = \frac{|A| - |B|}{|A| + |B|} \tag{2.1}$$

Where,

|A|: percentage change in stress, and

|B|: percentage change in strain for some fixed percentage reduction of stiffness.

The MF assumes a value of -1 for controlled-stress conditions and + 1 for controlled-strain conditions (Monismith, 1966). Researchers have evaluated several characteristics of the two modes of loading. For controlled-stress, the stress is constant and the strain increases as the number of load applications increases, which simulates

actual pavement structures with comparatively thick asphalt bound layers. For controlled-strain, the strain is constant and the stress decreases as the number of load applications increases, which simulates actual pavement structures with asphalt bound layers thinner than 3 inches. For a given specimen, the fatigue life under controlled-strain testing is longer than that under controlled-stress testing.

A comparison of fatigue life was performed by Raithby and Sterling (1972) to determine the effect of loading waveform. Three different waveforms were applied in their study and compared with the test result under sinusoidal waveform: the square waveform produced the shortest fatigue life while the triangular waveform produced the longest fatigue life. They also performed a series of tests to study the effects of rest periods on fatigue life. Based on their conclusion, the fatigue tests under continuous cyclic loading provided skeptical results in relation to real conditions under discontinuous traffic loads. The resultant fatigue life with strain recovery may increase by 5 or more times as the life indicated by continuous cyclic loading.

The effects of rest periods on fatigue response of asphalt concrete mixtures were also studied by other researchers. For example, Van Dijk et al. (1972) demonstrated the beneficial effects of rest periods on fatigue life, which was reflected by a significant increase in the fatigue life of laboratory specimens as compared with specimens tested with no rest period. They also found that a maximum rest period length exists, above which longer rest periods have no effect on fatigue life.

Bonnaure et al. (1982) carried out a laboratory investigation of the influences of rest periods on the fatigue characteristics of bituminous mixes. Based on their study, rest periods were shown to have a beneficial effect on fatigue life, and the benefits seem to reach a maximum when the rest period equals to 25 times the load cycle. They also found that higher temperature and softer binders increased the beneficial effect. Compared with constant-strain mode, the fatigue life under constant-stress mode benefited much more from the rest period. Hsu and Tseng (1996) applied a similar study on the effects of rest periods on asphalt concrete mixtures. They conducted a series of tests at different temperatures and loading ratio (rest period over times of the load cycle), and concluded that as the loading ratio increases, the fatigue life becomes longer due to the healing effect, resulting in higher stiffness modulus of the asphalt concrete mixtures.

Since rest period, loading frequency, and load duration are interdependent, studies were conducted on the effect of loading frequency on fatigue life of asphalt mixtures, while the effects of load period were studied (Pell and Taylor, 1969; Raithby and Sterling, 1970; Epps and Monismith, 1972). Gerritsen and Jongeneel (1988) focused on the fatigue properties of asphalt mixtures under conditions of very low loading frequency (0.00004Hz, such as diurnal temperature and stress variations) and summarized that unfavorable combinations of mix composition and test condition lead to significant deterioration of the mix samples. The low cycle fatigue resistance of asphalt mixes is a function of the mix composition, especially the binder content.

Environmental variables

Moisture and temperature are probably the most important environmentalal factors in laboratory and field testing. Several researchers have studied the effect of temperature and found that fatigue life increases with lower temperatures in controlled stress tests, and it decreases with lower temperatures in controlled strain tests (Pell and Taylor, 1969; Raithby and Sterling, 1970; Epps and Monismith, 1972; Hsu and Tseng, 1996). For controlled stress tests, the strain increases with the increasing temperature while the stress decreases for controlled strain tests. This could be further explained with the dissipation energy method.

Mixture variables

The composition of asphalt mixtures determines its fatigue performance. The most important factors identified that affect fatigue response are: asphalt content, asphalt type, aggregate type, aggregate gradation, and air void content. Several investigators have presented optimum asphalt content with respect to maximum fatigue life (Jiminez and Gallaway, 1962; Pell, 1967; Epps and Monismith, 1969; Pell and Taylor, 1969). For example, the effect of increasing air void content on fatigue life was quantified by Epps and Monismith (1969) in the United States and Pell and Taylor (1969) in the United Kingdom.

2.3 Fatigue Characteristics of Asphalt Mixtures

"The fatigue characteristics of asphalt mixes are usually expressed as relationships between the initial tensile stress or strain and the number of load repetitions to failure—determined by using repeated flexure, direct tension, or diametral tests performed at several stress or strain levels" (Tayebali et al., 1994). Early researchers have been expressing simple flexure results of fatigue tests in the form of relationships between the initial tensile stress or strain and the number of load repetitions to failure. It was found that fatigue life was often better correlated with tensile strains than with tensile stresses, and that the basic failure relationship could be characterized by the following equations (Monismith et al., 1966, 1981; Pell, 1967; Pell et al., 1975):

$$N_f = a\left(\frac{1}{\varepsilon_t}\right)^b \tag{2.2}$$

Where,

N_f: the number of load applications to failure (e.g. number of cycles to reach 50% of initial stiffness, number of load application to crack initiation),

ε_t,: the magnitudes of tensile strain and tensile stress repeatedly applied, and

a and b: experimentally determined material coefficients.

In an attempt to account for the effects of loading frequency and temperature on fatigue life, a mixture stiffness term can be added to Equation 2.2 as follows:

$$N_f = a\left(\frac{1}{\varepsilon_t}\right)^b (S_{mix})^c \quad (2.3)$$

Where,

S_{mix}: initial stiffness modulus of the asphalt mixture

a,b and c: experimentally determined parameters

The effects of the volumetric asphalt content (V_b) and the air void (V_a) content on the fatigue performance of hot mix asphalt (HMA) were introduced by Pell and Cooper (1975) as follows:

$$N_f = k_1\left(\frac{1}{\varepsilon_t}\right)^{k2}\left(\frac{1}{E}\right)^{k3}\left(\frac{V_b}{V_b + V_a}\right)^{k4} \quad (2.4)$$

Where,

E: stiffness modulus of the HMA mixtures,

V_b : volumetric asphalt content,

V_a : air void content,

k_1, k_2, k_3 and k_4: experimentally determined parameters.

Different models have been proposed by the Nottingham researchers (Brown et al., 1982), Shell (Shell, 1978), and the Asphalt Institute (AI, 1981) to account for the effects of other factors on fatigue life. The Nottingham researchers developed a general relationship between tensile strain, the number of loadings to failure, asphalt content (volume basis), and the ring and ball softening point of the asphalt in the mix as follows:

$$\log \varepsilon_t = \frac{14.39 \log V_B + 24.2 \log T_{RB} - 40.7 - \log N}{5.13 \log V_B + 8.63 \log T_{RB} - 15.8} \quad (2.5)$$

Where,

ε_t: allowable tensile stain

V_B : volumetric asphalt content,

N: number of load applications to failure

T_{RB}: ring and ball softening point temperature, °C

The Shell researchers developed a general approach to estimate the allowable fatigue strain expressed as follows. Where the mix stiffness (S_{mix}) can be estimated with the volume concentrations of the aggregate and asphalt and the stiffness of the asphalt (S_{asp}) contained in the mix.

$$\varepsilon_t = (0.856 \times V_B + 1.08) S_{mix}^{-0.036} \times N^{-0.2} \quad (2.6)$$

The Asphalt Institute (AI, 1982) took the volume of air voids into consideration and included a correction term C, thus the Asphalt Institute methodology expressed the number of load applications to failure from the following expression:

$$N = 18.4C(4.325 \times 10^{-3} \varepsilon_t^{-3.291} S_{mix}^{-0.854}) \quad (2.7)$$

Where,

$C = 10^M$,

$M = 4.84 \times (\frac{V_B}{V_B + V_V} - 0.69)$

Bonnaure et al. (1980) employed a statistical approach using 146 fatigue curves from various fatigue tests and found the following equations in the form of initial strain and fatigue life (Equations 2.8 and 2.9) to determine the fatigue resistance of a mix.

For constant strain test:

$$\varepsilon = (4.102 \times PI - 0.205 \times PI \times V_B + 1.094 \times V_B - 2.707) \times S_{mix}^{-0.36} \times N^{-0.2} \quad (2.8)$$

For constant stress test:

$$\varepsilon = (0.300 \times PI - 0.015 \times PI \times V_B + 0.080 \times V_B - 0.198) \times S_{mix}^{-0.28} \times N^{-0.2} \quad (2.9)$$

Where,

V_B: the volumetric bitumen content of the mix,

PI: the penetration index of the binder in the mix, and

S_{mix}: the stiffness modulus of the mix.

The 146 fatigue curves covered a wide range of mixes, bitumens and testing conditions. Although the accuracy of this method is only ±50 % (after discarding some 10% outliers) for the constant strain test and ±40 % for the constant stress test, it is considered sufficient given the wide range of testing mixes and conditions. From the above mentioned relationships, one simple nomograph has been prepared for the constant stress test and constant strain test, respectively. Initial strain and fatigue life relations can be determined once the volumetric bitumen content of the mix, the penetration index of the binder in the mix, and the stiffness modulus of the mix are provided.

Several researchers have used the energy approach for predicting the fatigue behavior of the asphalt mixes (Chomton and Valayer, 1972; Van Dijk et al., 1972, 1975, 1977). The relationship between fatigue life and cumulative dissipated energy can be characterized as follows:

$$W_N = A\left(N_f\right)^z \tag{2.10}$$

Where,

W_N: Cumulative dissipated energy to failure, and

A,z: experimentally determined coefficients.

With this approach, the fatigue life could be predicted only if the dissipated energy was determined for a given mix formulation. Dissipated energy captures both elastic and viscous effects and thus it is possible to predict the relative fatigue behavior of mixes in the laboratory from the results of fatigue tests when strain is the only test variable (Tayebali et al., 1994).

2.4 Accelerated Pavement Testing (APT)

Development of a protocol for the establishment and operation of LTPP sections in conjunction with APT sections, laboratory characterization of materials tested, and the development of testing protocols and specifications are potential components of LTPP studies being conducted in all regions to investigate the relationships between field and APT performance and the results of laboratory characterization.

APT programs have led to advances in practice and economic savings from the evaluation of new pavement configurations, stress level related factors (such as a vehicle's weight, axle configuration, traveling speed, tire type, tire inflation pressure, and wheel arrangements), new materials and design improvements. APT could be traced back to as early as 1909 with a test track in Detroit. Historically, the most notable APT program on highway pavement engineering is the Road Test conducted by the Association of State Highway Officials (AASHO) in the late 1950s (AASHO, 1961). The United States was not as active and productive as Australia, Denmark, South Africa, France, Britain, and the Netherlands in APT activities during the period between the 1970s and 1980s (Coetzee et al., 2000). Since the mid-1980s, the situation changed dramatically. The Federal Highway Administration (FHWA), U.S. Army Corps of Engineers (USACE, both at Waterways Experiment Station (WES) and at the Cold Regions Research and Engineering Laboratory (CRREL)), and the states of Minnesota, California, and Louisiana have made significant investments in APT programs. The State of Florida and the National Center for Asphalt Technology (NCAT), in collaboration with the Alabama Department of Transportation, have taken the leadership in new APT programs of the 21st Century (Coetzee et al., 2000).

However, because of the limited ability to address long-term phenomena, the same pavement structure may exhibit different response and performance under APT than when in-service. Therefore, to fully utilize the benefits of APT, there is a need for a

methodology to predict the long-term performance of in-service pavement structures from the results of APT tests that will account for such differences. Moreover, APT programs must be supplemented with laboratory testing programs to gain full benefit. Three approaches are generally suggested to account for the difference: (1) shift factors, (2) statistical models, and (3) mechanistic models.

Shift factors

Shift factors have been used by many APT programs to obtain quick correlations between APT and in-service performance when limited data are available (Al-Qadi and Nassar, 2003; Al-Balbissi and Little, 1990). This is similar to the approach followed to estimate in-service performance based on laboratory results. Shift factors can be estimated for each APT pavement structure for which in-service performance data are available. In order to generalize, the estimated shift factors of all structures should be compared and multivariate statistical analysis should be performed to investigate the manner in which each loading and climatic condition influences the shift factor. The main disadvantage of this approach, although relatively simple and straightforward, is that shift factors cannot be extrapolated. Thus, shift factors can only be developed when both APT and in-service performance results are available.

Empirical or statistical models

The empirical approach is based on experience, experimentation or a combination of both to establish the relationships between design inputs (pavement structures, material

properties, traffic loading and environment) and pavement performance indicators (such as rutting, cracking and roughness). Many pavement structural design procedures such as the AASHTO and California methods use an empirical approach. The AASHTO method is the most common empirical design method that could be traced back to the 1960s, and remains popular for pavement structural design. The resulting design equation was developed from experimental data at the AASHO Road Test, which relates pavement structure to pavement performance, applied loads, service life and subgrade support. The California method is another common empirical design method developed in California during the early 1940s by Francis Hveem and others. This method was originally based on test track data from Brighton and Stockton. Similar to the AASHTO equation, the California method relates pavement structure to applied loads and subgrade support (HAPI, 2007).

Regression analysis in pavement performance prediction is the process used to estimate the parameter values of a prediction model, in which the model predicts the pavement performance as a function of the explanatory variables such as pavement structure, environmental condition and traffic loading. The goal of regression analysis is to determine the values of parameters for a model that cause the model to best fit a set of data observations provided. Regression analysis has been applied to develop empirical or statistical models to predict fatigue response of asphalt-aggregate mixes (Tangella et al., 1990; SHRP, 1994). The main disadvantage is that performance equations are only approximations of the real physical phenomena. Linear and multi-linear regression and

non-linear regression are the two statistical methods most commonly used. In order for the statistical methods to benefit from a generalized application, relatively large data sources are required.

Mechanistic-Empirical (M-E) models (Linear Elastic and Finite elements)

A mechanistic-empirical (M-E) model or mechanistic model consists of two main parts, including structural models and transfer functions. The first part, which is referred to as the mechanistic part, is used to compute critical stresses, strains, and displacements due to both traffic loads and climatic factors. Stress-dependent finite element programs (such as ILLI-PAVE, MICH-PAVE) and multi-layer linear-elastic computer programs (such as BISAR, WESLEA, JULEA, CHEVRON, ELSYM5, CIRCLY and KENLAYER) are both recommended for structural analysis. The second part, which is actually the empirical part, utilizes the resultant responses from the first part in damage models to accumulate damage over the design period, and further relates to specific distresses such as fatigue cracking or rutting by using a field calibrated model. The most common flexible pavement transfer functions are flexural strain to fatigue life and subgrade vertical strain to pavement rutting. Since transfer functions are the weak link in the M-E approach, field calibration and validation are essential for a reliable distress prediction model (Theyse et al., 1996; Thompson, 1996). The Mechanistic-Empirical Pavement Design Guide (MEPDG) developed under NCHRP 1-37A provides the most advanced and comprehensive method for the design of flexible pavements to date (www.trb.org/mepdg).

Besides the capability of accommodating stress-dependent properties such as granular materials stress hardening and fine-grained soils stress softening, the Finite Element Model (FEM) is used to estimate the effects of loading frequency, presence or lack of lateral wheel wandering, dynamic loading (several wave shapes, modeling those typically measured for APT wheel loading will be used), and unidirectional or bi-directional loading.

The approach for modeling the fatigue performance of pavement sections through APT is similar to that currently used for modeling in-service pavements based on laboratory testing. The laboratory transfer functions developed in this manner are correlated to the expected APT performance by means of a shift factor or other type of calibration approach (Prozzi and De Beer, 1997; Harvey et al., 1997; AL-Qadi and Nassar, 2003).

Predicting in-service fatigue life of HMA based solely on laboratory tests is still not a very reliable method. The differences between laboratory testing and field conditions are related to loading, material properties and specimen preparation and have typically been accounted for by using shift factors (AL-Qadi and Nassar, 2003). Four shift factors were identified in the literature: stress state, traffic wander, HMA healing and material properties. Based on truck testing at the Virginia Smart Road, a shift factor to account for the traffic wander can be calculated with Equation 2.11. This shift factor makes use of the density function to consider the lateral distribution of traffic, but it does

not reflect the sensitivity of a particular process to a change in the level of interested variable. Furthermore, it has been established independently of other factors.

$$SHF_{traffic-wander} = \frac{1}{\int f(x) \times \varepsilon_{ratio}(x)dx / \int \varepsilon_{ratio}(x)dx} \quad (2.11)$$

Where,

$SHF_{traffic\text{-}wander}$: shift factor to account for traffic wander,

f(x): probability density function of lateral traffic distribution , and

$\varepsilon_{ratio}(x) = \frac{\varepsilon}{\varepsilon_{\max}} = 0.931\exp(-1.7199x)$ (fitted to an exponential curve of truck testing at the Virginia Smart Road).

The development of fatigue cracking during an APT experiment can be captured through the direct or indirect monitoring of the changes in the stiffness of the asphalt surface or base layers or by monitoring the development of hairline surface cracks by visual or automated digital surveys (Long et al., 1996; Tsai et al., 2004). This monitoring enables the determination of the time between opening the pavement section to traffic and the end of the propagation phase (actual deterioration stage). However, given the difficulty in determining the first hairline cracks appearing on the surface, the transfer functions are calibrated to different levels of crack, e.g. 45% area cracked, etc. That is, crack initiation and some degree of crack propagation are merged together into one process.

The development of fatigue cracking is traditionally related to the maximum horizontal tensile strains that develop at the bottom of the asphalt layer under the action of the APT device. Through this approach, the classical bottom-up fatigue cracking is developed. Most recently, research conducted in South Africa was able to quantify the tensile stresses that develop at the surface of an asphalt layer due to higher tire inflation pressures and non-uniform stress distributions (De Beer, 1996). This research could help explain the development of top-down fatigue cracking, although reliable transfer functions for this type of failure are not available to date. Although the newly developed MEPDG (NCHRP, 2006) includes models for estimating bottom-up cracking, initial assessment of these models yielded unreasonable performance estimation results.

A number of attempts to model the asphalt fatigue and cracking performance of APT sections have been reported by Hugo in his recent Synthesis of Highway Practices 325 (Hugo, 2004). The Accelerated Loading Facility (ALF) at FHWA's Turner Fairbanks Research Center was used to evaluate the fatigue performance of a relatively thin asphalt pavement surface layer on top of a granular base (Tayebali et al., 1994). This research, part of the SHRP, involved the selection of a laboratory testing methodology for modeling fatigue performance (SHRP, 1994). Observed field performance was correlated with third-point bending fatigue testing of rectangular beams, which were sawed out of the test sections. The laboratory tests were conducted at 10 Hz and 20°C under controlled strain conditions.

A similar approach has been followed by other research groups such as the Minnesota Road Research Center (MnRoad). The regression equation (Newcomb et al., 1999) that was developed to estimate the fatigue performance at MnRoad sections is:

$$N_f = 2.83 \times 10^6 \times \left(\frac{1}{\varepsilon_t} \right)^{3.206} \quad (2.12)$$

Where,

N: number of cycles to the onset of fatigue cracking, and

ε_t: transverse strain at the bottom of the asphalt layer, microstrain.

The circular APT facility at the Laboratoire Central des Ponts et Chaussees (LCPC) in Nantes (France) has been used to determine fatigue performance of flexible pavement structures of varying surface thickness (Gramsammer et al., 1999; De La Roche et al., 1994). In this case, fatigue was correlated with surface deflection. Trapezoidal cantilever beams were used in the laboratory to estimate the fatigue resistance of the mixes under stress and strain-controlled conditions.

Very few pairs of APT and in-service sections have been found that can provide adequate data to validate and calibrate the various individual models, i.e. shift factors, statistical and mechanistic. Therefore, a reliability-based methodology is preferred since, in addition to better data usage, it provides an estimate of the expected performance as well as a probability associated with the estimate.

Chapter 3: Methodology

3.1 Principles of Methodology

Given a set of similar basic structural inputs (such as pavement type, material properties, layer thicknesses, and subgrade characteristics) a pavement site could be subjected to accelerated deterioration by means of APT or to the action of actual traffic and environmental conditions (in-service pavement). Let A denote the performance of the site under APT conditions and F denote the field performance of the in-service pavement site. If APT technology is able to simulate exact field conditions, the performance on the in-service pavement (F) could be directly estimated by the observed APT performance (A) (Prozzi et al., 2005)

$$F = A \tag{3.1}$$

Where,

F: in-service performance, e.g. number of trucks or Equivalent Single-Axle Load (ESALs) to a certain density of fatigue cracking (e.g. 45% of whole area with fatigue cracking, $3m/m^2$ crack density),

A: performance of the site under APT, e.g. number of trucks or ESALs of the APT device to the same severity of fatigue cracking as that of in-service.

Figure 3.1 shows a schematic representation of the main differences between the fatigue performance of in-service sites and those subjected to APT. The figure shows the

main differences that are considered in the fatigue methodology proposed in this dissertation. Some of these differences will be assessed by means of laboratory testing of asphalt mixtures.

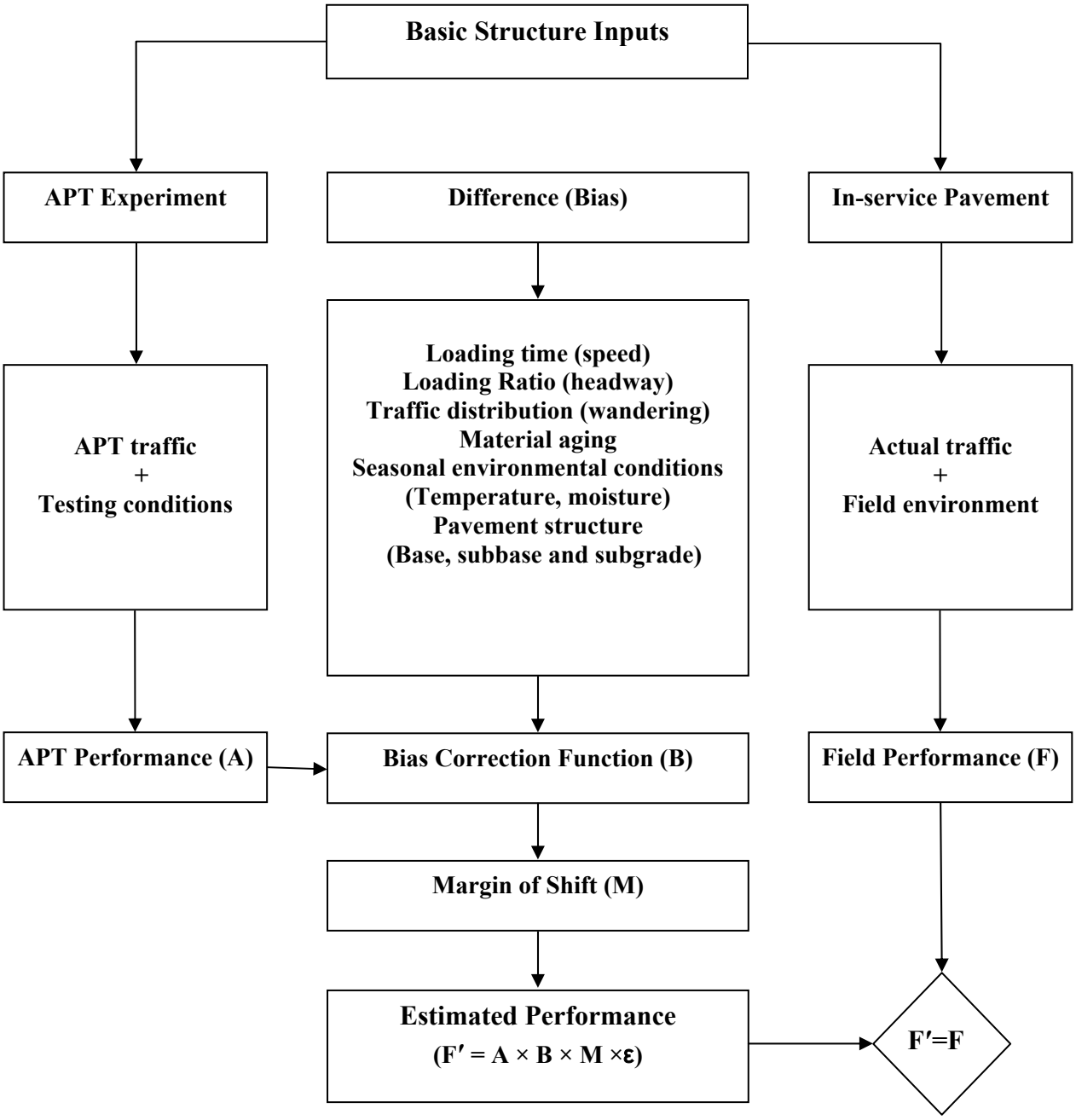

Figure 3.1 Main differences between in-service and APT fatigue performance

Due to the various conditions indicated in Figure 3.1, both sites perform differently. APT performance (A) constitutes a biased estimate of in-service performance (F). Therefore, a Bias Correction Factor (B) must be incorporated to account for these differences. In addition, due to the high variability and uncertainties inherent to the process and the effects of unobserved variables, the incorporation of a margin of shift (M) is desirable to account for the unquantifiable differences. By incorporating these two aspects into the formulation, the in-service performance can now be modified by (illustrated as in Figure 3.2):

$$F = A \times B \times M \tag{3.2}$$

Where,

B: Bias Correction Factor which accounts for all observed differences between APT and in-service conditions, and

M: marginal shift factor (M) which accounts for the unquantifiable differences

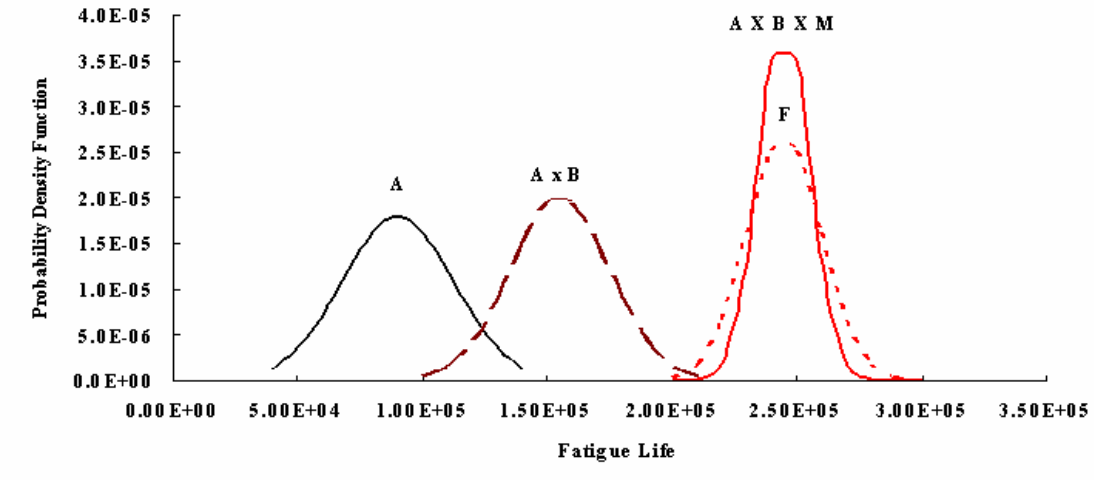

Figure 3.2 Estimation of field performance: F′ = A × B × M

This equation provides a means to estimate the expected in-service fatigue performance of a pavement site (F), when the expected performance of the same (or similar) site has been previously determined through APT (A). The equation provides for the incorporation of a margin of shift factor to account for expected but unobserved differences, field variability and other sources of uncertainty. All variables in Equation 3.2 are random variables, which are characterized by a given distribution function.

It should be noted that the "shift factor" approach commonly used to correlate laboratory and field performance is the simplest version of a Bias Correction Factor. While the shift factor is a deterministic number, usually determined in an ad-hoc manner, the bias factor is statistically determined and characterized: it has a distribution. In addition, by using a Bias Correction Function instead of a correction factor, an equation can be developed that can incorporate variables affecting the value of the factor.

Equation 3.2 represents the expected value of F. No matter how accurately the bias correction factor and the shift factor are estimated, due to unobserved variables and the random nature of A, B, M and F, a random model error is actually present, therefore:

$$F = A \times B \times M \times \varepsilon \tag{3.3}$$

Empirical evidence supports that performance functions such as F and A can be assumed to follow a log-normal distribution. Thus, if the formulation of the bias

correction function, B, and the marginal shift factor, M, are such that they can be assumed to be log-normal random variables, then the prediction error can be given by:

$$\log(\varepsilon) = \log(F) - \log(A \times B) - \log(M) \quad (3.4)$$

Under the above-mentioned assumptions, the prediction error defined by Equation 3.4 is a log-normal random variable with mean equal to zero. It takes the form:

$$\log(\varepsilon) \approx N\left(0, \sigma^2_{\log(\varepsilon)}\right) \quad (3.5)$$

Where,

ε: unbiased random error term,

$\sigma_{\log(\varepsilon)}$: std. deviation of the prediction error.

The reliability-based methodology for the estimation of the fatigue life of in-service sites based on the observed performance of similar sites under APT conditions will be implemented in four steps, which are discussed in the following section.

3.2 Methods and Procedures

To develop a reliability based methodology for fatigue cracking prediction, four main steps are required. The first step consists of obtaining and analyzing cracking performance data from sites tested under APT and similar in-service sites from FHWA's LTPP studies, the objective of which is to address the difference between APT results

and in-service pavement fatigue performance. In the second step, Bias Correction Functions will be developed to estimate Bias Correction Factors, the objective of which is to quantify the difference between APT and in service conditions. The third step is to develop the marginal shift factor and calibration, which will account for all unquantifiable differences between the performance of the pavement site under APT and in-service conditions. The final step consists of the reliability analysis, the objective of which is to account for uncertainties and to obtain pavement performance estimations and their respective variability.

The systematic component of the unobserved differences and other differences of secondary order effect will be considered by the incorporation of a marginal shift factor (M). The random differences between observed and predicted behavior will be part of the unbiased model error. As outlined in Figure 3.1, the shift factor approach, statistical and mechanistic modeling are combined into one general approach that builds on their individual strengths to overcome some of the shortcomings when the models are applied individually (Prozzi et al., 2005). By combining the three models into one methodology, the utilization of the available data is optimized. In addition, this combined methodology is preferred because:

1) It is scientifically sound,
2) It makes optimal use of limited available data, and
3) It provides an estimate of the expected performance as well as an estimate of its variability. This becomes very important for reliability calculations.

3.3 Reliability-based Fatigue Performance Prediction

In the past, prediction models developed from full scale or laboratory tests have been used to predict performance. It is also known that a great spatial variability exists among the numerous pavement structural components, such as layer material properties and layer thicknesses as a result of the construction of the pavement. There are also variations in layer material quality, homogeneity, environmental conditions, and construction techniques. Another source of spatial variability is due to the dynamic loads applied to the pavement structure by the moving traffic. As a result of all these spatial variations, the distributions of stresses, strains, and deformations within the pavement structure are by no means uniform and lead to the development of non uniform distribution of distresses in the pavement. Before reliability concepts were employed in probabilistic pavement design, shift factors were widely used to account for the many uncertainties in the deterministic pavement design method. This generally resulted in over-design or under-design, depending on the applied shift factors. The factors applied in the design usually reflected the magnitude of the variation of all the design variables.

A more realistic procedure called probabilistic design was applied for the first time in the 1993 AASHTO design method, which uses a reliability-based approach to account for the uncertainties in the design variables and introduced desired level of reliability into the pavement design. The AASHTO definition of reliability is: *"The reliability of the pavement design-performance process is the probability that a pavement site designed*

using the process will perform satisfactorily over the traffic and environmental conditions for the design period" (AASHTO, 1993). The limit state is assumed to be reached when the predicted number of ESALs reaches the number that the site can withstand before it reaches a specified terminal level of serviceability. In the AASHTO Design Guide (1993), closed form solutions are used to develop designs for the chosen reliability level.

Reliability based methodology for pavement performance (such as fatigue cracking) prediction was recently proposed (Prozzi et al., 2005; Sun and Hudson, 2005) and is further developed in the early part of this research (Prozzi and Guo, 2007). Through this approach, the three models suggested previously are combined into one general approach that builds on their individual strengths to overcome some of the shortcomings when the models are applied individually. The unobserved differences and other differences of secondary order effect are considered part of the model error. In this dissertation, a reliability based methodology for fatigue cracking prediction is developed. As shown in Figure 3.3, let W(t) = A×B×M denote the allowable traffic loading repetitions (or ESALs) predicted from APT and laboratory testing when the performance of pavement structure deteriorates to a certain level and let W(T) be the actual in-service pavement traffic loading repetitions, then the definition of reliability is expressed by Equation 3.6:

$$R = \text{Probability}\left[W(T) < W(t)\right] \tag{3.6}$$

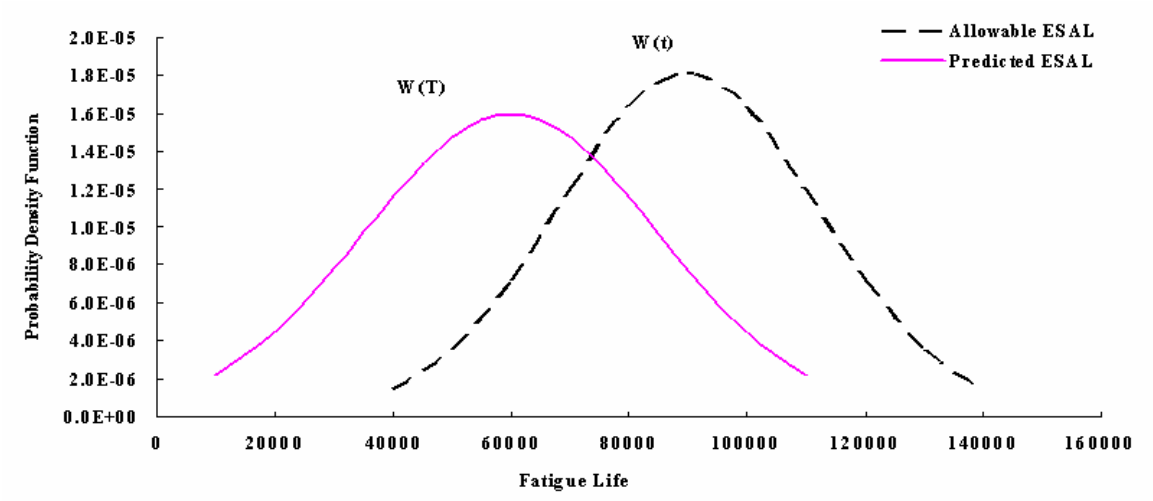

Figure 3.3 Reliability statement of performance prediction from APT

Log (A×B×M) is the performance equation which gives the predicted number of ESAL applications from APT; log (W_T) is the predicted number of ESAL applications from in service pavement. If log (W_T) is equal to log (A×B×M), the reliability of the prediction is 50% because all variables are based on mean values. To achieve a higher level of reliability, log (A×B×M) must be larger than log (W_T) by a normal deviate Z_R calculated as follows (Huang, 1993):

$$-Z_R = \frac{\log(W_T) - \log(A \times B \times M)}{\sigma_{\log(\varepsilon)}} \tag{3.7}$$

Where,

Z_R: normal deviate for a given reliability R,

$\sigma_{\log(\varepsilon)}$: stand deviation of log (F)-log (A×B×M) defined in Equation 3.5.

In this approach, the marginal shift is a direct function of the design reliability. The errors of pavement performance models can only be evaluated by calibration to a well designed experiment with accurate design and performance data. To this effect the data from the California APT (CAL/APT, as described later) and the LTPP studies are evaluated. These errors affect the accuracy of the design and performance predictions together with the variability expected for all input variables. Furthermore, a rigorous reliability approach is developed to assess the effect of the variation of selected variables on pavement performance prediction based on APT results. The reliability of the performance prediction is evaluated as the normal deviate Z_R, which can be determined from standard normal probabilities table. The final equation for fatigue life prediction is as follows:

$$\log(W_T) = -Z_R \times \sigma_{\log(\varepsilon)} + \log(A \times B \times M) \tag{3.8}$$

Chapter 4: Gathering and Processing of Performance Data

The first step in the reliability-based methodology consists of collecting cracking performance data from sites tested under APT and similar in-service sites from FHWA's LTPP databases. Caltrans' fleet of Heavy Vehicle Simulators (HVS) and FHWA's Accelerated Loading Facilities (ALF) represent the most successful APT programs worldwide and have been collecting performance information on numerous mixes and pavements for several years.

4.1 Caltrans Accelerated Pavement Testing Program (CAL/APT)

From 1994 to 1996, the University of California at Berkeley (UCB), in a joint effort with the California Department of Transportation (Caltrans) and other agencies, utilized two Heavy Vehicle Simulators (HVS) to study the accelerated loading on four full-scale pavements with untreated aggregate and asphalt treated permeable bases (ATPB). One of the HVS units was used to test in-service pavements while the other was utilized for testing environment-controlled full-scale pavements at UCB's Richmond Field Station (RFS). The primary objective was to develop data to quantitatively verify existing Caltrans design methodologies for different pavement types. A secondary objective was to determine and compare fatigue lives of the different types of pavement structures. For this research, test results from CAL/APT on pavement structure (Figure 4.1) containing untreated aggregate base site 501RF and 503RF were collected (Harvey et al., 1999).

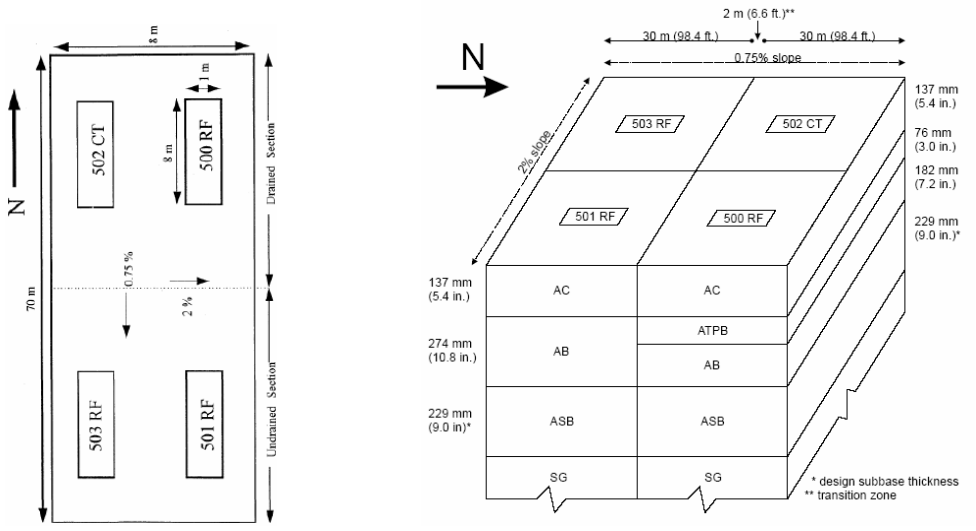

Figure 4.1 Structural pavement sites of CAL/APT program (Harvey et al., 1999)

Since accurate and complete fatigue performance data sets are scarce, the site with available fatigue performance data was disaggregated to create more subsections. For example, the 8.0-m HVS site is subdivided into 8 individual 1.0-meter sites. Then, after discarding three sections to avoid edge effects, data from 5 subsections for each site could be available (Sites 501RF2-3 through 503RF6-7 in Figure 4.2, Figure 4.3). By proceeding in this method, the mean cracking progression data and its distribution are both available. Spatial correlation of the six APT sections could be expected due to identical testing conditions. However, this correlation can be accounted for and incorporated into the data analysis.

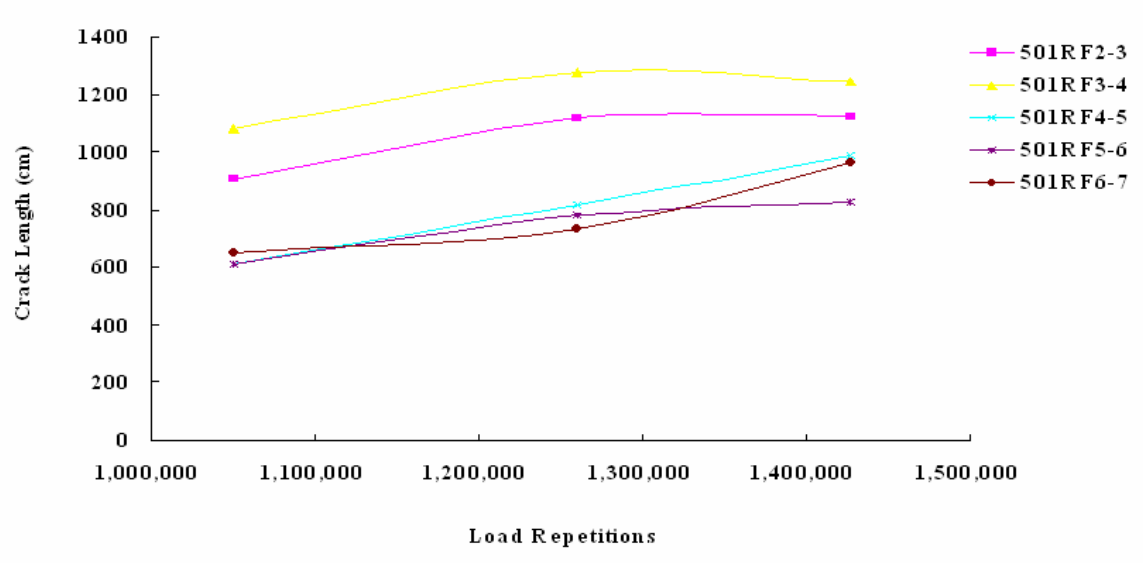

Figure 4.2 Performance fatigue data corresponding to 6 subsections of site 501RF

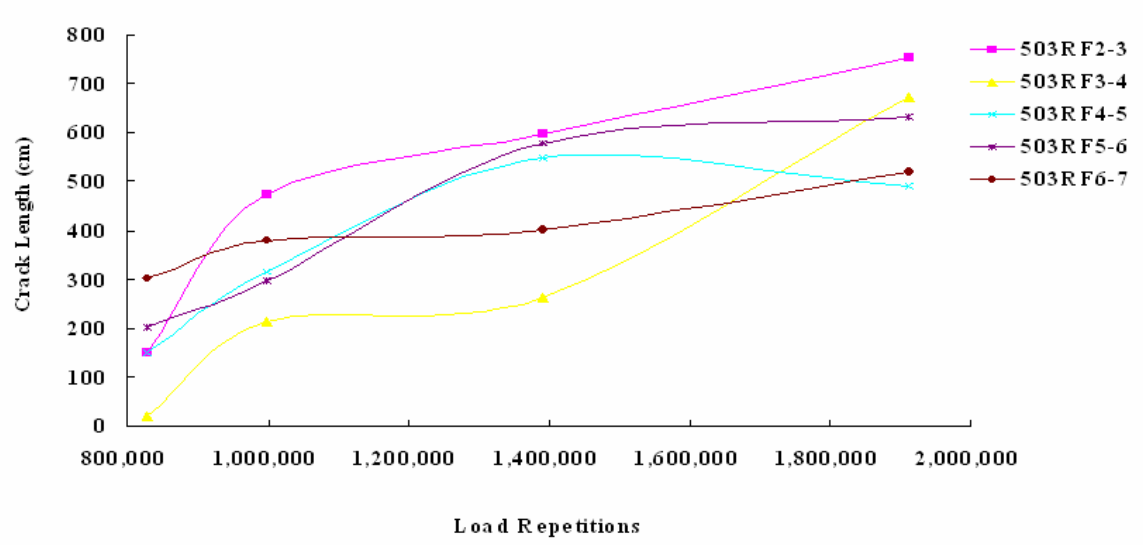

Figure 4.3 Performance fatigue data corresponding to 6 subsections of site 503RF

4.2 Federal Highway Administration's Accelerated Loading Facility (FHWA/ALF)

In 1993, twelve lanes of full scale pavement were constructed at the FHWA's pavement testing facility to validate the Superpave (SUperior PERforming asphalt PAVEments) binder parameters for rutting and fatigue cracking, among which Lane 3 through Lane 4 were primarily being used for fatigue tests (Sherwood et al., 1999) as shown in Figure 4.4. One of the specific objectives of the study was to provide a set of pavement performance data to validate the mechanistic pavement performance models in Superpave.

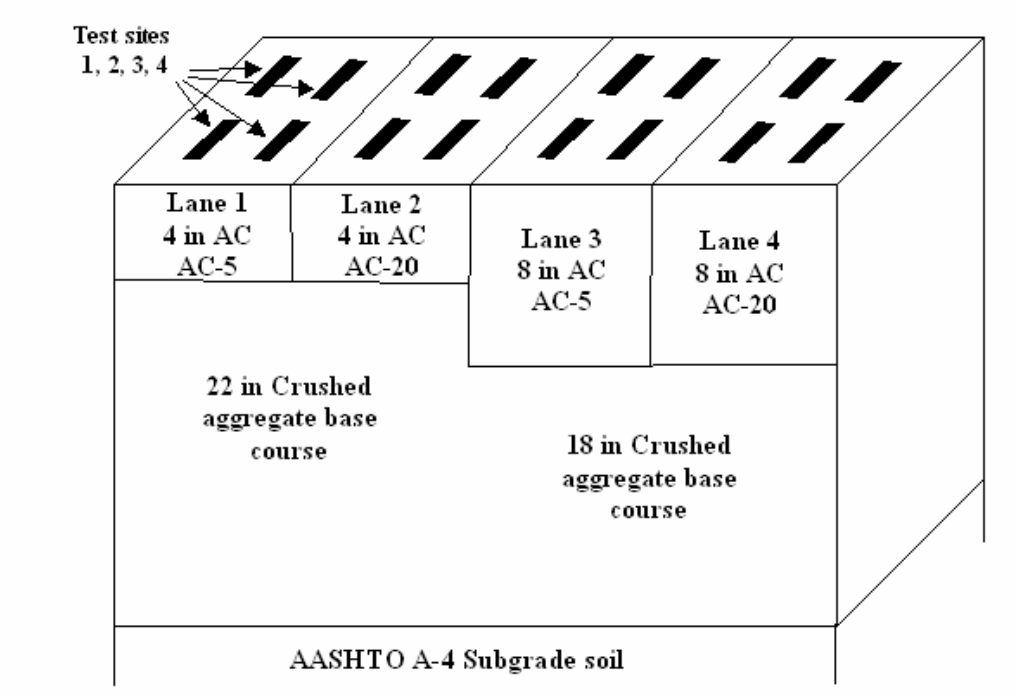

Figure 4.4 Layout of the pavement lanes for fatigue tests

Figure 4.5 shows the cracking data of the nine fatigue test sites. Lane 1 site 2 and lane 2 site 2 are not included in the data analysis because both of these sites failed prematurely under rutting. Lane 1 site 3 was also excluded because of poor drainage and early failure due to a heavy rain storm.

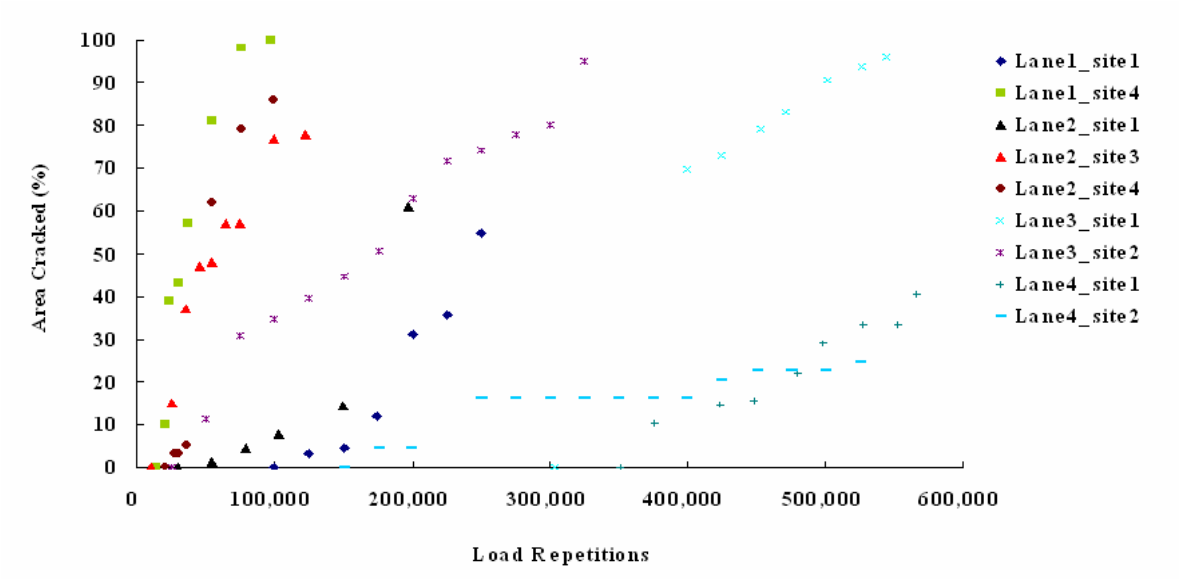

Figure 4.5 Percentage of area cracked corresponding to nine fatigue test sites

4.3 In-service Pavement Performance Data (LTPP)

Initiated as part of SHRP, the LTPP program was established by the Transportation Research Board (TRB) of the National Research Council in the early 1980's and sponsored by FHWA in cooperation with AASHTO. The motivation of the LTPP program is to better understand pavement performance under the effects of various variables. The overall objective of this program was to monitor and evaluate in-service pavement performance under a variety of affecting factors over a pavement's service life

for as long as 20 years (SHRP, 1994). Two main categories of pavement test sites are included in the LTPP database, among which General Pavement Studies (GPS) are existing pavements while Specific Pavement Studies (SPS) are sites where multiple test sites of differing experimental treatment factors were specifically constructed (FHWA, 2003).

The LTPP pavement performance database is divided into several modules containing multiple tables, among which the pavement monitoring (MON) module contains manual distress and inventory (INV) module contains inventory information for all GPS test sites. As one of the main LTPP products, the LTPP DataPave Online provides a fast and easy means of navigating the complex structure of the LTPP relational database.

According to the CAL/APT program, 3 similar in-service pavement sites with 5.8 inches (±5%) of asphalt concrete (AC) surface layer are selected from the LTPP database (Table 4.1). **A**ccording to the FHWA/ALF program, 4 similar in-service pavement sites with 4 inches and 8 inches (±5%) of asphalt concrete (AC) surface layer are selected from the LTPP database (Table 4.2).

Table 4.1 Selected LTPP sites match CAL/APT program

SHRP_ID	State_Code	Region	Climatic	Layer	Thickness (in)
1009	Maine (23)	North Atlantic	Wet freeze	Subgrade Subbase Base AC	 25.8 4.8 5.7
6007	British Columbia (82)	Western	Wet no freeze	Subgrade Base A	 12.4 5.8
1622	Ontario (87)	North Atlantic	Wet freeze	Subgrade Subbase Base A	 26.3 6.7 5.7

Table 4.2 Selected LTPP sites match FHWA/ALF program

SHRP_ID	State_Code	Region	Climatic	Layer	Thickness (in)
1030	North Carolina (37)	North Atlantic	Wet No Freeze	Subgrade Base A	 4.7 4
6160	Texas (48)	Southern	Dry Freeze	Subgrade Subbase Base AC	 4.8 8.4 4
109	New Mexico (35)	Southern	Dry No Freeze	Subgrade Subbase Base AC	 11.9 4.5 8
1004	Vermont (50)	North Atlantic	Wet Freeze	Subgrade Subbase Base AC	 22.8 24.3 8

The performance data from CAL/APT and FHWA/ALF provide the distribution of A, while the data from LTPP provide the distribution of F (Figure 3.1). The link between these two databases is established by means of Bias Correction Factor (variable *B*) and the marginal shift factor M. Data for the determination of F is obtained from the fatigue cracking tables contained in the LTPP pavement performance monitoring database. Initially, data for the equivalent LTPP sites is typically obtained from the fatigue cracking tables GATOR_CRACK_A contained in DataPave, which is expressed in squared meters and the data contained in the tables corresponding to alligator cracking are used at the various levels of severity (low, medium, high) (FHWA, 2006). Longitudinal cracking and transverse cracking data are also used as that contained in tables TRANS_CRACK_ L (L, M and H), TRANS_CRACK_ N (L, M and H), LONG_CRACK_WP_L (L, M and H) and LONG_CRACK_NWP_L (L, M, H). These data are updated every year and are available at http://www.ltpp-products.com. A most recent update can be obtained on request from FHWA.

Chapter 5: Development of the Bias Correction Factor

In addition to pavement and material properties, the main factors that need to be considered for developing an accurate methodology are traffic loading and environment-related variables. To be specific, these factors are loading frequency (speed), loading ratio (LR: rest periods over loading time), traffic distribution (wandering), moisture, temperature and other long term effects such as climate and age hardening of asphalt. The Bias Correction Factor should account for all quantifiable differences of these factors between the performance of the pavement site under APT and in-service conditions. In order to account for all differences, the Bias Correction Factor can be represented as the product of a number of independent Bias Correction Functions as in Equation 5.1:

$$B = BCF_{frequency} \times BCF_{loadingratio} \times BCF_{wander} \times BCF_{temperature} \times BCF_{moisture} \times \ldots \quad (5.1)$$

Where,

$BCF_{frequency}$: Bias Correction Function to account for differences in loading speed,

$BCF_{loading\ ratio}$: Bias Correction Function to account for differences in rest periods and loading time,

BCF_{wander}: Correction Function to account for differences in the lateral distribution of traffic: channelized versus wandering,

$BCF_{temperature}$: Bias Correction Function to account for differences in temperature, and

$BCF_{moisture}$: Bias Correction Function to account for differences in the moisture content of the untreated granular materials.

All these correction functions are aimed at capturing the overall differential effect of the specified variable between in-service pavements and similar pavements subjected to APT, which is represented by the ratio of a given moment between the distribution of the variables under in-service and APT, as in Equation 5.2, the parameter α reflects the sensitivity of a particular process to a change in the level of variable x. This parameter represents the order of the moment.

$$BCF_{generic} = \frac{\int g(x_{APT}^{\alpha}) f(x_{APT}) dx_{APT}}{\int g(x_{in}^{\alpha}) f(x_{in}) dx_{in}}$$

$$or \qquad (5.2)$$

$$BCF_{generic} = \frac{\int D(x_{in})] f(x_{in}) dx_{in}}{\int D(x_{APT}^{\alpha}) f(x_{APT}) dx_{APT}}$$

Where,

x_{in}: variable of interest under in-service conditions,

x_{APT}: variable of interest under APT conditions, and

α: parameter that reflects the sensitivity of a particular process to a change in the level of variable x. This parameter represents the order of the moment,

g(x): fatigue life as a function of variable x, and

D(x): damage as a function of variable x, and

f(x): density function of variable x.

When the variable of interest is not continuously distributed, the correction functions are then represented as in Equation 5.3:

$$BCF_{generic} = \frac{\sum_{1}^{m} g(x_{in.i}^{\alpha}) p(x_{in.i})}{\sum_{1}^{n} g(x_{APTi}^{\alpha}) p(x_{APTi})} \tag{5.3}$$

Where,

p(x.i): proportion of variable of interest in condition i,

m, n: number of conditions considered in the analysis (e.g. seasons).

During this research, BCFs are developed based on previous research results and experience or computer simulations. In those cases where appropriate data are not available for developing the specification form of the models or for testing the recommended methodology and "fine-tuning" of the actual factors, laboratory testing is carried out. This laboratory testing consists primarily of third-point bending tests and dynamic stiffness. In the hypothetical case when the testing of the APT site is such that all expected differences can be accounted for, then the value of the bias factor should be unity. For example, if the wandering under APT is the same as the wandering observed in-service, the Bias Correction Function for wandering will be one.

5.1 Bias Correction Function for Temperature and Loading Frequency (Speed)

Due to the fact that asphalt materials are thermorehologicaly simple, the principle of superposition is used to assess the effects of temperature and loading speed (frequency) by means of the same master curve.

5.1.1 Laboratory testing program

Limited laboratory testing consisting primarily of third-point bending tests and dynamic stiffness are carried out for the recommended methodology. As shown in Figure 5.1, the beam is simply supported at two points, such that equal loading is applied at those points which trisect the distance between the support points and the stress between the two central points is uniformly distributed.

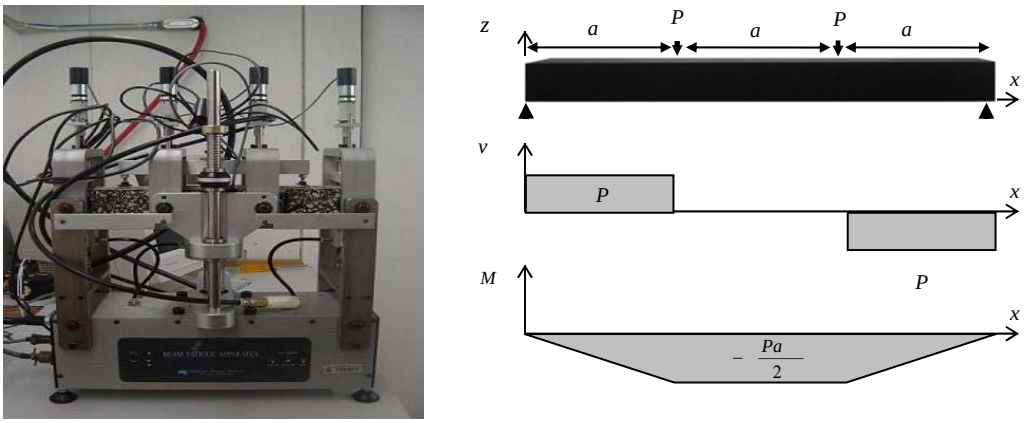

Figure 5.1 Four-point bending fatigue testing apparatus

The peak tensile stress (kPa) is:

$$\sigma_t = \frac{LP}{Wh^2} \times 10^6 \tag{5.4}$$

Where,

σ_t = peak tensile stress (kPa),

L = beam span (mm),

P = peak force excursion (kN),

w = beam width (mm),

h = beam height (mm).

And the peak tensile strain (mm/mm) is:

$$\varepsilon_t = \frac{108\delta h}{23L^2} \times 10^6 \tag{5.5}$$

Where,

ε_t: peak tensile strain (microstrain)

δ: peak displacement (mm)

The main purpose of carrying out the third-point beam bending fatigue tests is to analyze the fatigue response of the asphalt mixes at different temperatures and frequencies and to identify the joint effect of temperature and frequency on asphalt fatigue performance. Based on the laboratory test results, the Bias Correction Functions for temperature and frequency are developed. To establish the non-linear dependency, three temperature levels, four frequency levels, together with different strain levels and duplicate specimens are tested in the laboratory.

5.1.1 Test temperature setting

Asphalt pavements are known to exhibit fatigue distress or deterioration of binder stiffness under repeated traffic load in the intermediate temperature range from about 10°C to 30°C (Deacon et al., 1994; Stuart et al., 2002). Based on these findings, three test temperatures were selected in this research: 30°C, 20°C and 10°C.

5.1.2 Test loading frequency setting

The change in material temperature has the same effect as changing the loading speed. As shown in Figure 5.2, the loading frequency applied to the bottom of AC layer is a function of the length of tire contact area (a), the thickness of AC layer (h), the driving speed and the load spread angle (θ°). Suggested by Shell (1978), the loading time of 0.02s is representative of the range of a vehicle speed of 48 to 64 km/h, which corresponds to a loading frequency of 8 Hz according to Equation 5.6, which could also be referred to calculate loading frequencies at different speed (Table 5.1).

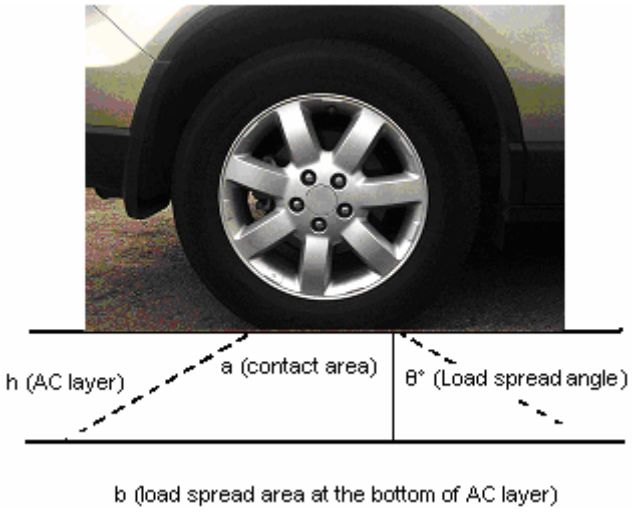

Figure 5.2 Mode for loading speed (frequency) calculation

The stiffness modulus of bitumen can be determined by either a creep test with a loading time or a dynamic test with a frequency (Huang, 1993). It has been suggested by Van Der Poel (1954) that when the loading time, t, is related to the frequency, f, by Equation 5.6, the same stiffness modulus is obtained.

$$t = \frac{1}{2\pi f} \tag{5.6}$$

Table 5.1 Loading frequencies at different speed and load spread area width (Hz)

Speed	Load spread area width (cm), a: 10-40 cm; h: 5-40 cm; θ°: 30°- 75°					
(km/H)	15	30	60	120	240	480
5	1.47	0.74	0.37	0.18	0.09	0.05
10	2.95	1.47	0.74	0.37	0.18	0.09
30	8.84	4.42	2.21	1.11	0.55	0.28
60	17.68	8.84	4.42	2.21	1.11	0.55
100	29.47	14.73	7.37	3.68	1.84	0.92
120	35.36	17.68	8.84	4.42	2.21	1.11

To capture the relationship between fatigue performance of asphalt concrete mixes and temperature and frequency, the test system shall be capable of providing repeated sinusoidal loading at a frequency of between 5 and 10 Hz (Harvey et al., 1996). Pell and Taylor's (1969) test results showed that the most significant change occurred at frequencies below 200 cycles per minute, according to which the critical loading frequency is 3.33 Hz. Considering all these facts and the limitations of the testing equipment, the test frequency is set at the range from a lower side 2.5Hz to a higher side of 20 Hz. Two intermediate frequencies were also included as 5 Hz and 10Hz.

5.1.3 Experiment design

Three temperature levels and four frequency levels are selected in this research according to previous discussion. Together with duplicates, 36 laboratory fatigue tests were conducted within a period of six months. Experimental arrangements of fatigue tests are listed as in Table 5.2.

Table 5.2 Experimental arrangement of fatigue tests

Specimen	Temperature (℃)	Frequency (Hz)	Strain level (10-6)
1	10	2.5	300
2	10	2.5	450
3	10	5	300
4	10	5	450
5	10	10	300
6	10	10	450
7	20	5	350
8	20	5	500
9	20	10	350
10	20	10	500
11	20	20	350
12	20	20	500
13	30	2.5	450
14	30	2.5	600
15	30	5	450
16	30	5	600
17	30	10	450
18	30	10	600

To account for the effects of loading time and temperature on the stiffness of the mix and on the fatigue performance, a master curve is developed with a reference temperature and loading time equal to those prevailing during the APT test. For a range of frequencies applied by the APT facility, the stiffness of the mixture can be determined in the

laboratory at different temperatures. Then, the data obtained at different temperatures is shifted horizontally so as to build the master curve, which is shown in Figure 5.3. The amount of shifting that takes place at each temperature reflects the frequency and temperature dependency of the material.

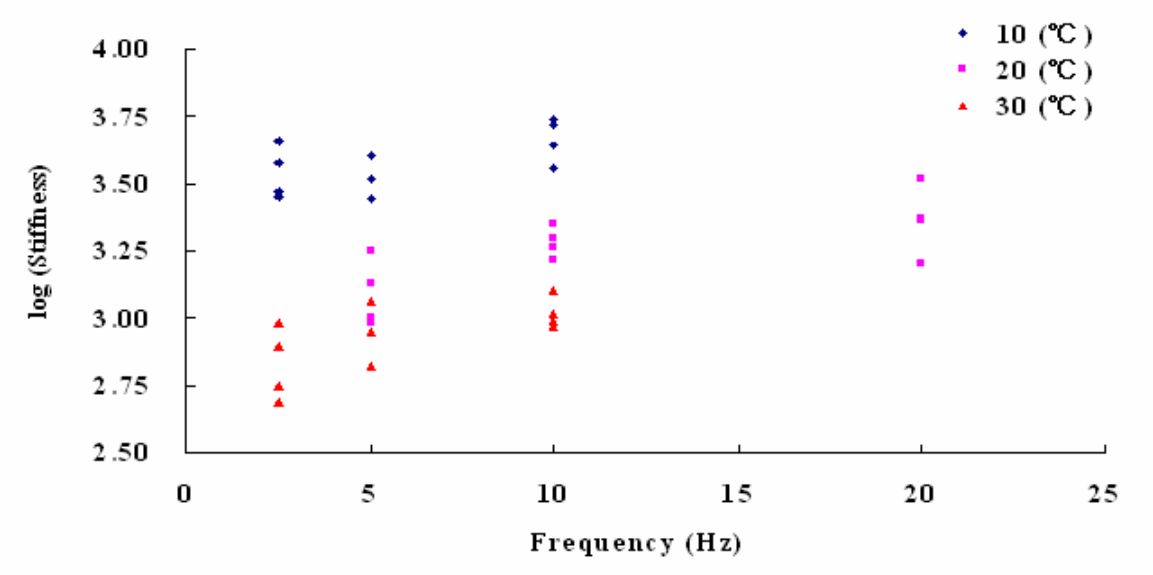

Figure 5.3 Master curve of a particular asphalt mixture

The master curve is typically developed from dynamic modulus testing of the material by means of tri-axial testing. For the purpose of this research, however, it is proposed to base the master curve on stiffness determinations performed by means of third-point bending test. The reasoning f this selection is that dynamic stiffness is closely related to fatigue performance as opposed to dynamic modulus. It has been shown that modified and unmodified asphalt mixtures with equivalent dynamic modulus may show significantly different fatigue performance.

Table 5.3 Laboratory four-point bending fatigue test results

Beam	Frequency (Hz)	Temp (°C)	Initial Stiffness (MPa)	Micro Strain	Cycles
APT 4-1-1	2.5	10.60	5845.0	449.13	8,525
APT 4-1-2	2.5	10.60	7505.0	434.56	25,960
APT 4-2-1	2.5	10.67	5613.9	298.93	324,040
APT 4-2-2	2.5	10.67	9192.1	290.55	87,310
APT 5-3-1	2.5	29.75	973.0	449.32	815,940
APT 5-3-2	2.5	29.75	1589.1	452.12	713,400
APT 6-1-1	2.5	29.99	1120.2	613.11	64,300
APT 6-1-2	2.5	29.99	1906.9	599.56	55,660
APT 2-2-1	5	20.79	1926.2	349.63	88,520
APT 2-2-2	5	20.80	2000.0	338.05	34,050
APT 2-3-1	5	20.77	2694.1	499.58	36,305
APT 2-3-2	5	20.77	3544.0	482.17	60,100
APT 4-3-1	5	10.09	5523.6	444.37	7,650
APT 4-3-2	5	10.09	7993.8	289.48	358,920
APT 6-2-1	5	29.08	1315.6	477.87	395,520
APT 6-2-2	5	29.08	2316.0	452.00	116,500
APT 6-3-1	5	29.99	1328.9	600.86	58,800
APT 6-3-2	5	29.70	1780.0	599.78	25,310
APT 6-4-1	5	10.09	6642.2	299.67	142,465
APT 6-4-2	5	10.60	7978.7	434.26	28,910
APT 1-1-1	10	20.65	3689.6	500.00	30,980
APT 1-1-2	10	20.70	3290.8	507.07	34,140
APT 1-3-1	10	20.80	3963.7	350.01	100,380
APT 1-3-2	10	20.79	4523.6	336.83	222,160
APT 3-1-1	10	10.10	8765.7	300.03	106,330
APT 3-1-2	10	10.10	11000.0	289.03	151,930
APT 3-3-1	10	10.30	7275.4	450.07	11,360
APT 3-3-2	10	10.30	10500.0	433.25	25,630
APT 5-1-1	10	29.08	1947.2	449.95	122,080
APT 5-1-2	10	29.08	2525.2	451.29	106,330
APT 5-2-1	10	29.60	1846.4	599.96	37,630
APT 5-2-2	10	29.60	2050.0	601.40	41,260
APT 2-1-1	20	20.77	3200.4	500.39	32,020
APT 2-1-2	20	21.26	4706.7	481.39	5,260
APT 3-2-1	20	20.77	4656.6	350.24	48,100
APT 3-2-2	20	21.24	6594.0	336.64	90,270

Laboratory four-point bending fatigue test results are shown in Table 5.3. Based on laboratory test results and statistical analysis, a regression equation for predicting fatigue life was developed as follows:

$$\log(N_f) = 16.6 - 4.80 \log(Strain) - 0.0348\ Freq. + 0.0570\ Temp. \qquad (5.7)$$

The regression results, presented in Table 5.4, indicate that all the variables included in the model are significant. The higher the strain level, in other words, the larger the magnitude of the traffic loads, the shorter the pavement fatigue life. The pavement fatigue life is greatly affected by the temperature: the AC layer becomes more resistant to fatigue distress as the temperature increases.

Table 5.4 Regression analysis of temperature and loading frequency

Predictor	Coef	SE Coef	t	P
Constant	16.558	1.659	9.98	0
log strain	-4.804	0.668	-7.19	0
Freq	-0.035	0.010	-3.48	0.001
Temp	0.057	0.009	6.57	0
S = 0.310277	R-Sq = 67.1%	R-Sq(adj) = 64.0%		

In principle, the Bias Correction Function for loading frequency and temperature is the ratio of the expected performance of the mixes under the conditions in the field over the expected performance of the mixes under APT conditions, therefore:

$$BCF_{T\&F} = \frac{N_f^{in,T\&F}}{N_f^{APT,T\&F}} \qquad (5.8)$$

By replacing Equation 5.6 into Equation 5.7, thus, Bias Correction Function for fatigue life as a function of loading frequency (Hz) and temperature (°C) can be computed as:

$$BCF_{T\&F} = 10^{0.0570\,(T_{in}-T_{APT})-0.0348\,(Freq_{in}-Freq_{APT})} \quad (5.9)$$

Where,

T_{APT}: pavement temperature during APT testing (°C),

T_{in}: pavement temperature in the field (°C),

F_{APT}: loading frequency during APT testing (Hz), and

F_{in}: loading frequency of in service pavement (Hz).

5.2 Bias Correction Function for Traffic Wandering

Unlike APT traffic, which is tightly controlled, actual highway traffic on in-service pavements follows a random lateral distribution. Previous research has indicated that the distribution could be characterized as normal with mean and standard deviation of the lateral position being a function of the facility type, number of lanes and lane width (Wang et al., 2000). Independent of the actual distribution, the traffic distribution will produce a distribution of the maximum strain that develops in the asphalt concrete layer. By denoting ε_x the random variable that represents the value of the maximum tensile strain as a result of the horizontal traffic distribution and f(x) the probability density function of this random variable, the Bias Correction Factor for traffic wandering (BCFwander) can be calculated as follows:

$$BCF_{Wander} = \frac{\int (\varepsilon_{APT})^{-\beta} f(x_{APT})\, dx_{APT}}{\int (\varepsilon_{in})^{-\beta} f(x_{in})\, dx_{in}} \quad (5.10)$$

Where,

ε_{in}, ε_{APT}: maximum tensile strain as a function of the lateral position x,

β: parameter that represents the sensitivity of the pavement fatigue life to a change in strain, -4.8 based on laboratory test results,

f(x): probability density function of traffic distributed at lateral position x.

If APT is strictly controlled, which means there is no wandering for APT, this equation can be simplified as Equation 5.11:

$$BCF_{Wander} = \frac{\varepsilon_{\max}^{-\beta}}{\int (\varepsilon_{in})^{-\beta} f(x_{in})\, dx_{in}} \quad (5.11)$$

According to truck testing at the Virginia Smart Road, the maximum response as a function of the lateral position could be fitted to an exponential curve (Al-Qadi and Nassar, 2003):

$$\varepsilon_{in} = \varepsilon_{\max} \times 0.931 \times \exp(-1.7199\,|x|) \quad (5.12)$$

It is assumed that traffic is normally distributed along the lateral position x with a mean of zero, the probability density function becomes:

$$f(x) = \frac{1}{\sigma\sqrt{2\pi}} \exp\left(-\frac{1}{2}\left[\frac{x}{\sigma}\right]^2\right) \quad (5.13)$$

By replacing Equation 5.12 and 5.13 into Equation 5.11, we obtain:

$$BCF_{wander} = \frac{\sigma_{APT}}{\sigma_{in}} \frac{\int_0^b \exp(-8.256\, x - \frac{x^2}{2\sigma_{in}^2})dx}{\int_0^a \exp(-8.256\, x - \frac{x^2}{2\sigma_{iAPT}^2})dx} \tag{5.14}$$

Where,

σ_{in}: standard deviation of lateral position x of in service pavement,

σ_{APT}: standard deviation of lateral position x of APT.

a, b: the allowable lateral offset of the axles (0 to 0.6 m based on known lateral wander distributions) (Hiller and Roesler, 2005).

Once the standard deviation of lateral position x is accessed, the Bias Correction Function of fatigue life for wandering can be evaluated with the above model. If the wandering of APT is simulated as in service, i.e. with the same standard deviation, this BCF will be unity. The parameter β represents the fatigue resistance sensitivity of a particular asphalt mixture to changes in strain level. The value of the parameter is determined in the laboratory under third point bending tests at different strain levels. This strain level should cover a wide range of strain so as to cover strain levels expected under APT and in-service conditions.

5.3 Bias Correction Function for Moisture

Moisture condition of pavement subgrade under APT is well controlled while in-service subgrade is subjected to seasonal changes. This change relates primarily to the variation of the bottom tensile strains of asphalt concrete layer and, therefore, to the fatigue performance. With the multi-layer linear elastic assumption, the Bias Correction Factor for moisture ($BCF_{mositure}$) is determined with Equation 5.15:

$$BCF_{moisture} = \frac{\varepsilon_{APT}^{4.8}}{\sum_{I=1}^{n} \varepsilon_{in,i}^{4.8} p(\varepsilon_{in.i})} \tag{5.15}$$

Where,

ε_{APT}: maximum tensile strain in the asphalt layer under APT,

ε_i: maximum seasonal tensile strain in the asphalt layer as a result of differential support due to moisture changes,

$p(\varepsilon i)$: proportion of time in condition i,

n: number of seasons (typically 4 to 12 seasons are sufficient),

5.4 Bias Correction Function for Loading Ratio

The rest times in an APT experiment are shorter than those occurring on actual highways but the loading time is longer because of the lower speeds typical of APT. This can be illustrated by a loading ratio, which is defined as the ratio of rest period over loading time (Figure 5.4). This translates into an increased amount of dissipated energy

occurring on in-service pavements and, therefore, a longer fatigue life.

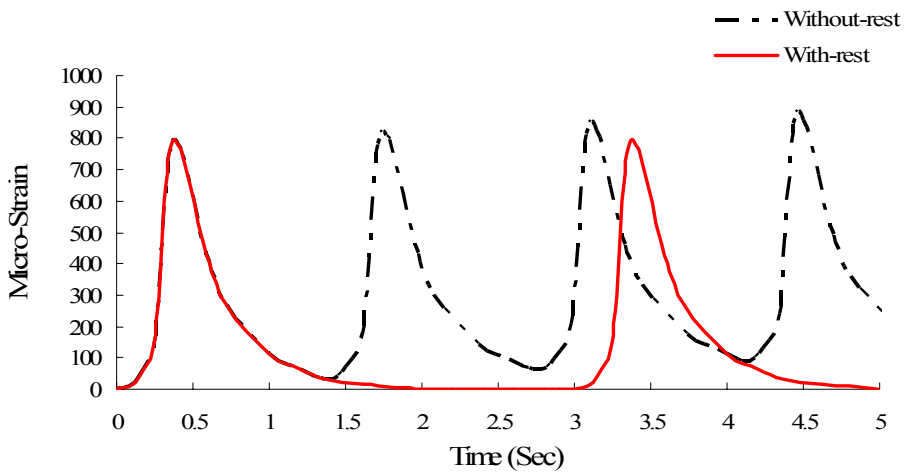

Figure 5.4 Traffic loading with or without rest period

The relationship between fatigue life under APT conditions and in-service performance can be related by means of a Bias Correction Function that accounts for the different loading ratios. In principle, this Bias Correction Function for loading ratio determines the ratio of the expected performance of the binder under the conditions in the field over the expected performance of the binder under APT conditions, as in Equation 5.16.

$$BCF_{LR} = \frac{N_f^{in,LR}}{N_f^{APT,LR}} \tag{5.16}$$

Based on previous laboratory investigation of the influence of rest periods on the fatigue characteristics of bituminous mixes (Raithby and Sterling, 1972), the regression equation for fatigue life prediction is:

$$\log(N_f) = -9.38 - 3.04\log(strain) + 0.0376\,Temp + 0.011\,LR \quad (5.17)$$

Table 5.5 Regression analysis of loading ratio based on laboratory investigation

Predictor	Coef	SE Coef	t	P
Constant	-9.380	0.634	-14.8	0
log strain	-3.040	0.144	-21.2	0
T(℃)	0.038	0.003	14.67	0
LR (Loading Ratio)	0.011	0.003	4.19	0

S = 0.288 R-Sq = 0.81 R-Sq(adj) = 0.80

The results in Table 5.5 indicate that all the estimated model parameters are significant (P-value < 0.001). The rest period has positive effect on fatigue performance and the effect of temperature and strain is further proved to be significant, which agrees with previous results although the coefficient is slightly different because of different tested materials.

Given the same strain and stiffness levels for both APT program and in-service pavement, by replacing Equation 5.16 into Equation 5.17, the Bias Correction Function for fatigue life that accounts for different loading ratios can now be given as:

$$BCF_{\mathrm{LR}} = 10^{0.011(LR_{\mathrm{in}} - LR_{\mathrm{APT}})} \quad (5.18)$$

Where,

LR_{in}: loading ratio of in-service pavement, and

LR_{APT}: loading ratio of APT program.

Furthermore, according to Bonnaure's results, the beneficial effect of rest periods on fatigue life seems to reach a maximum when the loading ratio is up to 25 (Bonnaure et al., 1982). LR will then take a value of 25 when the ratio is larger than 25.

5.5 Sensitivity Analysis of Bias Correction Functions

Sensitivity analysis is the determination of how variations in input parameters quantitatively affect predicted distress. The goals of a sensitivity analysis are as follows: (1) determination of the degree to which the distress prediction model can simulate observed trends in the development and progression of distress; (2) determination of what factors contribute to variability in the predicted distress; and (3) assessment of the reasonability of the influence of the model parameters on the variability of the predicted distress. With the use of Bias Correction Functions, sensitivity analyses were made to determine the effects of loading frequency (speed), loading ratio, traffic distribution (wandering), moisture, and temperature on pavement fatigue life prediction.

The Bias Correction Factor can now be represented as the product of a number of independent Bias Correction Functions as in Equation 5.19, which was used to determine the effect of various parameters on the Bias Correction Factor.

$$B = BCF_{frequency} \times BCF_{loadingratio} \times BCF_{wander} \times BCF_{temperature} \times BCF_{moisture}$$

$$= 10^{0.0570(T_{in}-T_{APT})-0.0348(Freq_{in}-Freq_{APT})+0.011(LR_{in}-LR_{APT})} \tag{5.19}$$

$$\times \frac{\int_0^{0.6} \sigma_{in} \exp(-8.26x - \frac{x^2}{2\sigma_{APT}^2})dx}{\int_0^{0.6} \sigma_{APT} \exp(-8.26x - \frac{x^2}{2\sigma_{in}^2})dx} \times \frac{\varepsilon_{in}^{-4.8}}{\varepsilon_{APT}^{-4.8}}$$

Figure 5.5 shows the effect of temperature on BCF. Increasing the temperature difference between in service pavement and APT from -10 ℃ to 10℃ increases the BCF by 14 times, indicating that the temperature has a marked effect on increasing the BCF, hence, the fatigue life of flexible pavement is very sensitive to temperature change.

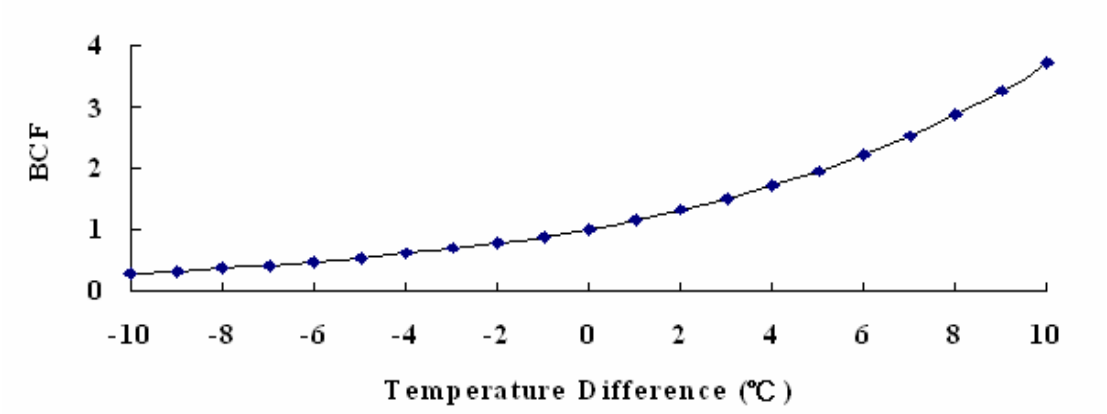

Figure 5.5 Effect of temperature on BCFs

Figure 5.6 shows the effect of driving speed on BCF. Increasing the driving speed from 50 km/hour to 100 km/hour increases the BCF by 65%, indicating that faster traffic

has a negative impact on pavement fatigue performance. One km/hour increase of driving speed will result in about 1% decrease of pavement fatigue life based on this research.

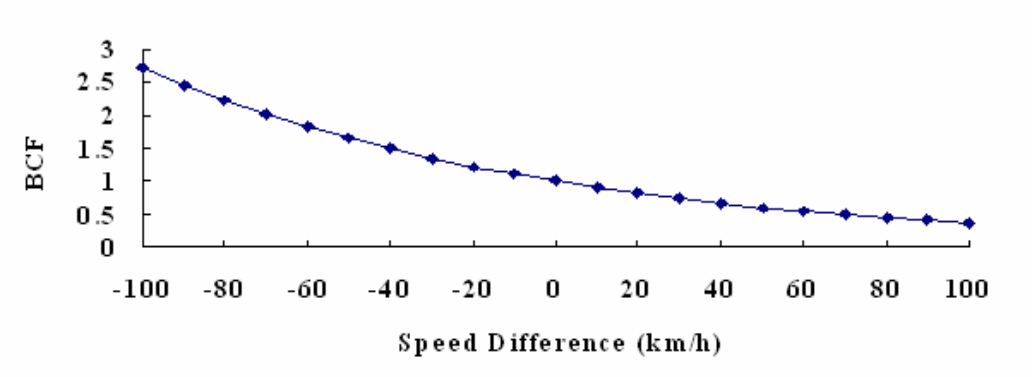

Figure 5.6 Effect of driving speed on BCFs

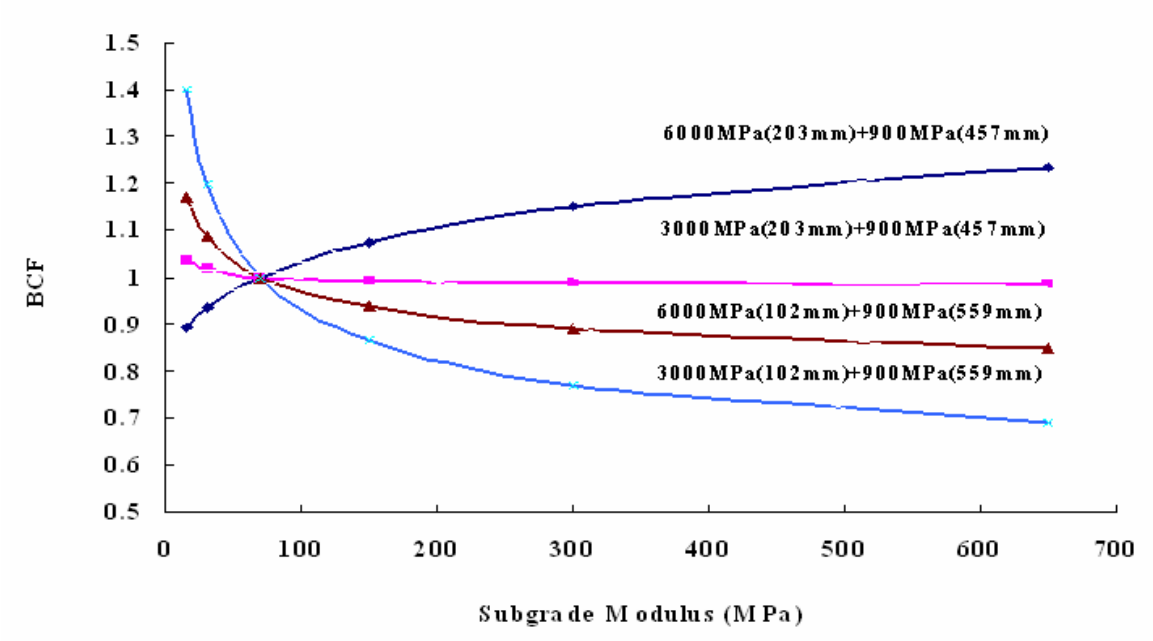

Figure 5.7 Effect of subgrade modulus change on BCFs

Figure 5.7 shows the effect of subgrade modulus on BCF. Increasing the subgrade modulus increases or decreases the BCF, depending on the strength of the pavement

structure. It is not economical to improve the subgrade modulus just for the purpose of increasing the fatigue life of a relatively strong pavement structure. The change in subgrade modulus affects the BCF only when it is very weak. Inclusion of seasonal variation in moisture condition may or may not result in pavement fatigue life change, depending on the relative strength of subgrade to the whole pavement structure.

Figure 5.8 shows the effect of the loading ratio on BCF. Rest periods have been proven to have a beneficial effect on fatigue life and the benefits seem to reach a maximum when the rest period equals to 25 times of the load cycle. Based on the sensitivity analysis, a unit increase of the loading ratio results in an increase of 2.6% of pavement fatigue life on average before it reaches 25.

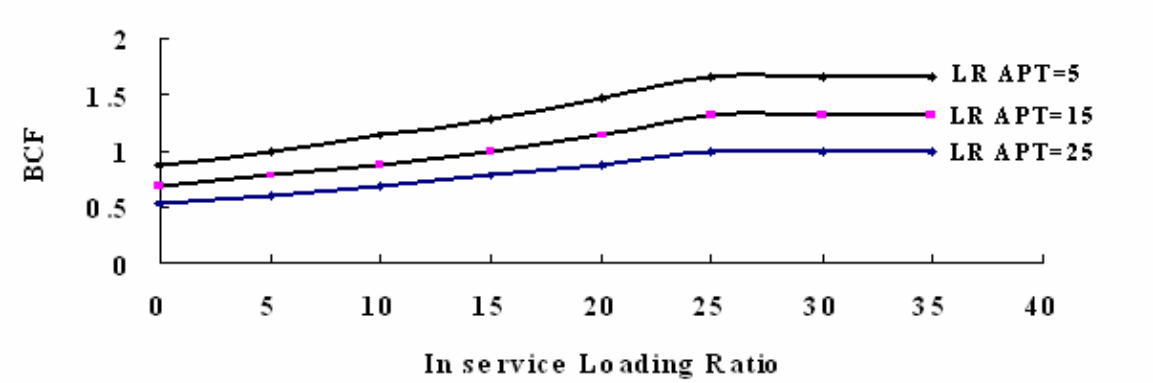

Figure 5.8 Effect of loading ratio on BCFs

Figure 5.9 shows the effect of standard deviation of lateral position on BCF. Increasing the standard deviation from 0.05 m to1.5 m may increase the BCF by as much as 12 times, indicating that the lateral position is very effective in changing the BCF.

As expected, the fatigue life of flexible pavement is very sensitive to standard deviation of lateral position.

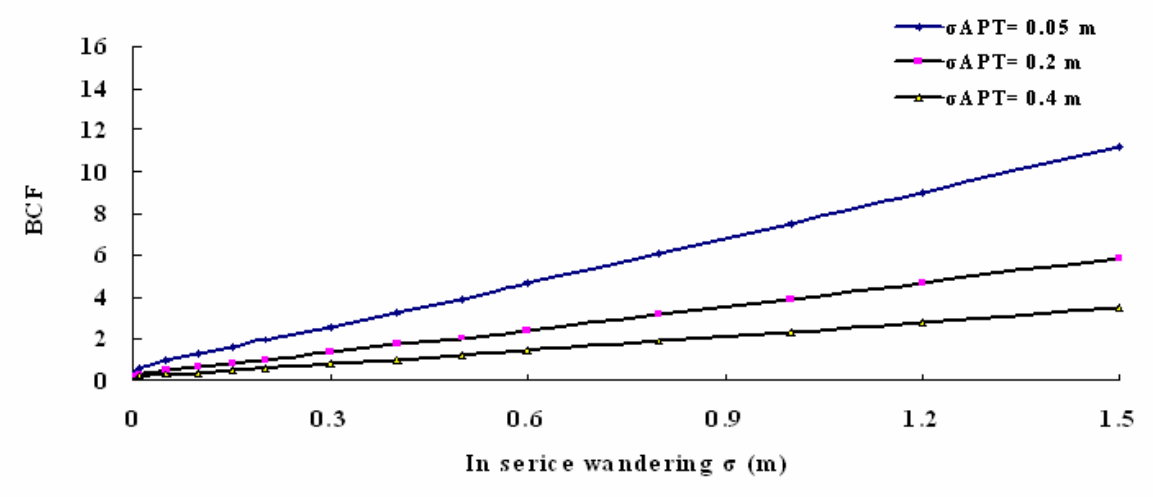

Figure 5.9 Effect of standard deviation of lateral position on BCFs

Chapter 6: Reliability Based Fatigue Life Prediction

6.1 Test Results of the Bias Correction Functions

Based on previously discussed methodology, together with existing pavement structure information, environmental condition records, traffic loading history and pavement performance database, the Bias Correction Function for each of the variables and the marginal shift factor are estimated.

6.1.1 Bias Correction Functions for temperature

The fatigue life of flexible pavement is very sensitive to temperature change. Since the air temperature at different LTPP sites varies hourly, daily, monthly and even yearly (Figure 6.1 through Figure 6.3), it is not possible to use just an average value to represent the in service pavement temperature conditions.

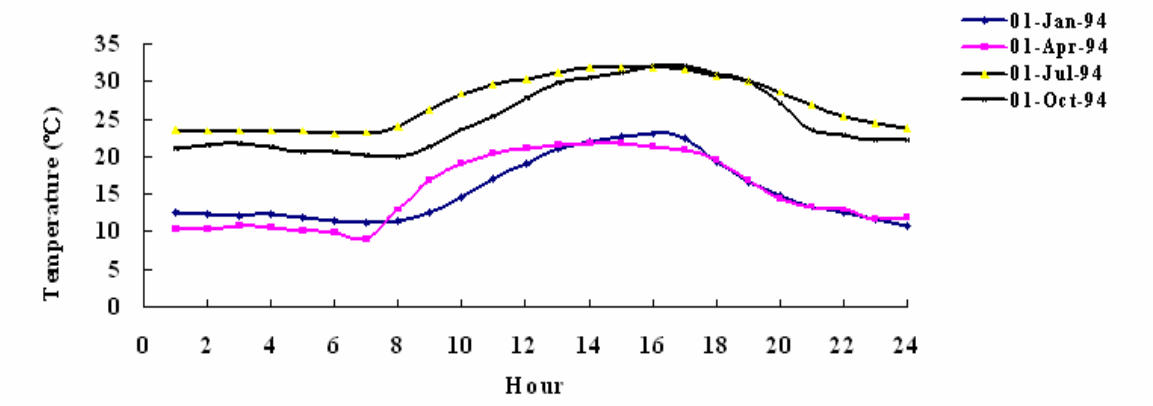

Figure 6.1 Hourly temperature change of LTPP site 48-6160 in different months

Because only a few pavement temperatures of LTPP sites at different depths are recorded (Figure 6.2), there is a need to predict the pavement temperature from available air temperature of special LTPP sites. The Asphalt Institute (AI) model (AI, 1982) relates the mean pavement temperature at depth Z to the mean monthly air temperature by Equation 6.1. The Integrated Climatic Model also predicts asphalt temperature more accurately.

$$T_p = T_a\left(1+\frac{1}{z+4}\right)-\frac{34}{z+4}+6 \qquad (6.1)$$

Where,

T_p = Mean pavement temperature at depth Z, ^oC

T_a = Mean monthly air temperature, ^oC

Z = Depth from surface at which temperature is to be predicted, mm

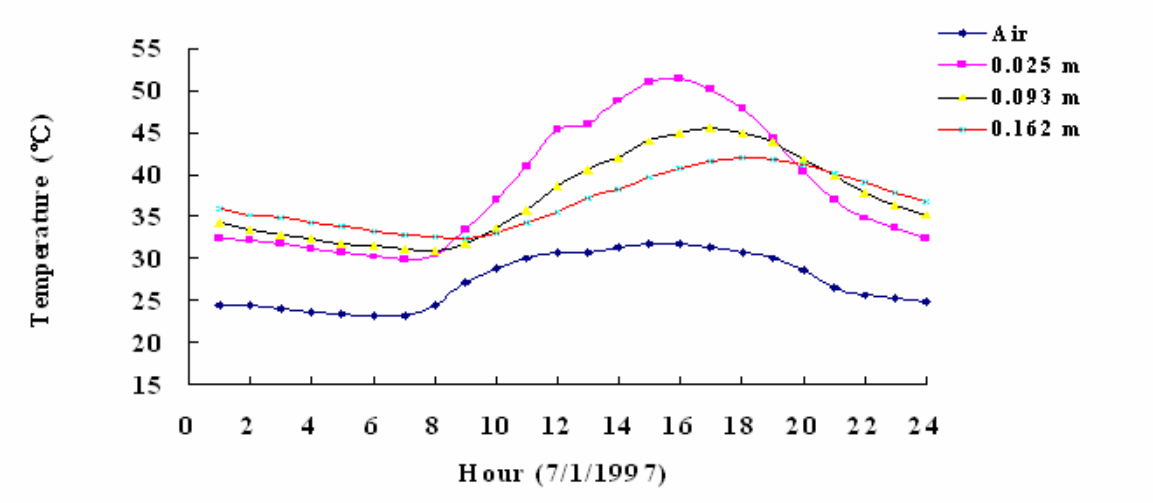

Figure 6.2 Hourly pavement temperature change of LTPP site 48-6160 at different depth

The necessary data are obtained from the operating weather stations (OWS) daily data in the table CLM_VWS_TEMP_DAILY stored offline (part of the LTPP database), in which daily temperature data computed from daily operating station data is recorded on a daily base. For the purposes of this research, daily minimum air temperature and daily maximum air temperature are used to predict the hourly air temperature with the following model:

$$T_i = \left(\frac{T_{\max} + T_{\min}}{2}\right) + \left(\frac{T_{\max} - T_{\min}}{2}\right) \times \sin\left(\frac{i - 10.5}{24} \times 2\pi\right) \qquad (6.2)$$

Hourly air temperature predicted with model 6.2 is a good estimation of real data (Figure 6.3), and any LTPP sites with maximum and minimum daily air temperature records will be able to estimate the hourly change of a day.

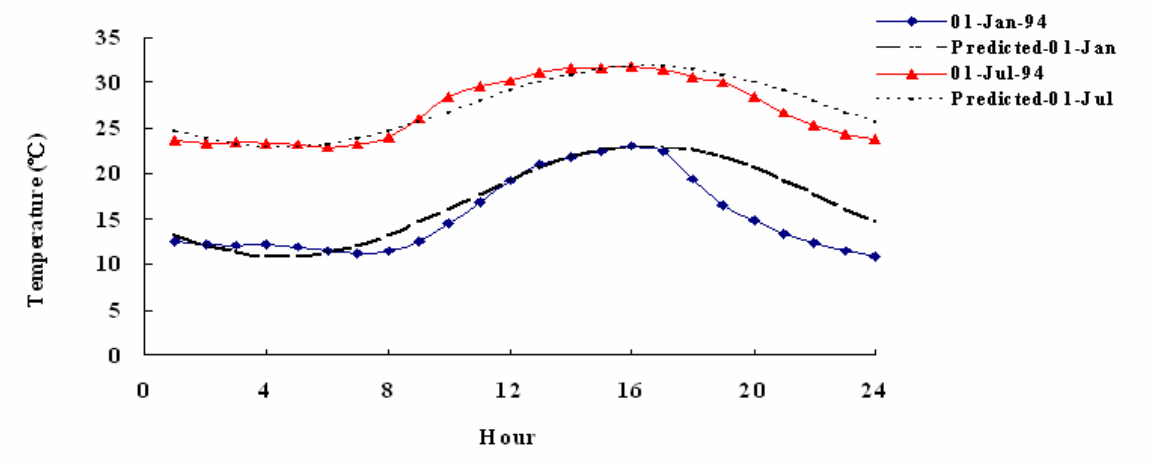

Figure 6.3 Sinusoidal curve fitted to hourly air temperature

Compared to the daily and monthly air temperature change, the variation between

years could be neglected confidently (Figure 6.4). Pavement temperature varies greatly during the year. It is necessary to account for this change and weight the effect of different seasons on pavement performance. To better capture the temperature characteristics of LTPP sites all the time, the Bias Correction Function of temperature becomes a weighted summary of all the hours. According to the general correction functions represented in Equation 5.3 and laboratory four-point fatigue test results, the Bias Correction Function on temperature can be calculated with Equation 6.3.

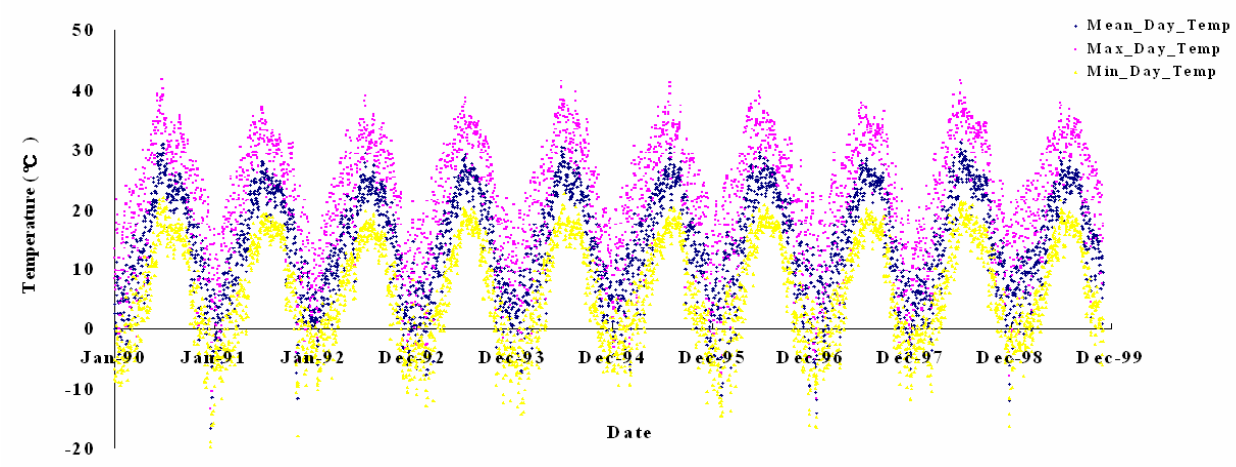

Figure 6.4 A 10-year air temperature record of LTPP site 48-6160

$$BCF_{T} = \frac{365}{\sum_{j=1}^{365}\sum_{i=1}^{24} 10^{-0.0570\,(T_{in.ij} - T_{APT})} \times a_i} \qquad (6.3)$$

Where,

$T_{in.ij}$: Pavement temperature at ith hour of a day and jth day of a year,

a_i: hour truck traffic distribution at ith hour of a year.

Table 6.1 is a summary Bias Correction Functions table of all the selected LTPP sites to different APT temperatures.

Table 6.1 BCF of LTPP sites to different APT temperatures

APT Temp (°C)	LTPP Sites						
	35-0100	37-1030	50-1004	48-6160	23-1009	87-1622	82-6007
10	2.12	3.52	0.78	1.47	0.56	0.32	1.61
19	0.65	1.08	0.24	0.45	0.17	0.10	0.50
28	0.20	0.33	0.07	0.14	0.05	0.03	0.15

6.1.2 Bias Correction Functions for frequency

At the seven LTPP sites selected, free flow conditions can be assumed; therefore, traveling speeds were assumed to be close to the speed limit of each site (rural interstate). Thus, the traffic loading frequency of in-service pavement (F_{in}) is assumed to be constant in this research. In areas subjected to traffic congestion, the change of loading frequency should be considered. Based on the speed limit information of each LTPP site, the loading time (loading frequency) is calculated with Equation 5.6. With loading frequency known, the Bias Correction Function can then be evaluated with Equation 5.9. Table 6.2 is a list of Bias Correction Functions on loading frequency for all seven LTPP sites.

6.1.3 Bias Correction Function for traffic wandering

Since the lateral wandering of APT sections was programmed to simulate the traffic wandering on a typical highway lane, the Bias Correction Function for traffic wandering should be set as one in this research.

Table 6.2 BCFs of LTPP sites to different APT loading speeds

LTPP Sites	Speed (km/h)	Loading time (s)	Loading frequency (Hz)	APT Speed (km/h)	BCFs
23-1009	90	0.014	11.20	9	0.45
82-6007	80	0.016	9.95	9	0.49
87-1622	100	0.013	12.44	9	0.40
37-1030	110	0.012	13.68	17.5	0.40
48-6160	110	0.012	13.68	17.5	0.40
35-0109	105	0.012	13.06	17.5	0.42
50-1004	90	0.014	11.20	17.5	0.49

6.1.4 Bias Correction Functions for rest period

The traffic flow changes hourly and thus the rest periods between traffic loading vary accordingly. Table 6.3 shows the hourly truck traffic distribution default values based on LTPP traffic data. The number of trucks counted within each hour of traffic differs at various times of the day; thus, different loading ratios should be used to account for this effect. Moreover, the Average Annual Daily Truck Traffic (AADTT) changes over years (Figure 6.5), which also effects the rest periods between traffic loading. For a given time period, the greater the amount of traffic, the shorter the rest periods will be. The loading ratio (LR) is assigned at different times of a day according to the hourly truck traffic. Considering the general correction functions represented in Equation 5.3 and dividing a whole day into 24 hour-periods, the Bias Correction Function for loading ratio can be calculated as follows:

$$BCF_{\text{rest period}} = \frac{24n}{\sum_{j=1}^{n}\sum_{i=1}^{24} 10^{-0.011\,(LR_{\text{in.ij}} - LR_{\text{APT}})}} \tag{6.4}$$

Where,

$LR_{in,ij}$: loading ratio of in-service pavement for ith hour of a day and jth year.

n: Years open to traffic.

Table 6.3 Typical hour truck traffic distribution values based on LTPP traffic data (NCHRP, 2006)

Time Period	Distribution (%)	Time Period	Distribution (%)
12:00 a.m. - 1:00 a.m.	2.3	12:00 p.m. - 1:00 p.m.	5.9
1:00 a.m. - 2:00 a.m.	2.3	1:00 p.m. - 2:00 p.m.	5.9
2:00 a.m. - 3:00 a.m.	2.3	2:00 p.m. - 3:00 p.m.	5.9
3:00 a.m. - 4:00 a.m.	2.3	3:00 p.m. - 4:00 p.m.	5.9
4:00 a.m. - 5:00 a.m.	2.3	4:00 p.m. - 5:00 p.m.	4.6
5:00 a.m. - 6:00 a.m.	2.3	5:00 p.m. - 6:00 p.m.	4.6
6:00 a.m. - 7:00 a.m.	5.0	6:00 p.m. - 7:00 p.m.	4.6
7:00 a.m. - 8:00 a.m.	5.0	7:00 p.m. - 8:00 p.m.	4.6
8:00 a.m. - 9:00 a.m.	5.0	8:00 p.m. - 9:00 p.m.	3.1
9:00 a.m. - 10:00 a.m.	5.0	9:00 p.m. - 10:00 p.m.	3.1
10:00 a.m. - 11:00 a.m.	5.9	10:00 p.m. - 11:00 p.m.	3.1
11:00 a.m. - 12:00 p.m.	5.9	11:00 p.m. - 12:00 a.m.	3.1

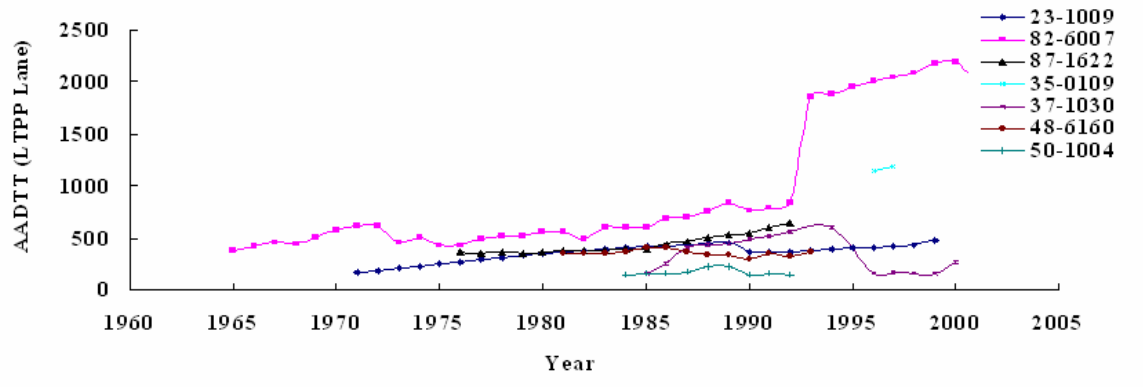

Figure 6.5 Estimated annual average daily number of trucks in the LTPP lane

The minimum rest period is calculated with the maximum AADTT and the busiest hour of a day. In this research, the loading ratios of the seven selected LTPP sites and APT programs are all above 25 and thus a value of 25 is used, as shown in Table 6.4.

Table 6.4 BCFs of LTPP sites to different APT loading ratio

Section	Speed	Loading time (s)		Min rest periods (s)		Loading ratio		BCF
	(km/H)	In-service	APT/ALF	In-service	APT	In-service	APT	
23-1009	90	0.011	0.111	11.20	10.30	>25	>25	1.00
82-6007	80	0.013	0.111	5.00	10.30	>25	>25	1.00
87-1622	100	0.010	0.111	12.50	10.30	>25	>25	1.00
37-1030	110	0.009	0.057	13.90	5.40	>25	>25	1.00
48-6160	110	0.009	0.057	31.30	5.40	>25	>25	1.00
35-0109	105	0.010	0.057	9.80	5.40	>25	>25	1.00
50-1004	90	0.011	0.057	16.80	5.40	>25	>25	1.00

6.1.5 Bias Correction Functions for moisture

The KENLAYER computer program (Huang, 2004) is used to calculate the tensile strain at the bottom of the asphalt layer under the application of a 40 kN dual-tire load having 690 kPa tire pressure and 30 cm (13.5 inches) dual spacing. Pavement layer properties differ from each other at different seasons because of the changes in moisture conditions, and hence the maximum tensile strain in the asphalt layer. The maximum strains obtained are shown in Table 6.4 through Table 6.6, with different layer properties discussed in the following paragraphs; the BCF for moisture can then be calculated with Equation 5.10.

Seasonal variation in elastic modulus of base and subbase layers

The base and subbase layer modulus in LTPP sites are assumed constant throughout

the year, which is valid since these layers are much less affected by moisture variation compared to subgrade soils. In the absence of base and subbase materials data, typical value from AASHTO is used in this research.

Seasonal variation in subgrade resilient modulus

The seasonal variation in no-freeze zone subgrade resilient modulus is expressed with a sinusoidal function as follows (Ali and Parker, 1996):

$$M_R = A + B \sin(2\pi fT + C) \quad (6.5)$$

Where,

M_R: subgrade resilient modulus AC elastic modulus at any season,

A: average value,

B: amplitude value,

T: time of observation,

f: number of increments per cycle (1/12 if months), and

C: phase angle that controls the starting point on the curve and the months.

The seasonal moduli are displayed in Table 6.5 through Table 6.7. The seasonal subgrade resilient modulus cycles of LTPP site 87-1622 and 82-6007 are illustrated in Drumm and Meier's NCHRP report (2003). Information for site 23-1009 is not accessible; thus, a neighbor LTPP site, 23-1026 (within one hundred miles), is set as reference.

Table 6.5 Maximum tensile strains in the asphalt layer matched with CAL/APT

Season (Month)	23-1009 (Wet-freeze)		82-6007 (Wet-no-freeze)		87-1622 (Wet-freeze)	
	Subgrade (MPa)	Strain (10^-6)	Subgrade (MPa)	Strain (10^-6)	Subgrade (MPa)	Strain (10^-6)
January	196	67.84	92	71.83	145	73.27
February	222	67.73	95	71.65	140	73.29
March	153	68.07	92	71.83	250	73.01
April	116	68.34	83	72.4	145	73.27
May	111	68.38	70	73.34	160	73.22
June	127	68.25	58	74.39	160	73.22
July	148	68.1	48	75.43	160	73.22
August	153	68.07	45	75.78	150	73.22
September	148	68.1	48	75.43	155	73.23
October	175	67.94	57	74.48	155	73.23
November	188	67.87	70	73.34	155	73.23
December	201	67.81	82	72.47	160	73.22
APT Strain (10^-6)	66.55		66.55		66.55	
BCFs	0.899		0.617		0.632	

Table 6.6 Maximum tensile strains in the asphalt layer matched with FHWA/ALF Lane 1&2 (10^{-6})

Season (Month)	37-1030 (Wet-no-freeze)				48-6160 (Dry-freeze)			
	Subgrade (MPa)	10 °C	19 °C	28 °C	Subgrade (MPa)	10 °C	19 °C	28 °C
Jan	115	96.77	121.70	146.20	124	80.71	100.30	119.90
Feb	113	97.09	122.10	146.60	121	80.83	100.50	120.00
Mar	107	98.09	123.30	148.00	112	81.23	100.80	120.30
Apr	102	98.98	124.40	149.20	102	81.71	101.20	120.50
May	94	100.50	126.20	151.30	94	82.14	101.60	120.80
Jun	86	102.20	128.30	153.50	78	83.14	102.50	121.40
Jul	82	103.10	129.40	154.80	83	82.80	102.20	121.20
Aug	84	102.60	128.80	154.10	84	82.74	102.20	121.20
Sep	90	101.30	127.20	152.40	87	82.55	102.00	121.10
Oct	96	100.10	125.80	150.70	101	81.76	101.30	120.60
Nov	109	97.75	122.90	147.50	111	81.27	100.80	120.30
Dec	113	97.09	122.10	146.60	128	80.55	100.20	119.80
APT Strain (10^-6)		187.10	243.50	309.60		187.10	243.50	309.60
BCFs		20.50	24.27	32.21		53.05	67.30	92.35

Table 6.7 Maximum tensile strains in the asphalt layer matched with FHWA/ALF Lane 3&4 (10^-6)

Season (Month)	35-0109 (Dry-no-freeze)				50-1004 (Wet-freeze)			
	Subgrade (MPa)	10 °C	19 °C	28 °C	Subgrade (MPa)	10 °C	19 °C	28 °C
Jan	106	43.12	57.85	74.54	179	54.76	71.43	90.77
Feb	105	43.16	57.89	74.59	186	54.75	71.43	90.77
Mar	93	43.64	58.47	75.23	173	54.77	71.44	90.76
Apr	84	44.06	58.97	75.79	150	54.83	71.45	90.72
May	80	44.26	59.21	76.06	139	54.86	71.47	90.71
Jun	68	44.95	60.04	76.97	123	54.90	71.48	90.68
Jul	72	44.70	59.75	76.65	117	54.92	71.49	90.66
Aug	75	44.53	59.54	76.42	117	54.92	71.49	90.66
Sep	75	44.53	59.54	76.42	130	54.88	71.47	90.69
Oct	86	43.96	58.85	75.66	144	54.84	71.46	90.72
Nov	95	43.55	58.37	75.12	160	54.80	71.45	90.74
Dec	105	43.16	57.89	74.59	177	54.77	71.43	90.76
APT Strain (10^-6)		80.11	109.30	146.30		80.11	109.30	146.30
BCFs		17.78	19.47	23.65		6.17	7.69	9.91

Table 6.8 Summary table of Bias Correction Functions

Machine	Section (Site)	LTPP	BCF (Temp)	BCF (Freq)	BCF (Strain)	BCF (Wander)	BCF (Rest)	BCFs
CAL/APT	501RF/503RF	23-1009	0.17	0.45	0.90	1.00	1.00	0.07
CAL/APT	501RF/503RF	82-6007	0.50	0.49	0.62	1.00	1.00	0.15
CAL/APT	501RF/503RF	87-1622	0.10	0.40	0.63	1.00	1.00	0.02
FHWA/ALF	3_1/4_1	35_0109	0.20	0.42	23.65	1.00	1.00	1.98
FHWA/ALF	3_2/4_2	35_0109	0.65	0.42	19.47	1.00	1.00	5.29
FHWA/ALF	1_1/2_1	37_1030	0.33	0.40	21.03	1.00	1.00	2.76
FHWA/ALF	1_3/2_3	37_1030	1.08	0.40	16.43	1.00	1.00	7.06
FHWA/ALF	1_4/2_4	37_1030	3.52	0.40	14.18	1.00	1.00	19.85
FHWA/ALF	1_1/2_1	48_6160	0.14	0.40	52.47	1.00	1.00	2.92
FHWA/ALF	1_3/2_3	48_6160	0.45	0.40	67.30	1.00	1.00	12.05
FHWA/ALF	1_4/2_4	48_6160	1.47	0.40	32.36	1.00	1.00	18.92
FHWA/ALF	3_1/4_1	50_1004	0.07	0.49	9.91	1.00	1.00	0.34
FHWA/ALF	3_2/4_2	50_1004	0.24	0.49	7.69	1.00	1.00	0.90

Table 6.8 is a summary of all the Bias Correction Functions including the effects of temperature, travel speed, traffic wandering, moisture condition and rest periods.

6.2 Marginal Shift Factor (M)

The marginal shift factor M to account for all other unquantifiable differences is developed by combing APT and LTPP datasets. APT recorded the crack length under different load repetitions while LTPP records the area. Since the fatigue distress recording systems of APT and LTPP differ from each other, there is a need to standardize the test results to make them compatible. The Damage Ratio (DR) concept is used in this research, which is defined as the ratio of total crack length to the maximum crack length when the whole area is cracked. According to LTPP distress identification manual, the crack length of a fatigue area is usually less than 0.3 meters (FHWA, 2003). Accordingly, the DR is defined as 100% when the cracked area is comprised of less than 0.3 meters cracks (Figure 6.6).

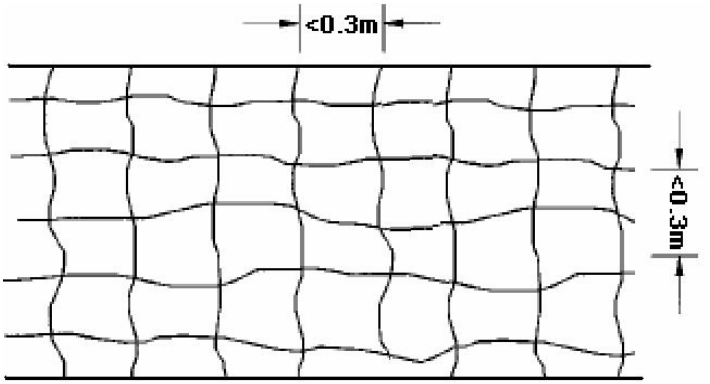

Figure 6.6 Definition of a fully damaged fatigue cracking area
(DR=1, crack density = 6.7m/m^2 correspondingly)

In this research, the differences between APT and LTPP sites are captured by the addressed variables. To account for all unquantifiable differences (such as aging) between the performance of the pavement site under APT and in-service conditions, the margin of shift factor M is calibrated by combining data sets as shown in Equation 3.2, M will be calculated explicitly using the equation developed earlier:

$$\log(M) = \log(F) - \log(A \times B) \tag{6.6}$$

The APT performance data provide the distribution of log (A), while the data from LTPP will provide the distribution of log (F). With the previously-mentioned log-normal assumptions, the prediction error is a normal random variable with mean equal to zero, together with the calculated B, margin of shift factor M is calibrated by means of constrained regression analysis between log (F) and log (A×B). As shown in Figure 6.7, when the coefficient before log (A×B) is constrained as 1, the intercept (constant part of this regression) represents the expected value of log (M). If it is statistically significantly different from zero, the marginal shift factor is necessary and can only be released when all variables to account for the difference are included. In other words, M can be calculated by minimizing the squared differences between Log (A×B) and Log (F).

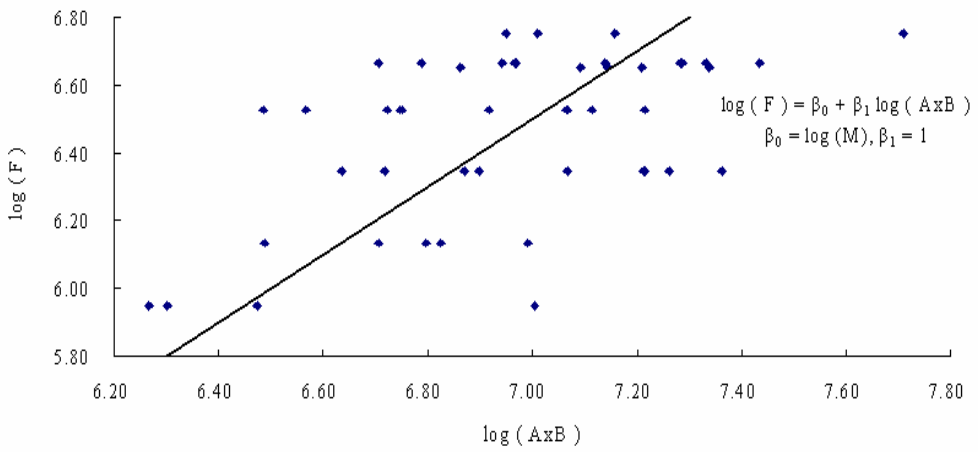

Figure 6.7 Constrained regressions on marginal shift factor M

Table 6.9 presents the load repetitions (ESALs) of CAL/APT and FHWA/ALF to different damage levels (damage ratio) of area cracked. Associated with that, load repetitions of selected LTPP sites are collected at the same fatigue cracking level. It should be noted that the accumulated load repetitions are not proportional to fatigue cracking level, so the calibrated marginal shift M may be different according to different failure criteria.

With the constrained regression analysis between log (F) and log (A×B), the estimated intercept is 0.191. Then, the margin of shift, M, is estimated as 1.552 (i.e. $10^{0.191}$) when 45% area cracked ($3m/m^2$) is set as the failure criterion. This means that despite the quantified differences, the APT program tends to predict shorter pavement fatigue life. The fatigue performance of pavement is underestimated and this marginal shift factor M should be included.

Table 6.9 Load repetitions (in ESALs) of LTPP and APT at different DR

APT/LTPP/SITES	Damage Ratio					
	0.5	0.4	0.3	0.2	0.1	0.05
CAL/APT_501RF2-3	12,528,248	12,528,248	5,063,585	2,902,319	1,120,815	432,835
CAL/APT_501RF3-4	10,379,757	10,379,757	2,305,097	1,155,491	354,850	108,974
CAL/APT_501RF4-5	19,030,030	19,030,030	17,470,782	12,876,036	7,642,235	4,535,849
CAL/APT_501RF5-6	18,972,759	18,972,759	11,603,217	7,405,595	3,436,954	1,595,098
CAL/APT_501RF6-7	17,893,847	17,893,847	15,622,036	11,076,693	6,153,654	3,418,661
CAL/APT_503RF2-3	41,873,714	39,613,944	31,998,384	25,846,872	17,943,288	12,456,501
CAL/APT_503RF3-4	56,952,197	55,470,636	50,119,840	45,285,192	38,075,562	32,013,741
CAL/APT_503RF4-5	47,185,278	44,068,806	33,878,981	26,045,301	16,615,047	10,599,217
CAL/APT_503RF5-6	42,493,076	39,202,408	28,747,448	21,080,739	12,404,854	7,299,574
CAL/APT_503RF6-7	34,263,741	28,075,370	13,043,876	6,060,212	1,634,404	440,789
FHWA/ALF_1_1	795,750	774,337	64,688	603,191	548,575	496,404
FHWA/ALF_1_4	109,232	101,081	74,210	69,710	65,213	62,964
FHWA/ALF_2_1	606,538	589,700	539,188	505,513	386,118	271,402
FHWA/ALF_2_3	183,321	140,209	103,748	88,928	65,213	48,910
FHWA/ALF_2_4	163,720	158,571	143,126	13,163	122,533	117,384
FHWA/ALF_3_1	1,214,526	1,191,863	1,123,877	1,078,553	1,033,229	1,010,567
FHWA/ALF_3_2	562,728	496,989	240,845	199,675	154,955	118,236
FHWA/ALF_4_1	2,008,679	1,922,249	1,645,450	1,533,542	1,223,202	1,184,012
FHWA/ALF_4_2	2,693,934	2,499,846	1,917,584	1,378,201	729,202	658,738
LTPP_23-1009	5,173,655	4,656,290	3,104,193	2,069,462	1,034,731	517,366
LTPP_35_0109	5,785,360	5,679,378	5,289,321	4,926,053	4,361,880	3,862,321
LTPP_37_1030	1,379,630	1,367,118	1,320,014	1,274,534	1,200,384	1,130,548
LTPP_48_6160	4,578,003	4,524,624	4,324,947	4,134,081	3,827,097	3,542,909
LTPP_50_1004	995,544	895,990	597,327	398,218	199,109	99,554
LTPP_82-6007	2,246,999	2,239,720	2,211,926	2,184,478	2,138,340	2,093,178
LTPP_87-1622	3,455,588	3,376,668	3,089,410	2,826,590	2,428,028	2,085,666

6.3 Reliability Based Fatigue Life Prediction

The prediction error is then given by:

$$\log(\varepsilon_i) = \log(F_i) - \log(A_i \times B_i) - \log(M) \tag{6.7}$$

Figure 6.8 is the histogram of log(εi). It is chosen to perform an Anderson-Darling test for normality, which is a test based on the empirical cumulative distribution function (Anderson and Darling, 1952). A P-value larger than 0.05 will fail to reject the null hypothesis that the log(εi) follows normal distribution at a 95% confidence level (Figure 6.9). Thus the distribution of the error term can be evaluated with existing database, which is as follows:

$$\log(\varepsilon) \approx N\left(0, 0.265^2\right) \tag{6.8}$$

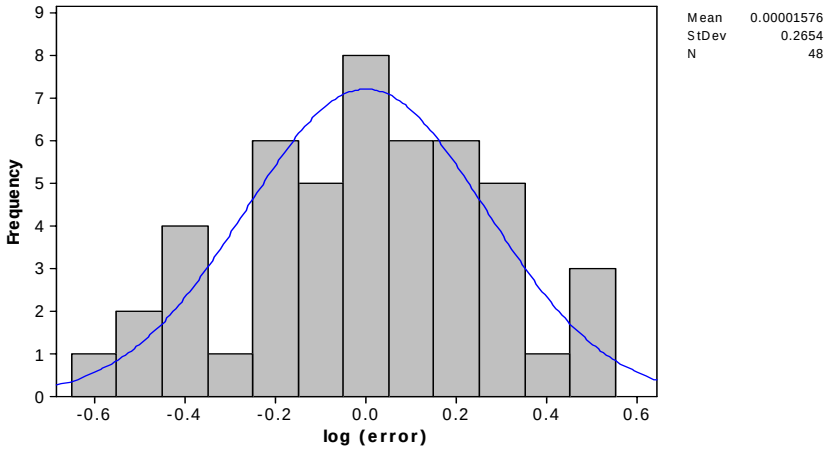

Figure 6.8 Histogram of log (ε_i)

The equation for fatigue life prediction is now updated as follows:

$$\log(W_T) = -Z_R \times 0.265 + \log(A \times B) + 0.161 \qquad (6.9)$$

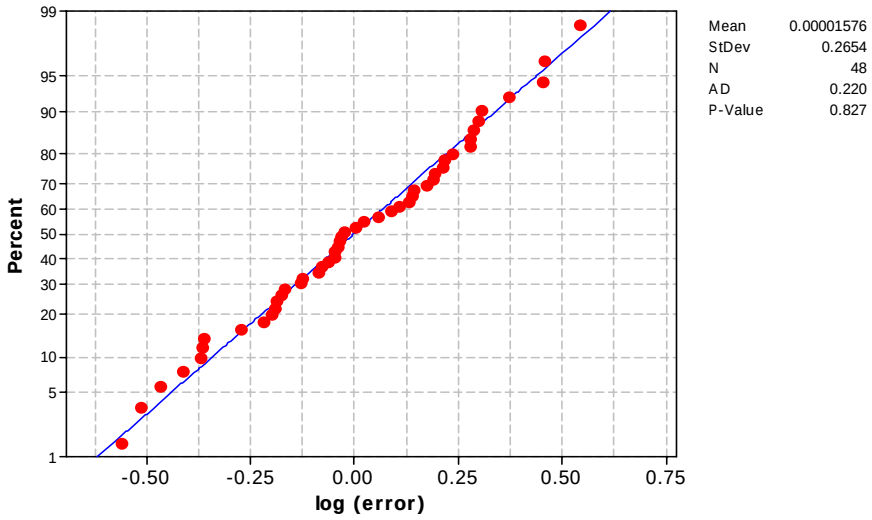

Figure 6.9 Probability plot of log (ε_i)

The reliability of the performance prediction is evaluated as the normal deviate Z_R, which is determined from standard normal probabilities table and, more conveniently, from Table 6.10.

Table 6.10 Standard normal deviate for various levels of reliability

Reliability (%)	Standard normal deviate (Z_R)	Reliability (%)	Standard normal deviate (Z_R)
50	0	92	1.405
55	0.126	93	1.476
60	0.253	94	1.555
65	0.385	95	1.645
70	0.524	96	1.751
75	0.674	97	1.881
80	0.842	98	2.054
85	1.036	99	2.326
90	1.282	99.5	2.576
91	1.341	99.9	3.09

Chapter 7: Validation of the Fatigue Life Prediction

7.1 Principles of Validation

The proposed approach should be validated using different dataset to examine the predictive capacity and accuracy. Comparison of the model distress predictions to observed distress were made by applying the following steps: (1) assemble a database of in-service pavements and test sites, containing information regarding design, material, construction, climate, traffic, and measure pavement distress in the form of fatigue cracking; (2) for each test pavement, run the distress model using the data assembled in step 1; and (3) compare the predicted distress to measured distress from the in-service test sections and evaluate the predictive capacity and accuracy of the model.

The predictive capacity and accuracy of the distress model was evaluated using statistical analysis as follows: (1) determine the correlation between predicted and measured distress (R^2); (2) determine the residual error between predicted and measured distress (mean square error, MSE); and (3) use paired t-test to determine whether there is a significant difference on average between measured and predicted distress for the in-service pavements analyzed.

7.2 Data Gathering and Processing

A dataset different from that used for methodology development was prepared for the validation of fatigue life prediction. A comprehensive search and review of publications documenting the performance of in-field and in-service pavements was the first task undertaken to conduct this study. Several studies, implementation projects and investigation programs were identified as potential sources of data. Based on the type, quality and potential usage of the data available, two programs were considered for inclusion in this study. Details of each of these programs are presented in the following sections.

7.2.1 APT Performance Data (FHWA/ALF)

In 2002, twelve lanes of full scale pavement were constructed at the FHWA's pavement testing facility to study the performance of Superpave mixtures containing modified asphalt binders. Lane 2 used unmodified asphalt binder, and this lane served as the control reference section. For this research, test results pertaining to FHWA/ALF lane 2 site 3 were utilized. Details of the structural and material properties of these test sections can be found in Figure 7.1. Additional information can be found in Qi et al. (2004).

The progressive cracking patterns in terms of the cracked area are shown in Figure 7.2.

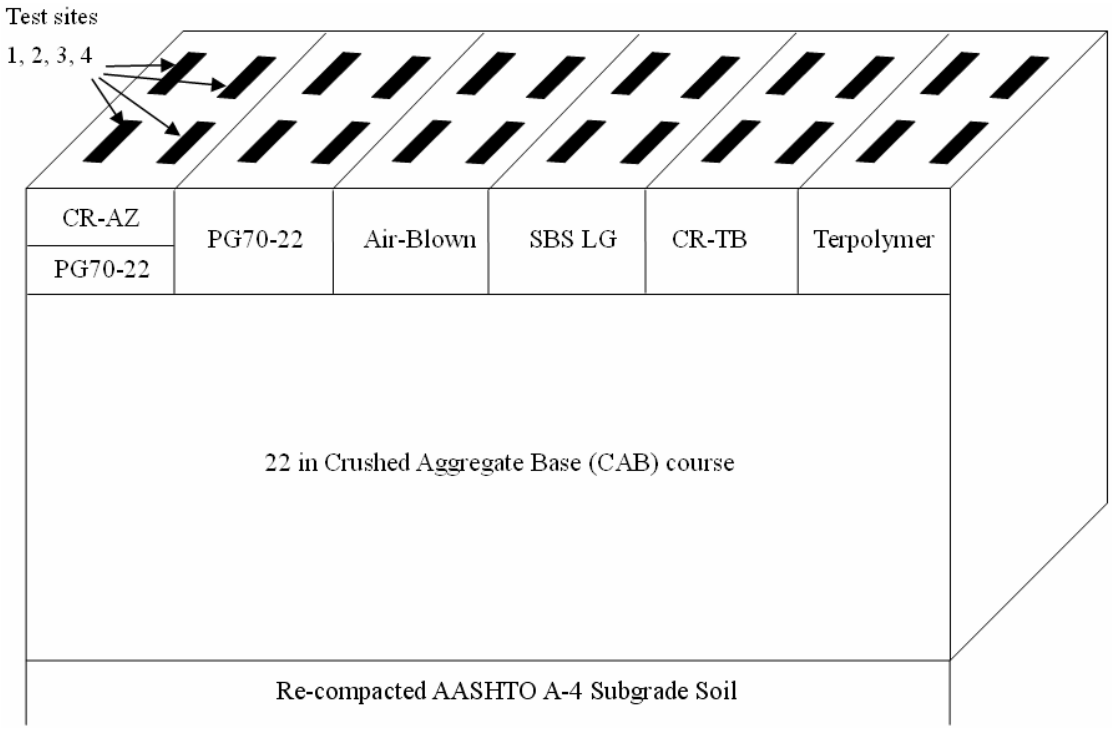

Figure 7.1 Layout of part of the 12 pavement test lanes

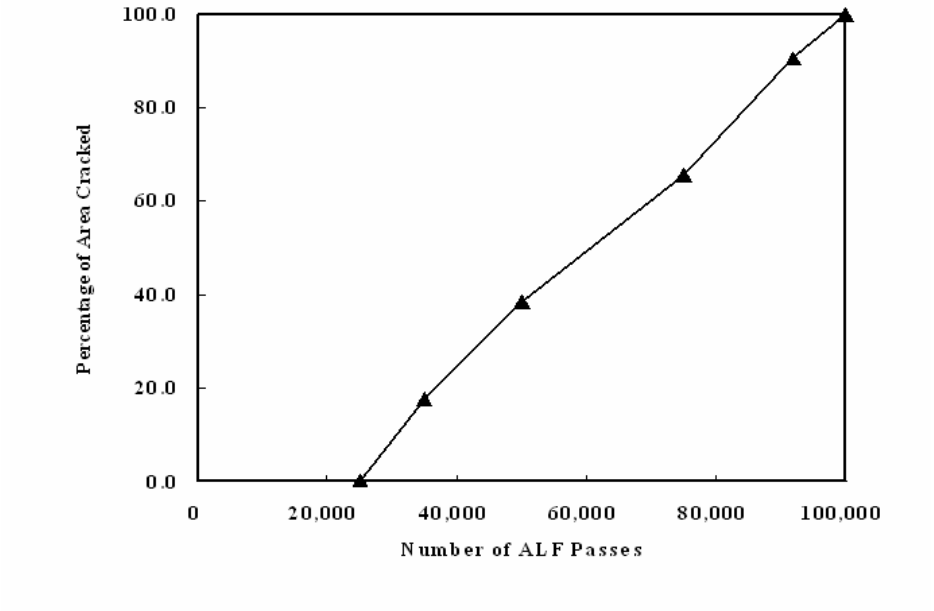

Figure 7.2 Performance fatigue data corresponding to Lane 2 site 3

7.2.2 In-service pavement performance data

The main source for in-service pavement data selected to conduct the validation was the Long Term Pavement Performance database (LTPP). The LTPP database is part of a comprehensive program established by the Strategic Highway Research Program designed specifically to investigate the long-term performance of various pavement structures, both new and rehabilitated, subject to different loads, environments, subgrade soils, and maintenance practices. This thorough program consists of over 2,400 pavement test sections of in-service, new and rehabilitated pavements located across the United States, Canada and Puerto Rico. These pavement sections are classified in the LTPP program as General Pavement Studies (GPS) or Specific Pavement Studies (SPS). Essentially, the main difference between them is that the GPS test sections are existing pavements at the start of the program and the SPS test sections are newly constructed sections or existing pavement sections subject to maintenance or rehabilitation treatments. Regardless of what experiment classification a test section pertains to, similar data is housed within the database. This data includes original construction data, inventory data, material data, performance data and climatic information.

As one of the main LTPP products, the LTPP DataPave Online web-page provides fast and easy means for navigating the complex structure of the LTPP relational database. One of the principal advantages of this database management system is that it allowed the generation of summary reports of the pavement information. In addition, in order to obtain the latest updates of the data, performance data was retrieved from the LTPP

standard data release version 21.0. For the purpose of this study, only data pertaining to new flexible pavements with asphalt concrete (AC) thicknesses ranging from 4.0 to 4.2 inches that were not subject to any major maintenance or rehabilitation treatment were used.

According to the as-built pavement information of the control sections, and considering the availability of the performance data, five similar in-service pavement sites with 4.1 inches (±5%) of asphalt concrete (AC) surface layer are selected from LTPP database (Table7.1). Figure 7.3 is a display of all these selected sites.

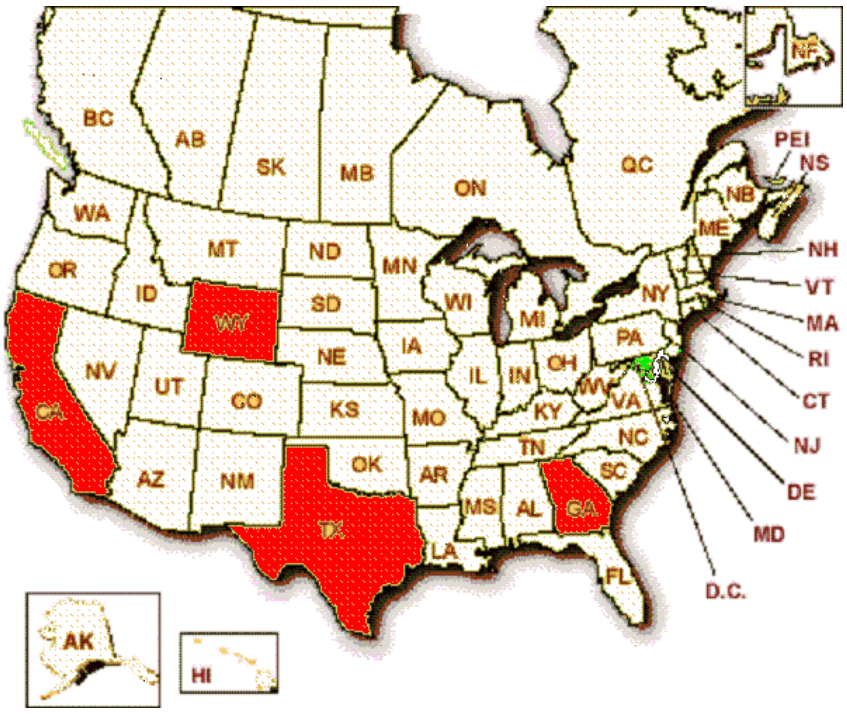

Figure 7.3 LTPP sites selected for approach validation

Table 7.1 Selected LTPP sites match FHWALF program

SHRP_ID	State_Code	Region	Climatic	Layer information	Thickness (Inches)
7454	California (06)	Western	Dry No Freeze	Seal Coat (AC) Original Surface Layer (AC) Base Layer (GB) Subgrade (SS)	0. 1 4 16.2
8153	California (06)	Western	Wet No Freeze	Seal Coat (AC) Original Surface Layer (AC) Base Layer (GB) Subbase Layer (GS) Subbase Layer (GS) Subgrade (SS) Inch	0.3 3.8 6.2 12 6
4096	Georgia (13)	Southern	Wet No Freeze	Original Surface Layer (AC) AC Layer Below Surface (AC) Base Layer (TB) Subgrade (SS) Inch	1.3 2.8 6.3
3609	Texas (48)	Southern	Wet No Freeze	Seal Coat (AC) Original Surface Layer (AC) AC Layer Below Surface (AC) Base Layer (GB) Subgrade (SS)	0.3 1.6 2.3 6.6
3669	Texas (48)	Southern	Wet No Freeze	Original Surface Layer (AC) AC Layer Below Surface (AC) Base Layer (TB) Subbase Layer (TS) Subgrade (SS) Inch	1.5 2.7 8 7.9

7.3 Verification and Validation Analysis of the Proposed Fatigue Life Prediction

In order to check the prediction accuracy of the aforementioned model, a verification and validation study was conducted. For this study, verification and validation were defined as follows:

1) Verification is a process by which the model service-life predictions are compared to observed traffic counts of similar in-service pavements.
2) Validation is ensuring that the model within its domain of applicability possesses a satisfactory range of accuracy consistent with the intended application of the model.

Table 7.2 is a summary table of the predictions. The specification process of all the Bias Correction Functions is included, together with the proposed marginal shift factor M, the predicted fatigue lives of the five LTPP sites based on ALF test results are calculated. The last column, "Predicted/Observed", gives the ratios of predicted over observed, which is a symbol of prediction accuracy.

Table 7.2 Summary table of the fatigue life prediction

STATE CODE	SHRP ID	log (ESALs) at 0.45 DR	Bias Correction Functions					Predicted (Log A×B×M)	Predicted/ Observed
			Temp	Frequency	Moisture	Loading	Wander		
6	7454	5.45	0.79	0.49	1.33	1	1	5.45	1
6	8153	5.9	1.01	0.49	1.06	1	1	5.45	0.92
13	4096	5.03	1.61	0.6	1.01	1	1	5.73	1.14
48	3609	5.89	0.66	0.38	1.07	1	1	5.17	0.88
48	3669	6.03	1.31	0.44	4.56	1	1	6.16	1.02

A statistical verification was conducted to assess the predictive capacity of the model. Results of the statistical analysis are presented in Table 7.3 and Figure 7.4. An analysis of Figure 7.4 shows that there was an adequate correlation between predicted and observed load traffic repetitions. A one-to-one line is included on the graph. Figure

7.4 also shows that the model does not have a bias towards under predicting or over predicting service-life.

Table 7.3 Summary statistics for the measured and predicted traffic*

	Observed	Predicted
Mean	5.660	5.592
Variance	0.172	0.140
Observations	5	5
Hypothesized Mean Difference	0	
df	4	
t Stat	0.276	
P(T<=t) one-tail	0.398	
t Critical one-tail	2.132	
P(T<=t) two-tail	0.796	
t Critical two-tail	2.776	

*t-Test: Paired Two Sample for Means

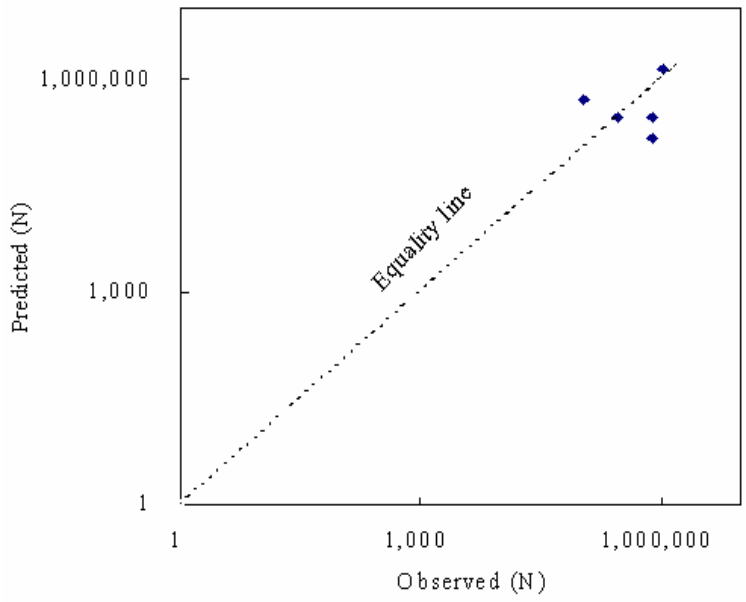

Figure 7.4 Plot of observed vs. predicted number of ESALs

Furthermore, an analysis of the summary statistics proves that the null hypothesis that the average of the differences between the paired observations is zero could not be rejected.

The proposed approach for fatigue life prediction is valid.

Chapter 8: Summary, Conclusions and Future Work

8.1 Summary

The main objective of this research is to analyze and quantify the difference between APT and in-service pavements and their impacts on the overall pavement fatigue life. To achieve this objective, a methodology framework for using results for APT to predict the life of in-service pavements has been presented. The methodology proposed in this research is generic, independent of facility, conditions or environment. However, it has been initially calibrated for the specific set of data available at this time, (Caltrans APT programs, FHWA's ALF program and LTPP Studies). By applying this methodology, APT performance results from a structure similar to an in-service structure can be used to run limited third-point bending tests and computer simulations in order to obtain an accurate estimate of the necessary Bias Correction Factors to estimate in-service performance. This methodology represents a significant improvement on the current state-of-practice and enables more accurate pavement performance predictions. The methodology enables not only the estimation of mean expected performance but also its expected variability (standard deviation), thus facilitating the implementation of reliability-based predictions and the incorporation of risk.

8.2 Conclusions

From the results of tests and associated analyses, the following preliminary conclusions have been established. It is expected that these conclusions may change as further data are incorporated into the analysis. The LTPP program will end in 2009 and as the final database is compiled, there will be an invaluable opportunity to enhance and validate the models developed in this dissertation. The work on this regard is not complete but this methodology represents an important step in the right direction. To date, the most significant findings can be summarized as follows:

1) Some of the important factors that help to explain the differences between the performance of APT sites and LTPP sites have been recognized and evaluated. These factors include: loading frequency (loading speed), loading ratio (rest period), traffic wandering, seasonal moisture change, and pavement temperature. The factors are individually assessed instead of being aggregated into one "shift factor" as is generally done.

2) Based on laboratory third-point beam fatigue test results, a general model relating pavement temperature and loading frequency to the difference of fatigue life between APT and in-service pavement was developed. The model shows that pavement temperature contributes the most to the difference. The most significant advantage of this model is that it is based on the observed fatigue life in the

laboratory as opposed to current models that estimate life based on the dynamic modulus. In addition, dynamic stiffness is preferred because it correlates closely to fatigue performance.

3) Heavier and faster traffic has been proven to have a negative impact on pavement performance, reducing the fatigue life. A heavier truck generates larger strains at the bottom of the asphalt layer, thus resulting in shorter fatigue life. According to these preliminary results, higher loading frequency (all else being equal) results in higher material stiffness and, therefore, in higher stress levels and shorter fatigue lives under the strain-controlled test. It should be noted that these results apply to thin asphalt structures (asphalt surface on granular base); however, the results may be opposite for full-depth asphalts (asphalt surface and asphalt base). The evaluation of thick asphalt layers was out of the scope of the current dissertation because of the lack of APT and field data. These findings are practical for pavements in use in Texas; the pavement life would be greatly shortened due to heavy and high speed traffic.

4) Traffic-induced pavement strains vary with the modulus of various pavement layers. The effect of differential moisture conditions between APT and in-service pavements relates primarily to the loss of support of the asphalt concrete base or surface and the consequential increase in tensile strains for the same applied wheel loads. For the same applied wheel loads, the tensile strains at the bottom of

asphalt concrete layer may increase significantly due to the loss of support from subgrade. The results show that the seasonal water content variations of subgrade affect the estimation of pavement fatigue life conditionally: the poorer the pavement structure, the greater the effect will be.

5) Rest periods have been proven to have a beneficial effect on pavement fatigue life. Rest periods in an APT experiment are shorter than those occurring on actual highways, resulting in a longer fatigue life of in-service pavement for the same traffic volume. The benefits seem to reach a maximum when the rest period equals to 25 times the load cycle. Unfortunately, for the cases studied, the loading ratios were larger than 25, and therefore the corresponding BCF were similar. The methodology, however, allows the determination when the loading ratios in the field are variable. This can be assessed by including urban highways where traffic congestion will cause differential loading ratio during the day.

6) Because of the inability to quantify all variables that affect the differences of overall pavement fatigue life between APT and in-service pavement, a marginal shift factor, M, should be introduced at this time. For the cases studied, this factor was estimated as 1.552. This research represents a significant improvement on pavement performance prediction. This marginal shift cannot be ignored and will only be released in the future when all the differences are taken into account. The

APT sections tend to present shorter pavement fatigue life and the fatigue performance of pavement is underestimated.

7) Sensitivity analyses were performed to numerically determine the effects of temperature, loading speed, lateral wander, rest period and subgrade moisture content. The fatigue life of flexible pavement is very sensitive to temperature change. On average, and for the cases studied in this dissertation, the following conclusions are valid:
   a) Increasing the temperature from -10 ℃ to 10℃ will result in fatigue life extension by as much as 14 times, indicating that the fatigue life of flexible pavement is very sensitive to temperature change.
   b) One km/hour increase of driving speed will result in about 1% decrease of pavement fatigue life based on this research.
   c) A unity increase of the loading ratio results in an increase of 2.6% of pavement fatigue life on average but this beneficial effect reaches a maximum when the loading ratio reaches 25.
   d) Increasing the standard deviation of lateral wandering from 0.05 m to1.5 m may increase the fatigue life by as much as 12 times, indicating that the fatigue life of flexible pavement is very sensitive to standard deviation of lateral position.
   e) Validation process proved that the proposed approach for fatigue life prediction is valid.

8.3 Methodology Limitations and Further Research

Due to the lack of data, there is a main difference between APT and in service pavements not addressed in this research, which contributes the most to the marginal shift factor M. The difference not addressed is material aging properties of in service pavement. This aspect has effect on pavement fatigue performance and should be calibrated into future work.

Appendix A: Specification of the Bias Correction Functions

A.1 Specification of General Bias Correction Function

All these correction functions are aimed at capturing the overall differential effect of the specified variable between in-service pavements and similar pavements subjected to APT, which is represented by the ratio of the expected performance of the mixes under the conditions in the field over the expected performance of the mixes under APT conditions, as in Equation A.1.

$$BCF_{generic} = \frac{N_f^{in}}{N_f^{APT}} = \frac{D_f^{APT}}{D_f^{in}} \quad \text{(A.1)}$$

Since the variable of interest may be in different levels (under different conditions), and under different loading and environmental conditions pavement structure performs differently, there is a need to account for the overall damage under all the levels. Miner's law was used in the development of the Bias Correction Functions. To account for the difference and the overall damage ascended, a particularly convenient form known as Linear Cumulative Damage (Miner's law) was proposed. The life of a pavement experiencing fatigue at various situations can be assessed through the cumulative damage (D) as follows:

$$BCF_{generic} = \frac{\int D(APT)\, f(x_{APT})\, dx_{APT}}{\int D(in)\, f(x_{in})\, dx_{in}} \quad \text{(A.2)}$$

Given that the fatigue life of a pavement structure under condition $x_{in.i}$ is $g(x_{in.i}^{a})$, the damage of one pass of traffic loading to pavement structure from condition x_i can be expressed as:

$$\text{Damage of one pass from condition } x_{in.i} = D_{in.i} = \frac{1}{g(x_{in.i}^{a})} \tag{A.3}$$

Where,

x_{in}: variable of interest under in-service conditions,

α: parameter that reflects the sensitivity of a particular process to a change in the level of variable x. This parameter represents the order of the moment,

g(x): fatigue life as a function of variable x, and

Provided the portion in condition $x_{in.i}$ is $f(x_{in.i})$, the overall damage of one pass of traffic loading to pavement structure from all conditions can be expressed as the summary of all the damages:

$$\text{Damage of one pass} = \int \frac{1 \times f(x_{in.i})}{g(x_{in.i}^{a})} dx_{in.i}$$

$$= \int [g(x_{in.i}^{a})]^{-1} f(x_{in.i}) dx_{in.i} \tag{A.4}$$

So the fatigue life of a pavement structure under all conditions is the reciprocal of the overall damage of one pass of traffic loading:

$$N_{in} = \frac{1}{\int [g(x_{in.i}^{a})]^{-1} f(x_{in.i}) dx_{in.i}} \tag{A.5}$$

In principle, this Bias Correction Function is the ratio of the expected performance of the pavement structure under the conditions in the field over the expected performance of the pavement structure under APT conditions, therefore,

$$BCF_{generic} = \frac{\frac{1}{\int [g(x_{in.i}^{a})]^{-1} f(x_{in.i}) dx_{in.i}}}{\frac{1}{\int [g(x_{APT}^{\alpha})]^{-1} f(x_{APT}) dx_{APT}}} = \frac{\int [g(x_{APT}^{\alpha})]^{-1} f(x_{APT}) dx_{APT}}{\int [g(x_{in.i}^{a})]^{-1} f(x_{in.i}) dx_{in.i}} \quad \text{(A.6)}$$

If the portion in condition x_i is given as probability mass function $p(x_{in.i})$ and the condition of a controlled APT is uniform, the Bias Correction Function can then be simplified as:

$$BCF_{generic} = \frac{\sum_{J=1}^{m} [g(x_{APT}^{a})]^{-1} p(x_{APT,J})}{\sum_{I=1}^{n} [g(x_{in.i}^{\alpha})]^{-1} p(x_{in.i})} \quad \text{(A.7)}$$

A.2 Specification of Bias Correction Function for Moisture

The change of subgrade moisture content relates primarily to the variation of the strength of the subgrade and, therefore, to the bottom tensile strains of asphalt concrete layer. The fatigue life as a function of the bottom tensile strains can be expressed as:

$$N_f = k_1 \varepsilon^{-4.8} \quad \text{(A.8)}$$

And based on the general form the Bias Correction Function for Moisture is**:**

$$BCF_{moisture} = \frac{[g(x^{\alpha}_{APT})]^{-1}}{\sum_{I=1}^{n}[g(x^{\alpha}_{in.i})]^{-1} p(x_{in.i})} = \frac{[k_1 \varepsilon^{-4.8}_{APT}]^{-1}}{\sum_{I=1}^{n}[k_1 \varepsilon^{-4.8}_{in,i}]^{-1} p(x_{in.i})} = \frac{\varepsilon^{4.8}_{APT}}{\sum_{I=1}^{n} \varepsilon^{4.8}_{in,i} p(x_{in.i})} \quad \text{(A.9)}$$

If a whole year is divided into 12 seasons to represent different subgrade moisture conditions, the Bias Correction Function for Moisture should be:

$$BCF_{moisture} = \frac{12\varepsilon^{4.8}_{APT}}{\sum_{I=1}^{12} \varepsilon^{4.8}_{in,i}} \quad \text{(A.10)}$$

A.3 Specification of Bias Correction Function for Temperature

A regression equation based on laboratory four-point bending fatigue test results shows fatigue life as a function of temperature was developed as follows:

$$N_f = k_2 10^{0.057T} \quad \text{(A.11)}$$

Since pavement temperature varies hourly and daily, and the traffic volume changes hourly (a_i), the Bias Correction Function for Temperature should account for all three variables. Still based on the general form the function is developed as follows:

$$BCF_{Temperature} = \frac{[g(x^{\alpha}_{APT})]^{-1}}{\sum_{I=1}^{n}[g(x^{\alpha}_{in.i})]^{-1} p(x_{in.i})}$$

$$= \frac{[k_2 10^{0.057 T_{APT}}]^{-1}}{\sum_{j=1}^{365} \sum_{i=1}^{24} [k_2 10^{0.057 T_{in.ij}}]^{-1} a_i \times \frac{1}{365}}$$

$$= \frac{365}{\sum_{j=1}^{365} \sum_{i=1}^{24} 10^{-0.0570(T_{in.ij} - T_{APT})} \times a_i} \qquad \text{(A.12)}$$

A.4 Specification of Bias Correction Function for Loading Ratio

A regression equation based on the research of the effect of rest period on fatigue performance shows fatigue life as a function of loading ratio as follows:

$$N_f = k_3 10^{0.011 LR} \qquad \text{(A.13)}$$

Since traffic loading ratio varies hourly and yearly, the Bias Correction Function for loading ratio should account for these. The function is developed as follows:

$$BCF_{LadingRatio} = \frac{[g(x^{\alpha}_{APT})]^{-1}}{\sum_{I=1}^{n} [g(x^{\alpha}_{in.i})]^{-1} p(x_{in.i})}$$

$$= \frac{[k_3 10^{0.011 LR_{APT}}]^{-1}}{\sum_{j=1}^{n} \sum_{i=1}^{24} [k_3 10^{0.011 LR_{in.ij}}]^{-1} \times \frac{1}{24} \times \frac{1}{n}}$$

$$= \frac{24n}{\sum_{j=1}^{n} \sum_{i=1}^{24} 10^{-0.011(LR_{in.ij} - LRA_{PT})}} \qquad \text{(A.14)}$$

Appendix B: Estimation of Correlation Matrix for the Parameters in Fatigue Life Prediction

Table B.1 Specification of the Parameters

SHRP_ID	State_Code	Region	Climatic	Moisture	Temperature	Speed (km/h)	Loading time	Loading Frequency	AADTT	Loading Ratio	Beneficial LR
0109	New Mexico (35)	Southern	Dry No Freeze	dry (0)	No Freeze (1)	105	0.012	13.1	6201	806	25
1004	Vermont (50)	North Atlantic	Wet Freeze	wet (1)	Freeze (0)	90	0.014	11.2	3635	1179	25
1009	Maine (23)	North Atlantic	Wet freeze	wet (1)	Freeze (0)	90	0.014	11.2	5430	789	25
1030	North Carolina (37)	North Atlantic	Wet No Freeze	wet (1)	No Freeze (1)	110	0.012	13.7	4400	1191	25
1622	Ontario (87)	North Atlantic	Wet freeze	wet (1)	Freeze (0)	100	0.013	12.4	4900	972	25
3609	Texas (48)	Southern	Wet No Freeze	wet (1)	No Freeze (1)	115	0.011	14.3	4400	1245	25
3669	Texas (48)	Southern	Wet No Freeze	wet (1)	No Freeze (1)	100	0.013	12.4	3964	1202	25
4096	Georgia (13)	Southern	Wet No Freeze	wet (1)	No Freeze (1)	70	0.018	8.7	1600	2085	25
6007	British Columbia (82)	Western	Wet no freeze	wet (1)	No Freeze (1)	80	0.016	10.0	12257	310	25
6160	Texas (48)	Southern	Dry Freeze	dry (0)	Freeze (0)	110	0.012	13.7	1950	2688	25
7454	California (06)	Western	Dry No Freeze	dry (0)	No Freeze (1)	90	0.014	11.2	2800	1531	25
8153	California (06)	Western	Wet No Freeze	wet (1)	No Freeze (1)	90	0.014	11.2	5700	752	25

Table B.2 Estimation of Correlation Matrix for the Parameters

	Moisture	**Freeze**	Speed (km/h)	Loading time	**Loading Frequency**	AADTT	**Loading Ratio**
Moisture	1.000						
Freeze	**0.000**	1.000					
Speed (km/h)	-0.265	-0.093	1.000				
Loading time	0.274	0.142	-0.987	1.000			
Loading Frequency	-0.265	**-0.094**	1.000	-0.987	1.000		
AADTT	0.245	0.212	-0.173	0.127	-0.173	1.000	
Loading Ratio	-0.422	**-0.206**	0.126	-0.043	**0.125**	-0.807	1.000

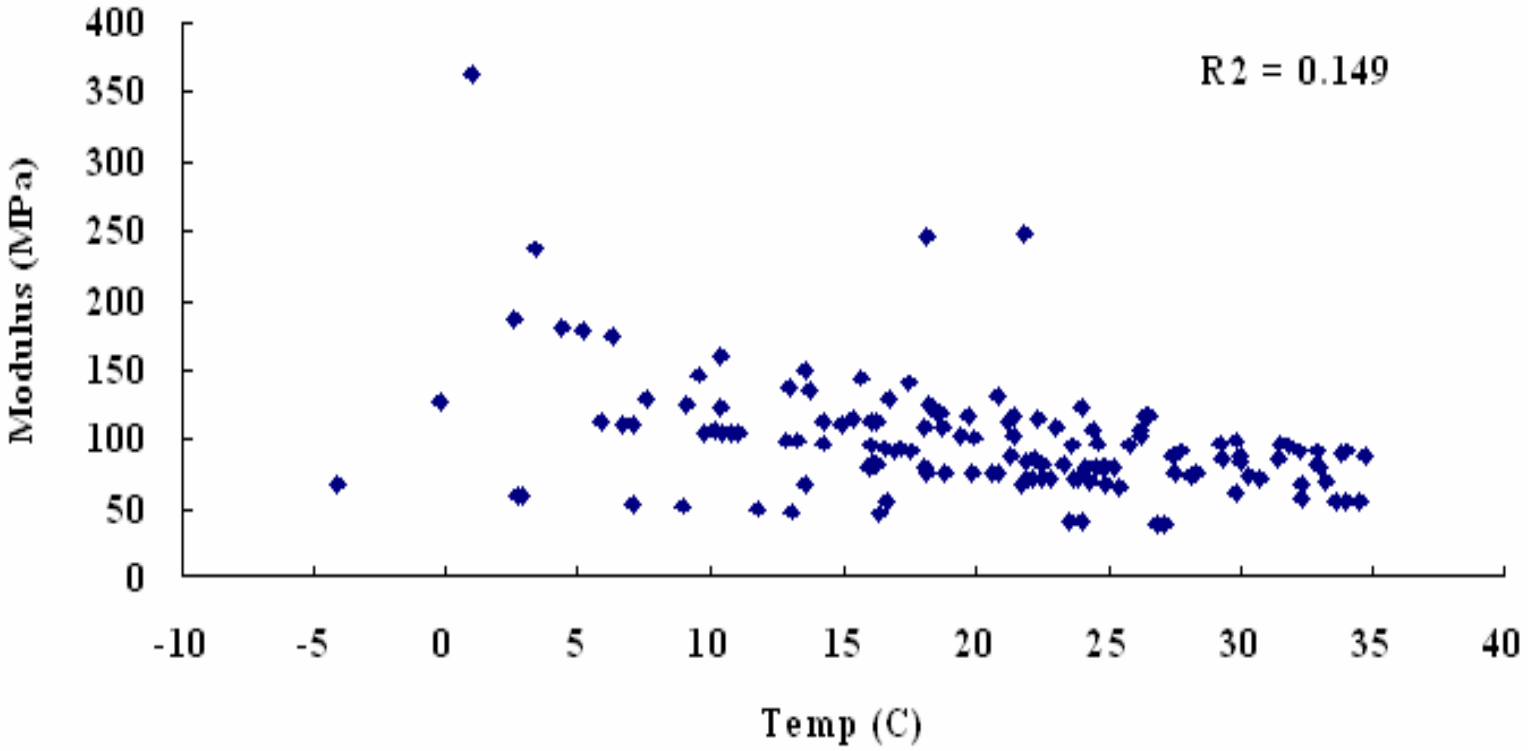

Figure B.1 Correlation between subgrade moisture (modulus) and temperature

Appendix C: Laboratory Fatigue Tests[1]

C.1 Introduction

The main purpose of carrying out the four point beam bending fatigue tests as described in Chapter 5 was to analyze the fatigue response of the asphalt mixes with different loading frequency, loading magnitude and environment temperature. The purpose of the tests also included quantification of the variability associated with the results and identification of the sources of variability for the results.

C.2 Materials Used

The testing procedure consists of manufacturing the beams and then testing them by the Fatigue Testing apparatus as shown in Figure C.1.

Figure C.1 Fatigue beam testing apparatus

[1] Section C.1 through C.4 cited Vishal Gossain's work.

The 36 tests consisted of premanufactured mixes designated as Accelerated Pavement Testing (APT) mixes obtained from the pavement constructed at the J.J. Pickle Research Campus (PRC) for Accelerated Pavement Testing with the Texas Mobile Load Simulator (TxMLS).

C.3 AASHTO TP – 8

The AASHTO TP-8 (AASHTO TP8, 1996) standard provides procedures for determining the fatigue life and fatigue energy of 380 mm long by 50 mm thick by 63 mm wide hot mix asphalt (HMA) beam specimens sawed from laboratory or field compacted HMA and subjected to repeated flexural bending until failure. The fatigue life and failure energy determined by this standard can be used to estimate the fatigue life of HMA pavement layers under repeated traffic loading.

The four point beam bending test procedure (constant strain) involves applying repeated loading and unloading on a beam specimen till the flexural stiffness of the specimen reduces to a calculated value. One such application of loading and unloading is termed as a load cycle.

The load is so applied that the specimen experiences a constant level of strain during each loading cycle. Repeated sinusoidal loading at a frequency range of 2.5 to 20 Hz is usually applied subjecting specimens to four points bending with free rotation and

horizontal translation at all load and reaction points with the flexural stiffness estimated after every 10 cycles. The constant strain level can be fixed from 250-750 micro strains as specified by AASHTO TP – 8. The flexural stiffness measured after the first 50 conditioning cycles is termed as initial stiffness and 50% of the initial stiffness is termed as termination stiffness or point of failure. The test is stopped after the termination stiffness has been achieved.

C.4 Manufacture of Beams

The asphalt mixes used for the construction of the section for Accelerated Pavement Testing at PRC were transported to the laboratories for testing.

AASHTO TP – 8 specifies the desired void content of 7 ± 0.5 % in the beam, which is representative of the void content of a new pavement. Based on the void content, the amount of mix to be compacted to a specified volume can be computed by volumetric calculations. The volume is determined based on the volume of the mold used for compaction. The mold is made out of steel with a width of 152.4 mm and length of 393.7 mm, and is supplied with the Asphalt Vibratory Compactor (AVC). The amount of aggregate blend can then be calculated from the amount of mix as the percentage of binder by mass of mix is known. The amounts of individual aggregates required to prepare the blend are then calculated from the amount of blend. The various volumetric

equations involved are listed as Equations (C.1) – (C.5). A conservative value of Gmm is used in the calculations.

$$M_b = \frac{P_b * M_s}{1 - P_b} \tag{C.1}$$

$$M_t = M_s + M_b \tag{C.2}$$

$$V = l * b * h \tag{C.3}$$

$$G_{mb} = \frac{M_t}{V} \tag{C.4}$$

$$VIM = 1 - \frac{G_{mb}}{G_{mm}} \tag{C.5}$$

Where,

Mb: Mass of binder

Mt: Total mass of mix

Pb: Percentage of binder by weight of the mix

Ms: Mass of aggregate

l ,b,h: Dimensions of the mold

V: Volume of the mold

Gmb: Bulk density

Gmm: Maximum theoretical specific gravity

VIM: Voids in mix

Thus, it is essentially a backcalculation procedure to estimate Ms based on a known VIM. After determining the Ms, the desired proportions of the aggregates are mixed and then heated to the mixing temperatures.

The mix is then aged in the oven for 4 hours at 135 ℃ to simulate the aging in the field in the time taken to transport the mix from the plant to the pavement. Two thousand grams of the mix is taken out (in total) from the pans after 4 hours for tests to determine theoretical maximum density in accordance with AASHTO T 209 (AASHTO T 209, 99).

Figure C.2 Rotatory mixer for mixing binder with aggregates

AASHTO T 209 test method covers the determination of the theoretical maximum specific gravity and density of uncompacted bituminous paving mixtures at 25°C. The obtained rice value (Gmm, maximum theoretical specific gravity) is then used to estimate the mass of the mix required to achieve the desired void content based on volumetric calculations. The mix is then heated to the compaction temperature.

Two steel plates are provided with the mold to facilitate easy removal of the specimen after compaction. The mold is also heated along with the steel plates. The mix is then poured into the mold, and then the mold is placed in the Asphalt Vibratory Compactor (AVC) (shown in Figure C.3) and compacted.

Figure C.3 Asphalt Vibratory Compactor

The AVC was designed to form rectangular and cylindrical specimens of asphalt mixes. The AVC compacts samples at the same amplitude, frequency and relative weight that a contractor applies with a vibratory compactor on the roadway (AVC manual). After

the samples are compacted, they are extracted with the help of an air cylinder. After extraction, the top plate is immediately removed. The slab is kept on a flat surface for 10-12 minutes to cool down, and then the bottom plate is also removed. After compaction, the slabs are left overnight and then tested for their bulk density.

The slabs are then sawed to derive two beams 380 mm long (L) by 50 mm high (h) by 63 mm wide (b) out of each slab, which serve as replicates. The slabs are cut such that each side is sawed. The beams are then aged for 7 days in a temperature control chamber at 20 ℃. They are then tested in accordance with AASHTO TP – 8. The strain levels and the loading frequency were selected based on experimentation discussed in Chapter 5. The test was terminated at a stiffness level of 20% instead of the traditional 50%.

The beam is subjected to both tension and compression in a constant strain test. It can be observed in Figure C.4 that the strain is not in phase with the load indicating the viscoelastic nature of asphalt, and the difference represents the phase angle of asphalt binder. The phase angle provides a relative indication of the viscous and elastic behavior of the asphalt binder. Materials with a phase angle of 90 degrees are completely viscous; while materials with a phase angle of 0 degrees are completely elastic. At intermediate temperatures, such as 20ºC, asphalt binders are said to be viscoelastic (phase angle near 45 degrees).

It is also important to mention that the compactive effort provided by AVC is non uniform. Hence, although the width of the mold (152.4 mm) and the length of the mold (393.7 mm) are known with certainty, the height of the mold or the slab needs to be estimated for the volumetric calculations. It is not always the case that the compactor "bottoms out", which means that the compactor is able to compact the slab by being able to reach the minimum slab height (75 mm). It was later found by backcalculation and actual measurement of height of the slab that the compactor was bottoming out in most of the cases.

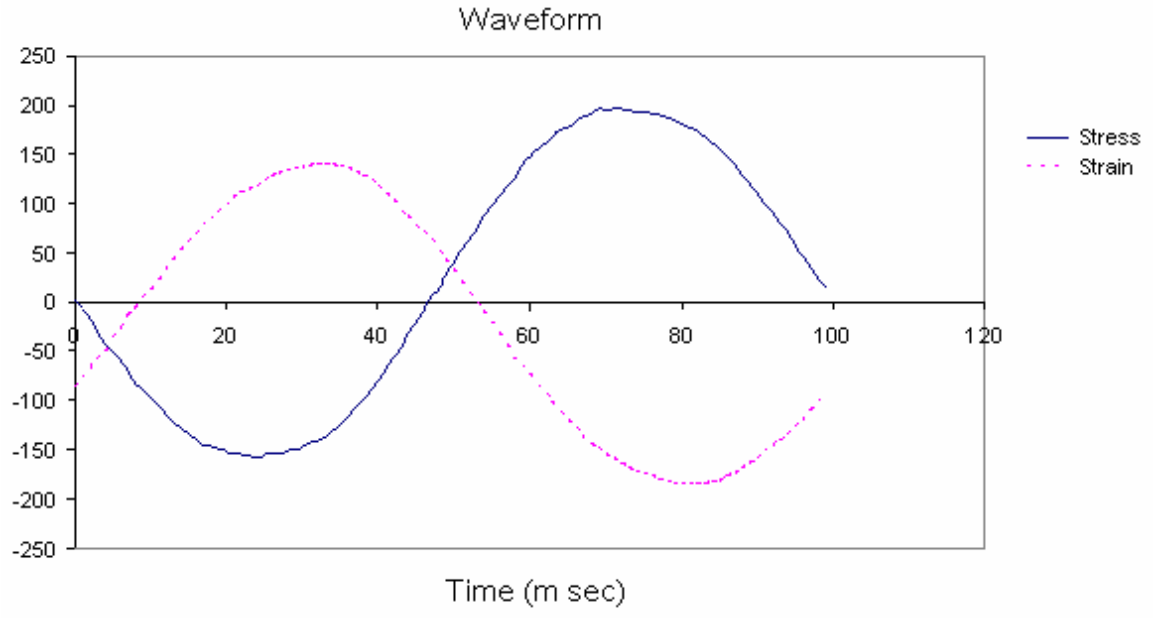

Figure C.4 Sinusoidal loading waveform

C.5 Laboratory fatigue test results

Figure C.5 is a sample fatigue test record (Beam APT 5-2-1 10Hz@30C 600ue). Tables C.1 through C.9 are summary tables of all the laboratory fatigue test results at different remaining material stiffness.

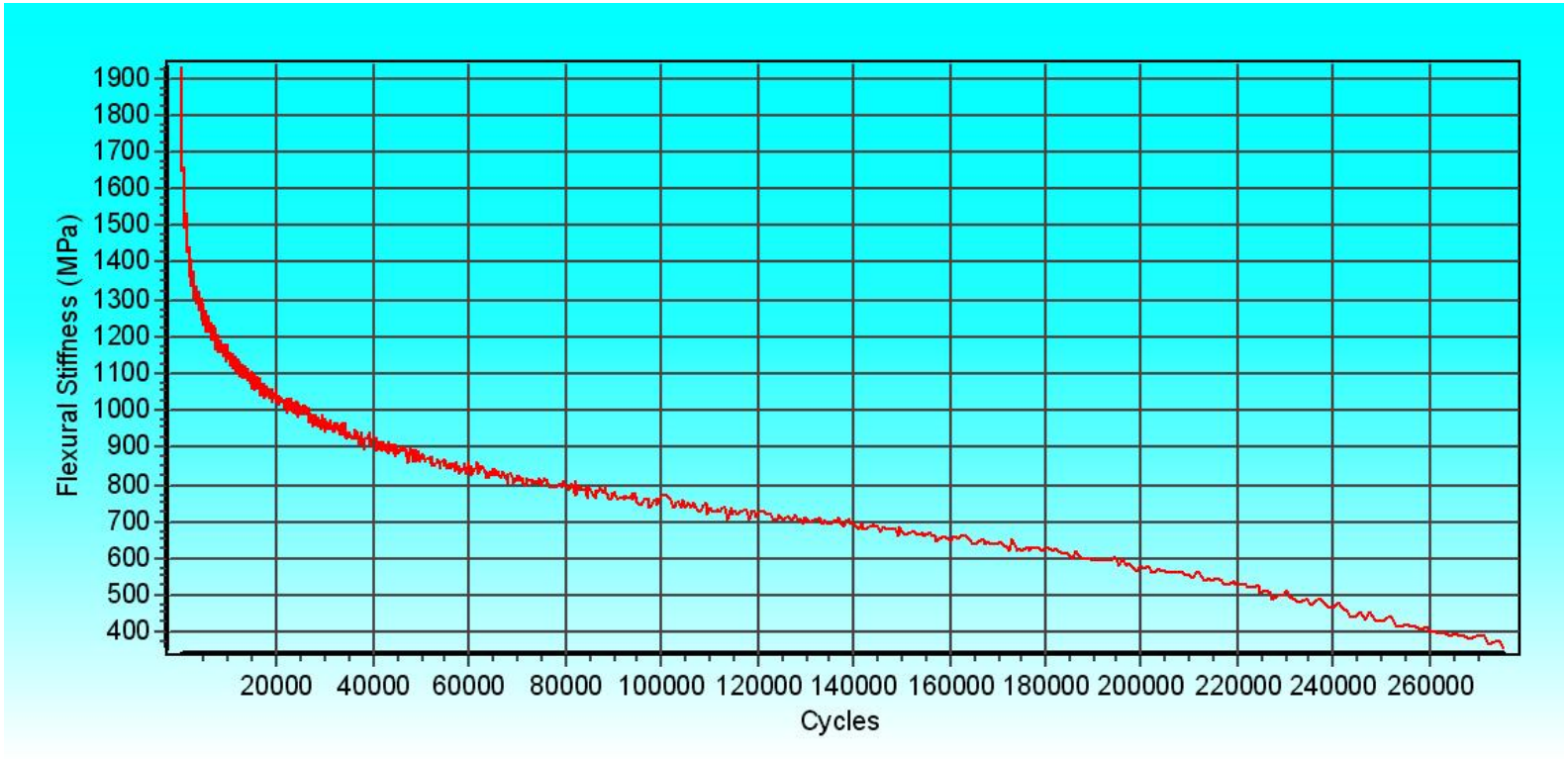

Figure C.5 Sample fatigue test record (Beam APT 5-2-1 10Hz at 30C 600ue)

Table C.1 Fatigue test results at 100% remaining stiffness

Objective	Stiffness	Strain	cycles	Temp	Freq	Beam
100%	7505.0	434.56	50	10.60	2.5	APT 4-1-2
100%	5845.0	449.13	50	10.60	2.5	APT 4-1-1
100%	5613.9	298.93	50	10.67	2.5	APT 4-2-1
100%	9192.1	290.55	50	10.67	2.5	APT 4-2-2
100%	1589.1	452.12	50	29.75	2.5	APT 5-3-2
100%	973.0	449.32	50	29.75	2.5	APT 5-3-1
100%	1120.2	613.11	50	29.99	2.5	APT 6-1-1
100%	1906.9	599.56	50	29.99	2.5	APT 6-1-2
100%	7993.8	289.48	50	10.09	5	APT 4-3-2
100%	5523.6	444.37	50	10.09	5	APT 4-3-1
100%	6642.2	299.67	50	10.09	5	APT 6-4-1
100%	7978.7	434.26	50	10.60	5	APT 6-4-2
100%	3544.0	482.17	50	20.77	5	APT 2-3-2
100%	2694.1	499.58	50	20.77	5	APT 2-3-1
100%	1926.2	349.63	50	20.79	5	APT 2-2-1
100%	2000.0	338.05	50	20.80	5	APT 2-2-2
100%	1315.6	477.87	50	29.08	5	APT 6-2-1
100%	2316.0	452.00	50	29.08	5	APT 6-2-2
100%	1780.0	599.78	50	29.70	5	APT 6-3-2
100%	1328.9	600.86	50	29.99	5	APT 6-3-1
100%	8765.7	300.03	50	10.10	10	APT 3-1-1
100%	11000.0	289.03	50	10.10	10	APT 3-1-2
100%	7275.4	450.07	50	10.30	10	APT 3-3-1
100%	10500.0	433.25	50	10.30	10	APT 3-3-2
100%	3689.6	500.00	50	20.65	10	APT 1-1-1
100%	3290.8	507.07	50	20.70	10	APT 1-1-2
100%	4523.6	336.83	50	20.79	10	APT 1-3-2
100%	3963.7	350.01	50	20.80	10	APT 1-3-1
100%	1947.2	449.95	50	29.08	10	APT 5-1-1
100%	2525.2	451.29	50	29.08	10	APT 5-1-2
100%	1846.4	599.96	50	29.60	10	APT 5-2-1
100%	2050.0	601.40	50	29.60	10	APT 5-2-2
100%	3200.4	500.39	50	20.77	20	APT 2-1-1
100%	4656.6	350.24	50	20.77	20	APT 3-2-1
100%	6594.0	336.64	50	21.24	20	APT 3-2-2
100%	4706.7	481.39	50	21.26	20	APT 2-1-2

Table C.2 Fatigue test results at 90% remaining stiffness

Objective	Stiffness	Strain	cycles	Temp	Freq	Beam
90%	6754.5	434.56	710	10.60	2.5	APT 4-1-2
90%	5260.5	449.13	300	10.60	2.5	APT 4-1-1
90%	5052.5	298.93	1510	10.67	2.5	APT 4-2-1
90%	8272.9	290.55	1120	10.67	2.5	APT 4-2-2
90%	1430.2	452.12	130	29.75	2.5	APT 5-3-2
90%	875.7	449.32	210	29.75	2.5	APT 5-3-1
90%	1008.2	613.11	105	29.99	2.5	APT 6-1-1
90%	1716.2	599.56	60	29.99	2.5	APT 6-1-2
90%	7194.4	289.48	1520	10.09	5	APT 4-3-2
90%	4971.2	444.37	380	10.09	5	APT 4-3-1
90%	5978.0	299.67	1510	10.09	5	APT 6-4-1
90%	7180.8	434.26	700	10.60	5	APT 6-4-2
90%	3189.6	482.17	420	20.77	5	APT 2-3-2
90%	2424.7	499.58	395	20.77	5	APT 2-3-1
90%	1733.6	349.63	1550	20.79	5	APT 2-2-1
90%	1800.0	338.05	920	20.80	5	APT 2-2-2
90%	1184.0	477.87	145	29.08	5	APT 6-2-1
90%	2084.4	452.00	160	29.08	5	APT 6-2-2
90%	1602.0	599.78	110	29.70	5	APT 6-3-2
90%	1196.0	600.86	245	29.99	5	APT 6-3-1
90%	7889.1	300.03	2510	10.10	10	APT 3-1-1
90%	9900.0	289.03	3170	10.10	10	APT 3-1-2
90%	6547.9	450.07	590	10.30	10	APT 3-3-1
90%	9450.0	433.25	810	10.30	10	APT 3-3-2
90%	3320.7	500.00	430	20.65	10	APT 1-1-1
90%	2961.7	507.07	440	20.70	10	APT 1-1-2
90%	4071.3	336.83	330	20.79	10	APT 1-3-2
90%	3567.3	350.01	170	20.80	10	APT 1-3-1
90%	1752.5	449.95	270	29.08	10	APT 5-1-1
90%	2272.7	451.29	510	29.08	10	APT 5-1-2
90%	1661.7	599.96	260	29.60	10	APT 5-2-1
90%	1845.0	601.40	300	29.60	10	APT 5-2-2
90%	2880.4	500.39	540	20.77	20	APT 2-1-1
90%	4191.0	350.24	610	20.77	20	APT 3-2-1
90%	5934.6	336.64	680	21.24	20	APT 3-2-2
90%	4236.0	481.39	440	21.26	20	APT 2-1-2

Table C.3 Fatigue test results at 80% remaining stiffness

Objective	Stiffness	Strain	cycles	Temp	Freq	Beam
80%	6004.0	434.56	2350	10.60	2.5	APT 4-1-2
80%	4676.0	449.13	1300	10.60	2.5	APT 4-1-1
80%	4491.1	298.93	14970	10.67	2.5	APT 4-2-1
80%	7353.7	290.55	8680	10.67	2.5	APT 4-2-2
80%	1271.3	452.12	730	29.75	2.5	APT 5-3-2
80%	778.4	449.32	2010	29.75	2.5	APT 5-3-1
80%	896.2	613.11	280	29.99	2.5	APT 6-1-1
80%	1525.5	599.56	120	29.99	2.5	APT 6-1-2
80%	6395.0	289.48	9190	10.09	5	APT 4-3-2
80%	4418.9	444.37	1165	10.09	5	APT 4-3-1
80%	5313.8	299.67	5015	10.09	5	APT 6-4-1
80%	6383.0	434.26	2490	10.60	5	APT 6-4-2
80%	2835.2	482.17	1720	20.77	5	APT 2-3-2
80%	2155.3	499.58	1620	20.77	5	APT 2-3-1
80%	1541.0	349.63	6610	20.79	5	APT 2-2-1
80%	1600.0	338.05	3770	20.80	5	APT 2-2-2
80%	1052.5	477.87	2560	29.08	5	APT 6-2-1
80%	1852.8	452.00	2890	29.08	5	APT 6-2-2
80%	1424.0	599.78	560	29.70	5	APT 6-3-2
80%	1063.2	600.86	1510	29.99	5	APT 6-3-1
80%	7012.6	300.03	10360	10.10	10	APT 3-1-1
80%	8800.0	289.03	15680	10.10	10	APT 3-1-2
80%	5820.3	450.07	2050	10.30	10	APT 3-3-1
80%	8400.0	433.25	3280	10.30	10	APT 3-3-2
80%	2951.7	500.00	2200	20.65	10	APT 1-1-1
80%	2632.7	507.07	1900	20.70	10	APT 1-1-2
80%	3618.9	336.83	4800	20.79	10	APT 1-3-2
80%	3171.0	350.01	1760	20.80	10	APT 1-3-1
80%	1557.8	449.95	1920	29.08	10	APT 5-1-1
80%	2020.2	451.29	3100	29.08	10	APT 5-1-2
80%	1477.1	599.96	1070	29.60	10	APT 5-2-1
80%	1640.0	601.40	1280	29.60	10	APT 5-2-2
80%	2560.3	500.39	3380	20.77	20	APT 2-1-1
80%	3725.3	350.24	4270	20.77	20	APT 3-2-1
80%	5275.2	336.64	5440	21.24	20	APT 3-2-2
80%	3765.4	481.39	1390	21.26	20	APT 2-1-2

Table C.4 Fatigue test results at 70% remaining stiffness

Objective	Stiffness	Strain	cycles	Temp	Freq	Beam
70%	5253.5	434.56	7340	10.60	2.5	APT 4-1-2
70%	4091.5	449.13	3660	10.60	2.5	APT 4-1-1
70%	3929.7	298.93	73830	10.67	2.5	APT 4-2-1
70%	6434.5	290.55	39100	10.67	2.5	APT 4-2-2
70%	1112.4	452.12	9230	29.75	2.5	APT 5-3-2
70%	681.1	449.32	282180	29.75	2.5	APT 5-3-1
70%	784.1	613.11	1520	29.99	2.5	APT 6-1-1
70%	1334.8	599.56	540	29.99	2.5	APT 6-1-2
70%	5595.7	289.48	46530	10.09	5	APT 4-3-2
70%	3866.5	444.37	2620	10.09	5	APT 4-3-1
70%	4649.6	299.67	22660	10.09	5	APT 6-4-1
70%	5585.1	434.26	7020	10.60	5	APT 6-4-2
70%	2480.8	482.17	5740	20.77	5	APT 2-3-2
70%	1885.9	499.58	5180	20.77	5	APT 2-3-1
70%	1348.3	349.63	32490	20.79	5	APT 2-2-1
70%	1400.0	338.05	9480	20.80	5	APT 2-2-2
70%	920.9	477.87	29630	29.08	5	APT 6-2-1
70%	1621.2	452.00	8050	29.08	5	APT 6-2-2
70%	1246.0	599.78	2700	29.70	5	APT 6-3-2
70%	930.3	600.86	4195	29.99	5	APT 6-3-1
70%	6136.0	300.03	28110	10.10	10	APT 3-1-1
70%	7700.0	289.03	59640	10.10	10	APT 3-1-2
70%	5092.8	450.07	4650	10.30	10	APT 3-3-1
70%	7350.0	433.25	9000	10.30	10	APT 3-3-2
70%	2582.7	500.00	5740	20.65	10	APT 1-1-1
70%	2303.6	507.07	5450	20.70	10	APT 1-1-2
70%	3166.5	336.83	32440	20.79	10	APT 1-3-2
70%	2774.6	350.01	8480	20.80	10	APT 1-3-1
70%	1363.0	449.95	10050	29.08	10	APT 5-1-1
70%	1767.7	451.29	14160	29.08	10	APT 5-1-2
70%	1292.5	599.96	4060	29.60	10	APT 5-2-1
70%	1435.0	601.40	6120	29.60	10	APT 5-2-2
70%	2240.3	500.39	7890	20.77	20	APT 2-1-1
70%	3259.6	350.24	13870	20.77	20	APT 3-2-1
70%	4615.8	336.64	17870	21.24	20	APT 3-2-2
70%	3294.7	481.39	3030	21.26	20	APT 2-1-2

Table C.5 Fatigue test results at 60% remaining stiffness

Objective	Stiffness	Strain	cycles	Temp	Freq	Beam
60%	4503.0	434.56	18760	10.60	2.5	APT 4-1-2
60%	3507.0	449.13	6735	10.60	2.5	APT 4-1-1
60%	3368.3	298.93	153285	10.67	2.5	APT 4-2-1
60%	5515.3	290.55	64730	10.67	2.5	APT 4-2-2
60%	953.4	452.12	122550	29.75	2.5	APT 5-3-2
60%	583.8	449.32	696235	29.75	2.5	APT 5-3-1
60%	672.1	613.11	15090	29.99	2.5	APT 6-1-1
60%	1144.2	599.56	4490	29.99	2.5	APT 6-1-2
60%	4796.3	289.48	150770	10.09	5	APT 4-3-2
60%	3314.2	444.37	4710	10.09	5	APT 4-3-1
60%	3985.3	299.67	80730	10.09	5	APT 6-4-1
60%	4787.2	434.26	17640	10.60	5	APT 6-4-2
60%	2126.4	482.17	21930	20.77	5	APT 2-3-2
60%	1616.5	499.58	15590	20.77	5	APT 2-3-1
60%	1155.7	349.63	58010	20.79	5	APT 2-2-1
60%	1200.0	338.05	21000	20.80	5	APT 2-2-2
60%	789.4	477.87	141885	29.08	5	APT 6-2-1
60%	1389.6	452.00	20000	29.08	5	APT 6-2-2
60%	1068.0	599.78	12980	29.70	5	APT 6-3-2
60%	797.4	600.86	15590	29.99	5	APT 6-3-1
60%	5259.4	300.03	60560	10.10	10	APT 3-1-1
60%	6600.0	289.03	112200	10.10	10	APT 3-1-2
60%	4365.2	450.07	8200	10.30	10	APT 3-3-1
60%	6300.0	433.25	17020	10.30	10	APT 3-3-2
60%	2213.8	500.00	16930	20.65	10	APT 1-1-1
60%	1974.5	507.07	15010	20.70	10	APT 1-1-2
60%	2714.2	336.83	98720	20.79	10	APT 1-3-2
60%	2378.2	350.01	31220	20.80	10	APT 1-3-1
60%	1168.3	449.95	35570	29.08	10	APT 5-1-1
60%	1515.1	451.29	38700	29.08	10	APT 5-1-2
60%	1107.8	599.96	12910	29.60	10	APT 5-2-1
60%	1230.0	601.40	20310	29.60	10	APT 5-2-2
60%	1920.2	500.39	17910	20.77	20	APT 2-1-1
60%	2794.0	350.24	27890	20.77	20	APT 3-2-1
60%	3956.4	336.64	44440	21.24	20	APT 3-2-2
60%	2824.0	481.39	4090	21.26	20	APT 2-1-2

Table C.6 Fatigue test results at 50% remaining stiffness

Objective	Stiffness	Strain	cycles	Temp	Freq	Beam
50%	3752.5	434.56	25960	10.60	2.5	APT 4-1-2
50%	2922.5	449.13	8525	10.60	2.5	APT 4-1-1
50%	2806.9	298.93	324040	10.67	2.5	APT 4-2-1
50%	4596.1	290.55	87310	10.67	2.5	APT 4-2-2
50%	794.5	452.12	713400	29.75	2.5	APT 5-3-2
50%	486.5	449.32	815940	29.75	2.5	APT 5-3-1
50%	560.1	613.11	64300	29.99	2.5	APT 6-1-1
50%	953.5	599.56	55660	29.99	2.5	APT 6-1-2
50%	3996.9	289.48	358920	10.09	5	APT 4-3-2
50%	2761.8	444.37	7650	10.09	5	APT 4-3-1
50%	3321.1	299.67	142465	10.09	5	APT 6-4-1
50%	3989.3	434.26	28910	10.60	5	APT 6-4-2
50%	1772.0	482.17	60100	20.77	5	APT 2-3-2
50%	1347.1	499.58	36305	20.77	5	APT 2-3-1
50%	963.1	349.63	88520	20.79	5	APT 2-2-1
50%	1000.0	338.05	34050	20.80	5	APT 2-2-2
50%	657.8	477.87	395520	29.08	5	APT 6-2-1
50%	1158.0	452.00	116500	29.08	5	APT 6-2-2
50%	890.0	599.78	25310	29.70	5	APT 6-3-2
50%	664.5	600.86	58800	29.99	5	APT 6-3-1
50%	4382.9	300.03	106330	10.10	10	APT 3-1-1
50%	5500.0	289.03	151930	10.10	10	APT 3-1-2
50%	3637.7	450.07	11360	10.30	10	APT 3-3-1
50%	5250.0	433.25	25630	10.30	10	APT 3-3-2
50%	1844.8	500.00	30980	20.65	10	APT 1-1-1
50%	1645.4	507.07	34140	20.70	10	APT 1-1-2
50%	2261.8	336.83	222160	20.79	10	APT 1-3-2
50%	1981.9	350.01	100380	20.80	10	APT 1-3-1
50%	973.6	449.95	122080	29.08	10	APT 5-1-1
50%	1262.6	451.29	106330	29.08	10	APT 5-1-2
50%	923.2	599.96	37630	29.60	10	APT 5-2-1
50%	1025.0	601.40	41260	29.60	10	APT 5-2-2
50%	1600.2	500.39	32020	20.77	20	APT 2-1-1
50%	2328.3	350.24	48100	20.77	20	APT 3-2-1
50%	3297.0	336.64	90270	21.24	20	APT 3-2-2
50%	2353.4	481.39	5260	21.26	20	APT 2-1-2

Table C.7 Fatigue test results at 40% remaining stiffness

Objective	Stiffness	Strain	cycles	Temp	Freq	Beam
40%	3002.0	434.56	31140	10.60	2.5	APT 4-1-2
40%	2338.0	449.13	10385	10.60	2.5	APT 4-1-1
40%	2245.5	298.93	373625	10.67	2.5	APT 4-2-1
40%	3676.9	290.55	147910	10.67	2.5	APT 4-2-2
40%	635.6	452.12	755670	29.75	2.5	APT 5-3-2
40%	389.2	449.32	829330	29.75	2.5	APT 5-3-1
40%	448.1	613.11	91945	29.99	2.5	APT 6-1-1
40%	762.8	599.56	104310	29.99	2.5	APT 6-1-2
40%	3197.5	289.48	640710	10.09	5	APT 4-3-2
40%	2209.4	444.37	10845	10.09	5	APT 4-3-1
40%	2656.9	299.67	198070	10.09	5	APT 6-4-1
40%	3191.5	434.26	36490	10.60	5	APT 6-4-2
40%	1417.6	482.17	103110	20.77	5	APT 2-3-2
40%	1077.7	499.58	49440	20.77	5	APT 2-3-1
40%	770.5	349.63	102470	20.79	5	APT 2-2-1
40%	800.0	338.05	56950	20.80	5	APT 2-2-2
40%	526.2	477.87	471130	29.08	5	APT 6-2-1
40%	926.4	452.00	194600	29.08	5	APT 6-2-2
40%	712.0	599.78	34140	29.70	5	APT 6-3-2
40%	531.6	600.86	141310	29.99	5	APT 6-3-1
40%	3506.3	300.03	142340	10.10	10	APT 3-1-1
40%	4400.0	289.03	177140	10.10	10	APT 3-1-2
40%	2910.2	450.07	13180	10.30	10	APT 3-3-1
40%	4200.0	433.25	30430	10.30	10	APT 3-3-2
40%	1475.9	500.00	43420	20.65	10	APT 1-1-1
40%	1316.3	507.07	56230	20.70	10	APT 1-1-2
40%	1809.4	336.83	290620	20.79	10	APT 1-3-2
40%	1585.5	350.01	201060	20.80	10	APT 1-3-1
40%	778.9	449.95	199520	29.08	10	APT 5-1-1
40%	1010.1	451.29	213790	29.08	10	APT 5-1-2
40%	738.5	599.96	110490	29.60	10	APT 5-2-1
40%	820.0	601.40	68830	29.60	10	APT 5-2-2
40%	1280.2	500.39	46060	20.77	20	APT 2-1-1
40%	1862.6	350.24	75470	20.77	20	APT 3-2-1
40%	2637.6	336.64	119300	21.24	20	APT 3-2-2
40%	1882.7	481.39	6450	21.26	20	APT 2-1-2

Table C.8 Fatigue test results at 30% remaining stiffness

Objective	Stiffness	Strain	cycles	Temp	Freq	Beam
30%	2251.5	434.56	35930	10.60	2.5	APT 4-1-2
30%	1753.5	449.13	13290	10.60	2.5	APT 4-1-1
30%	1684.2	298.93	406945	10.67	2.5	APT 4-2-1
30%	2757.6	290.55	251180	10.67	2.5	APT 4-2-2
30%	476.7	452.12	#N/A	29.75	2.5	APT 5-3-2
30%	291.9	449.32	929385	29.75	2.5	APT 5-3-1
30%	336.1	613.11	111610	29.99	2.5	APT 6-1-1
30%	572.1	599.56	135930	29.99	2.5	APT 6-1-2
30%	2398.1	289.48	735640	10.09	5	APT 4-3-2
30%	1657.1	444.37	14450	10.09	5	APT 4-3-1
30%	1992.7	299.67	236895	10.09	5	APT 6-4-1
30%	2393.6	434.26	44550	10.60	5	APT 6-4-2
30%	1063.2	482.17	142880	20.77	5	APT 2-3-2
30%	808.2	499.58	58325	20.77	5	APT 2-3-1
30%	577.9	349.63	118150	20.79	5	APT 2-2-1
30%	600.0	338.05	107970	20.80	5	APT 2-2-2
30%	394.7	477.87	494700	29.08	5	APT 6-2-1
30%	694.8	452.00	275400	29.08	5	APT 6-2-2
30%	534.0	599.78	40320	29.70	5	APT 6-3-2
30%	398.7	600.86	177465	29.99	5	APT 6-3-1
30%	2629.7	300.03	165320	10.10	10	APT 3-1-1
30%	3300.0	289.03	193490	10.10	10	APT 3-1-2
30%	2182.6	450.07	14900	10.30	10	APT 3-3-1
30%	3150.0	433.25	34140	10.30	10	APT 3-3-2
30%	1106.9	500.00	53700	20.65	10	APT 1-1-1
30%	987.2	507.07	68300	20.70	10	APT 1-1-2
30%	1357.1	336.83	322350	20.79	10	APT 1-3-2
30%	1189.1	350.01	240800	20.80	10	APT 1-3-1
30%	584.2	449.95	251180	29.08	10	APT 5-1-1
30%	757.6	451.29	377280	29.08	10	APT 5-1-2
30%	553.9	599.96	212970	29.60	10	APT 5-2-1
30%	615.0	601.40	92840	29.60	10	APT 5-2-2
30%	960.1	500.39	53150	20.77	20	APT 2-1-1
30%	1397.0	350.24	95250	20.77	20	APT 3-2-1
30%	1978.2	336.64	136450	21.24	20	APT 3-2-2
30%	1412.0	481.39	7740	21.26	20	APT 2-1-2

Table C.9 Fatigue test results at 20% remaining stiffness

Objective	Stiffness	Strain	cycles	Temp	Freq	Beam
20%	1501.0	434.56	52210	10.60	2.5	APT 4-1-2
20%	1169.0	449.13	21290	10.60	2.5	APT 4-1-1
20%	1122.8	298.93	452310	10.67	2.5	APT 4-2-1
20%	1838.4	290.55	382360	10.67	2.5	APT 4-2-2
20%	317.8	452.12	#N/A	29.75	2.5	APT 5-3-2
20%	194.6	449.32	#N/A	29.75	2.5	APT 5-3-1
20%	224.0	613.11	139030	29.99	2.5	APT 6-1-1
20%	381.4	599.56	189630	29.99	2.5	APT 6-1-2
20%	1598.8	289.48	836650	10.09	5	APT 4-3-2
20%	1104.7	444.37	20875	10.09	5	APT 4-3-1
20%	1328.4	299.67	263325	10.09	5	APT 6-4-1
20%	1595.7	434.26	67260	10.60	5	APT 6-4-2
20%	708.8	482.17	171130	20.77	5	APT 2-3-2
20%	538.8	499.58	67745	20.77	5	APT 2-3-1
20%	385.2	349.63	156080	20.79	5	APT 2-2-1
20%	400.0	338.05	169170	20.80	5	APT 2-2-2
20%	263.1	477.87	#N/A	29.08	5	APT 6-2-1
20%	463.2	452.00	#N/A	29.08	5	APT 6-2-2
20%	356.0	599.78	60720	29.70	5	APT 6-3-2
20%	265.8	600.86	213390	29.99	5	APT 6-3-1
20%	1753.1	300.03	181020	10.10	10	APT 3-1-1
20%	2200.0	289.03	218460	10.10	10	APT 3-1-2
20%	1455.1	450.07	17240	10.30	10	APT 3-3-1
20%	2100.0	433.25	38210	10.30	10	APT 3-3-2
20%	737.9	500.00	62930	20.65	10	APT 1-1-1
20%	658.2	507.07	77620	20.70	10	APT 1-1-2
20%	904.7	336.83	378730	20.79	10	APT 1-3-2
20%	792.7	350.01	289170	20.80	10	APT 1-3-1
20%	389.4	449.95	319580	29.08	10	APT 5-1-1
20%	505.0	451.29	624380	29.08	10	APT 5-1-2
20%	369.3	599.96	275290	29.60	10	APT 5-2-1
20%	410.0	601.40	113060	29.60	10	APT 5-2-2
20%	640.1	500.39	69150	20.77	20	APT 2-1-1
20%	931.3	350.24	107560	20.77	20	APT 3-2-1
20%	1318.8	336.64	162180	21.24	20	APT 3-2-2
20%	941.3	481.39	8580	21.26	20	APT 2-1-2

Appendix D: Sensitivity Analysis of the Model Parameters on the Predicted Fatigue Life of Flexible Pavements

The model verification and validation process requires conducting a sensitivity analysis and assessing the reasonability of the influence of the model parameters on the predicted fatigue life of flexible pavements.

The approach adopted in this study requires running the distress prediction model for different combinations of input parameters within the experienced inference space. Figures D.1 through D.3 show the overall influence on pavement fatigue life of the different model parameters.

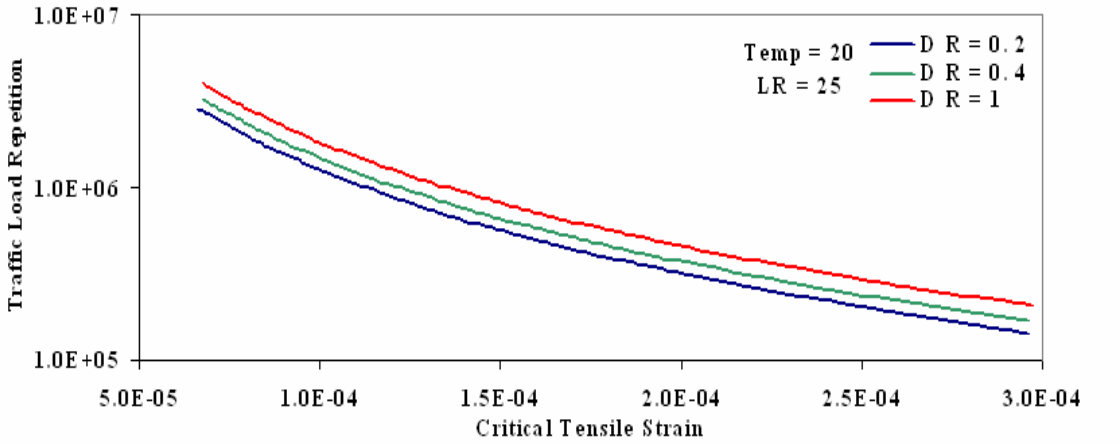

Figure D.1 Plot showing the influence of damage ratio on the predicted number of load applications

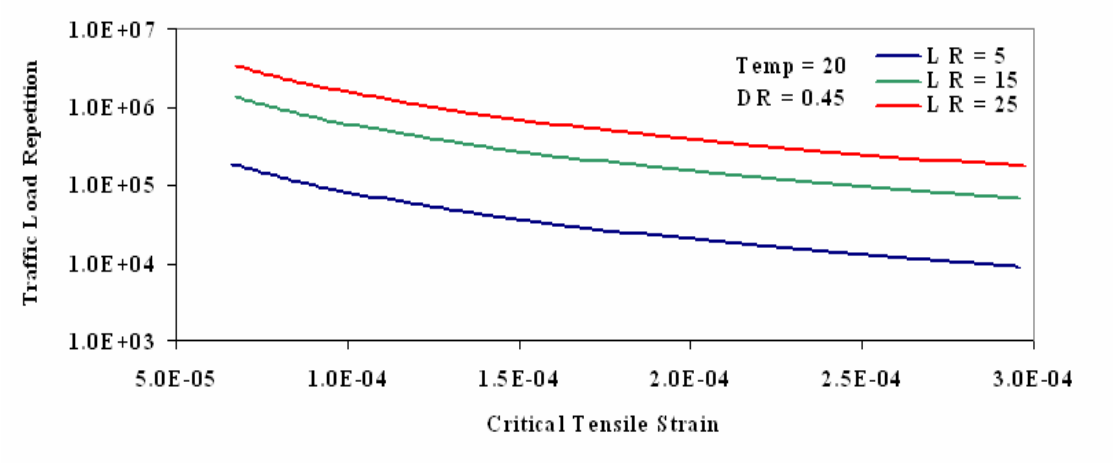

Figure D.2 Plot showing the influence of loading ratio on the predicted number of load applications

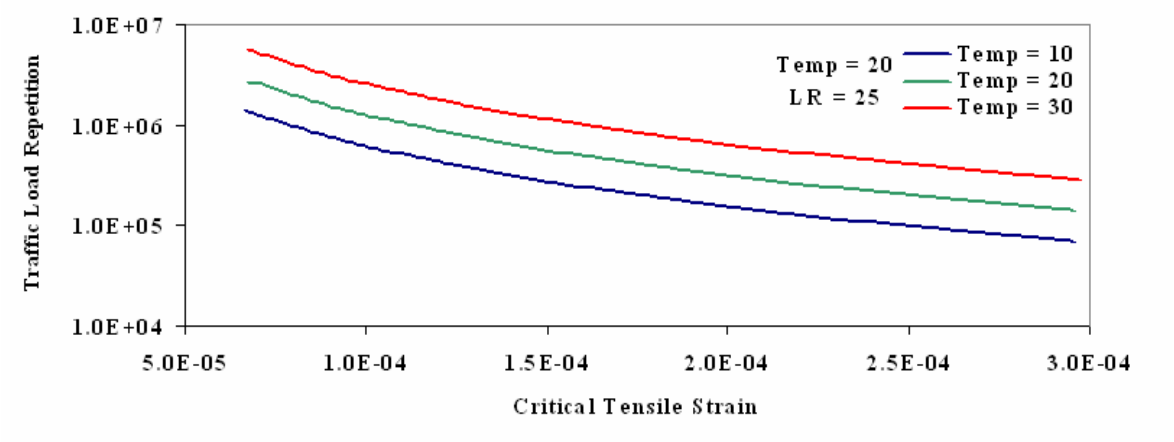

Figure D.3 Plot showing the influence of temperature on the predicted number of load applications

An analysis of the plots presented above leads to the conclusion that the total amount of variation in fatigue life that each variable accounted for and the trends in fatigue life performance with increasing critical tensile strain were reasonable.

List of References

Al-Balbissi, A. and D. N. Little, (1990). “Effect of fracture healing on laboratory-to-field shift factor.” Transportation Research Board No. 1286, National Research Council, Washington, D.C.

Ali, H. and A. Lopez (1996). “Statistical Analyses of Temperature and Moisture Effects on Pavement Structural Properties Based on Seasonal Monitoring Data.” Transportation Research Record No. 1540, Transportation Research Board, Washington, D.C.

Ali, H. and N. Parker (1996). “Using Time Series to Incorporate Seasonal Variations in Pavement Design.” Transportation Research Record No.1539, Transportation Research Board, Washington, D.C.

Al-Khateeb, G. and A. Shenoy (2004).”A Distinctive Fatigue Failure Criterion.” Journal of the Association of Asphalt Paving Technologists. Vol.73.

Al-Qadi, I. L. and W. N. Nassar (2003). “Fatigue Shift Factors to Predict HMA Performance.” International Journal of Pavement Engineering, Vol. 4, Number 2.

American Association of State Highway Officials (1961). “The AASHO Road Test: History and Description of the Project.” Special Report 61A. AASHO. Highway Research Board, Washington, D.C.

American Association of State Highway and Transportation Officials (1993). “Guide for design of pavement structures.” AASHTO. Washington, D.C.

Anderson, T. W. and D. A. Darling (1952). "Asymptotic theory of certain ‘goodness-of-fit’ criteria based on stochastic processes." Annals of Mathematical Statistics 23.

Asphalt Institute (1982). “Research and Development of the Asphalt Institute’s Thickness Design Manual (MS-1).” 9th. Edition, AI, Research Report 82-2, Asphalt Institute.

Barksdale, R. D. and J. H. Miller III, (1977). “Development of Equipment and Techniques for Evaluating Fatigue and Rutting Characteristics of Asphalt Concrete Mixes.” Report SCEGIT-77-147. School of Civil Engineering, Georgia Institute of

Technology, Atlanta.

Bazin, P. and J.B.Saunier (1967). "Deformability, fatigue and healing properties of asphalt mixes." Proceedings of the 2nd International Conference on the Structural Design of Asphalt Pavements, Ann Arbor, Michigan.

Bonnaure, F., A. Gravois and J. Udron (1980). “A New Method for Predicting the Fatigue Life of Bituminous Mixes.” Journal of the Association of Asphalt Paving Technologists, Vol.49.

Bonnaure, F., A. H. J. J. Huibbers, and A. Booders (1982) "A Laboratory Investigation of the Influence of Rest Periods on Fatigue Characteristics of Bituminous Mixes." Journal of the Association of Asphalt Paving Technologists, Vol. 51.

Brown, S. F., J. M. Brunton, and P. S. Pell (1982). "The Development and Implementation of Analytical Pavement Design for British Conditions." Proceedings, Fifth International Conference on the Structural Design of Asphalt Pavements, University of Michigan, Ann Arbor, Michigan.

Chatti, K., H. B. Kim, K. K. Yun, J.P. Mahoney and C. L. Monismith (1996). "Field Investigation into Effects of Vehicle Speed and Tire Pressure on Asphalt Concrete Pavement Strains." Transportation Research Record 1539, National Research Council, Washington, D.C.

Chomton, G. and P. J. Valayer (1972). “Applied Rheology of Asphalt Mixes - Practical Application.” Proceedings, Third International Conference on the Structural Design of Asphalt Pavements, London.

Coetzee, N. F., W. Nokes, C. L. Monismith, J. Metcalf, and J. Mahoney (2000). “Full-scale/Accelerated Pavement Testing: Current Status and Future Directions. A TRB Millennium paper, A2B52: Task Force on Full-Scale/Accelerated Pavement Testing.” Transportation Research Board, National Research Council, Washington, D.C. Internet Document, http://gulliver.trb.org/publications/millennium/00046.pdf, last accessed December 2006.

Cook, T. S. and F. Erdogan,. (1972). "Stresses in Bonded Materials with a Crack Perpendicular to the Interface.” International Journal of Engineering Science, Vol. 10.

Cowher, K. (1975). “Cumulative Damage of Asphalt Materials under Repeated-Load Indirect Tension.” Research Report Number 183-3. Center for Highway Research – University of Texas at Austin.

Daniel, J. S., W. Bisirri and Y. R. Kim (2004). "Fatigue Evaluation of Asphalt Mixtures Using Dissipated Energy and Viscoelastic Continuum Damage Approaches." Journal of the Association of Asphalt Paving Technologists, Vol. 73.

Deacon, J. A. (1965). “Fatigue of Asphalt Concrete.” Ph.D. dissertation, University of California. Berkeley.

Deacon, J. A., A. A. Tayebali, J. S. Coplantz, F. N. Finn, and C. L. Monismith (1994). “Fatigue Response of Asphalt-Aggregate Mixes, Part III—Mix Design and Analysis.” Strategic Highway Research Program Report No. SHRP-A-404, National Research Council, Washington, D.C.

Deacon, J. A., J. S. Coplantz, A. A. Tayebali, and C. L. Monismith (1994). “Temperature Considerations in Asphalt-Aggregate Mixture Analysis and Design.” Transportation Research Record 1454, National Research Council, Washington, D.C.

De Beer, M. (1996). “Measurement of tyre/pavement interface tresses under moving wheel loads.” International Journal of Vehicle Design. Special Issue on Vehicle-Road and Vehicle-Bridge Interaction, Vol. 3, Nos. 1-4.

De la Roche, C., H. Odeon, J.P. Simoncelli, and A. Spernol (1994). “Study of the fatigue of asphalt mixes using the circular test track of the laboratoire central des Ponts et Chaussées in Nantes, France.” Transportation Research Record 1436, National Research Council, Washington, D.C.

Drumm, E. C. and R. Meier (2003). “LTPP Data Analysis: Daily and Seasonal Variations in Insitu Material Properties.” NCHRP Web Document 60, Transportation Research Board, National Research Council, Washington, D.C.

Epps, J. and C. L. Monismith (1969). "Influence of mixture variables on the flexural fatigue properties of asphalt concrete.” Journal of the Association of Asphalt Paving Technologists, Vol.38.

Epps, J. and C. L. Monismith (1972). "Fatigue of asphalt concrete mixtures—A summary of existing information." Fatigue of Compacted Bituminous Aggregate Mixtures, Special Technical Publications 508, American Society for Testing and Materials.

Federal Highway Administration (2003). "Long-term pavement performance information management system pavement performance database user guide." FHWA, U.S. Department of Transportation, Report No. FHWA-RD-03-088.

Federal Highway Administration (2003). "Distress Identification Manual for the Long-Term Pavement Performance Program (Fourth Revised Edition)." FHWA, U.S. Department of Transportation, Report No. FHWA-RD-03-031.

Federal Highway Administration (2007). "LTPP DataPave Online", FHWA, available at http://www.ltpp-products.com/, last accessed March 2007.

Gerritsen, A. H. and D. J. Jongeneel. (1988). "Fatigue Properties of Asphalt Mixes Under Conditions of Very Low Loading Frequencies." Journal of the Association of Asphalt Paving Technologists, Vol. 57.

Ghuzlan, K.A.and S.H. Carpenter (2006)."Fatigue damage analysis in asphalt concrete mixtures using the dissipated energy approach." Canadian Journal of Civil Engineering, Vol. 33, Number 7.

Gramsammer, J. C., J. P. Kerzreho, and H. Odeon (1999). "The LCPC's APT Facility." Proceedings, 9th International Conference on Accelerated Pavement Testing, Reno, Nevada.

Hawai'i Asphalt Paving Industry (HAPI) (2007). "HAPI Asphalt Pavement Guide." available at http://www.hawaiiasphalt.com/HAPI/index.htm, last accessed March 2007.

Harvey, J. T, L. du Plessis, F. Long, S. Shatnawi, C. Scheffy, B. Tsai, I. Guada, D. Hung, N. Coetzee, M. Reimer, and C. L. Monismith (1996). "Initial CAL/APT Program: Site Information, Test Pavement Construction, Pavement Materials Characterizations, Initial CAL/APT Test Results, and Performance Estimates." Pavement Research Center, CAL/APT Program, Institute of Transportation Studies, University of California, Berkeley.

Harvey, J. T., L. Louw, I. Guada, D. Hung, J. A. Prozzi, F. Long, and L. du Plessis. (1999). “CAL/APT Program: Test Results from Accelerated Pavement Test on Pavement Structure Containing Untreated Aggregate Base—Section 501RF.” Pavement Research Center, CAL/APT Program, Institute of Transportation Studies, University of California, Berkeley.

Hiller, J. E.and J. R. Roesler (2005). "Determination of Critical Concrete Pavement Fatigue Damage Locations Using Influence Lines." Journal of Transportation Engineering, Vol. 131, Issue 8.

Hsu, T. W. and K. H. Tseng (1996), “Effect of Rest Periods on Fatigue Response of Asphalt Concrete Mixtures.” Journal of Transportation Engineering, ASCE. Vol. 122, No. 4.

Huang, Y.H. (1993). Pavement Analysis and Design. Prentice Hall, NJ.

Hugo, F., B. F. McCullough, and B. van der Walt (1991). “Full-Scale Accelerated Pavement Testing for the Texas State Department of Highways and Public Transportation.” Transportation Research Record 1293, National Research Council, Washington, D.C.

Hugo, F. and A. L. Epps (2004). “NCHRP Synthesis Practice 325: Significant Findings from Full-Scale Accelerated Pavement Testing.” Transportation Research Board, National Research Council, Washington, D.C.

Hveem, F. N. and R. M. Carmany (1948). “The Factors Underlying the Rational Design of Pavements. Proceedings of the Highway Research Board, Vol. 28, Highway Research Board, Washington, D.C.

Jiminez, R. Z. and B. M. Gallaway (1962). “Behavior of asphalt concrete diaphragms to loading.” International Conference on the Structural Design of Asphalt Pavements, Ann Arbor, Michigan.

Kallas, B. F. (1970). “Dynamic modulus of asphalt concrete in tension and compression.” Journal of the Association of Asphalt Paving Technologists. Vol.39.

Kallas, B. F. and V. P. Puzinauskas (1972). “Flexural Fatigue Tests on Asphalt Paving Mixtures.” Fatigue of Compacted Bituminous Aggregate Mixtures, Special Technical Publications 508, American Society for Testing and Materials.

Kennedy, T. W. (1977). “Characterization of asphalt pavement material using the indirect tensile test.” Journal of the Association of Asphalt Paving Technologists, Vol. 46.

Kim, B. and R. Roque (2006). “Evaluation of Healing Property of Asphalt Mixtures.” Transportation Research Record 1970, Transportation Research Board, National Research Council, Washington, D.C.

Long, F., J. T. Harvey, C. Scheffy, and C. L. Monismith (1996). “Prediction of Pavement Fatigue for California Department of Transportation Accelerated Pavement Testing Program: Drained and Undrained Test Sections.” Transportation Research Record 1540, National Research Council, Washington, D.C.

Majidzadeh, K., E. M. Kauffmann and D. V. Ramsamooj (1971). "Application of Fracture Mechanics in the Analysis of Pavement Fatigue.” Journal of the Association of Asphalt Paving Technologists, Vol. 40.

Majidzadeh, K., E. Kauffmann, and C. Saraf (1972). “Analysis of Fatigue of Paving Mixtures from the Fracture Mechanics Viewpoint.” Fatigue of Compacted Bituminous Aggregate Mixtures, Special Technical Publications 508, American Society for Testing and Materials.

Majidzadeh, K., C. Buranrom, and M. Karakomzian.(1976). "Applications of fracture mechanics for improved design of bituminous concrete." Report No.76-91, FHWA, U.S. Dept. of Transportation.

McLean, D. B. (1974). “Permanent Deformation Characteristics of Asphalt Concrete.” Ph.D. thesis, University of California, Berkeley.

Metcalf, J. B. (1996). “NCHRP Synthesis of Highway Practice 235: Application of Full-Scale Accelerated Pavement Testing.” Transportation Research Board, National Research Council, Washington, D.C.

Metcalf, J. B. (2005). “NCHRP Active Project 10-66: Predicting In-Service Performance of Flexible Pavements from Accelerated Pavement Testing.” Transportation Research Board, National Research Council, Washington, D.C.

Mirza, M. W. and M. W. Witczak (1995). “Development of a Global Aging System for Short and Long Term Aging of Asphalt Cements.” Journal of the Association of Asphalt Paving Technologists, Vol. 64.

Molenaar, A.A.A., J. Groenendijk and A.E. van Dommelen (1999). “ Development of performance models from APT.” Proceedings, 9th International Conference on Accelerated Pavement Testing, Reno, Nevada.

Monismith, C. L. (1966). “Asphalt Mixture Behavior in Repeated Flexure.” Report No. TE 66-66, ITIE, to California Division of Highways, University of California.

Monismith, C. L. and Deacon, J. A. (1969). "Fatigue of asphalt paving mixtures." Transportation Engineering Journal. ASCE 95(2).

Monismith, C. L. and Y. M. Salam (1973). "Distress Characteristics of Asphalt Concrete Mixes.” Journal of the Association of Asphalt Paving Technologists, Vol.42.

Monismith, C. L., K. Inkabi, D. B. McLean, and C. R. Freeme (1977). “Design Considerations for Asphalt Pavements.” Report No. TE 77-1, University of California, Berkeley.

Monismith, C. L. (1981). "Fatigue characteristics of asphalt paving mixtures and their us in pavement design.” Proceedings, 18th Paving Conference, University of New Mecico, Albuquerque.

Moore, R. K. and T. W. Kennedy (1971). “Tensile Behavior of Subbase Materials Under Repetitive Loading.” Research Report 98-12, Center for Highway Research, University of Texas at Austin, Austin, TX,

Navarro, D. and T, W. Kennedy (1975). "Fatigue and Repeated-Load Elastic Characteristics of In-service Asphalt-Treated Pavement.” Research Report No.183-2, Center for Highway Research, the University of Texas at Austin.

NCHRP (2006). “Mechanistic-Empirical Guide for the Design of New and Rehabilitated Pavement Structures”, National Cooperative Highway Research Program, Project 1-37A, available at www.trb.org/mepdg/guide.htm, last accessed December 2006.

Newcomb, D. E., G. Engstrom, D. A. Van Deusen, J. A. Siekmeier, and D. H. Timm. (1999). “Minnesota Road Research Project: A Five-Year Review of Accomplishments.” Proceedings, 9th International Conference on Accelerated Pavement Testing, Reno, Nevada.

Nijboer, L. W. and Van der Poel, C. (1953). “A Study of Vibration Phenomena in Asphaltic Road Constructions.” Proceedings of the Association of Asphalt Paving Technologists, Vol. 22.

Paris, P. and F. Erdogan (1963). “A critical analysis of crack propagation laws.” Journal of Basic Engineering, Transactions of the American Society of Mechanical Engineers, Vol. 85.

Pell, P.S. (1962). “Fatigue characteristics of bitumen and bituminous mixes.” International conference on the structural design of asphalt pavements, Ann Arbor, Michigan.

Pell, P.S. (1967). “Fatigue of asphalt pavement mixes.” Proceedings, Second International conference on the structural design of asphalt pavements, Ann Arbor, University of Michigan.

Pell, P. S. and I. F. Taylor (1969). "Asphaltic Road Materials in Fatigue.” Journal of the Association of Asphalt Paving Technologists, Vol. 38.

Pell, P. S. and S. F. Brown (1972). “The characteristics of materials for the design of flexible pavement structures.” Proceedings, Third International Conference on the Structural Design of Asphalt Pavements, London.

Pell, P. S. and K. E. Cooper (1975). "The effect of testing and mix variables on the fatigue performance of bituminous materials." Journal of the Association of Asphalt Paving Technologists, Vol. 44.

Porter, B. P. and T. W. Kennedy (1975). “Comparison of Fatigue Test Methods for Asphaltic Materials.” Research Report 183-4, Center for Highway Research, the

University of Texas at Austin.

Pronk, A.C. and P.C. Hopman (1990). "Energy dissipation: the leading factor of fatigue. In Highway Research: Sharing the Benefits." Proceedings of the Conference of the United States Strategic Highway Research Program, London, UK.

Prozzi, J. A. and M. de Beer (1997), "Mechanistic determination of equivalent damage factors for. multiple load and axle configurations", Proceedings of the 8th International Conference on Asphalt Pavements, Vol. 1, Seattle.

Prozzi, J. A. and S. M. Madanat (2000). "Using duration models to analyze experimental pavement failure data." Transportation Research Record 1699, Transportation Research Board, National Research Council, Washington, D.C., 87–94.

Prozzi, J.A., M. Sánchez Silva, S. Caro Spinel (2005). Uso de Ensayos Acelerados para Predecir el Comportamiento Real de carreteras. Proceedings, Congres Ibero-Latinoamericano del Asfalto, San José, Cost Rica.

Prozzi, J.A. and R. Guo (2007). Reliability-Based Approach for Using LTPP and APT Test Results for Estimating Fatigue Performance. Session 508, the 86th Transportation Research Board Annual Meeting, National Research Council, Washington D.C.

Raithby, K. D. and A. B. Sterling (1970). "Effect of Rest Periods on Fatigue Performance of Hot-Rolled Asphalt under Reversed Axial Loading." Association of Asphalt Paving Technologists, Vol. 39.

Raithby, K. D. and A. B. Sterling (1972). "Some Effects of Loading History on the Performance of Rolled Asphalt." TRRL-LR 496, Crowthorne, England.

Raithby, K. D. and J. T. Ramshaw (1972). "Effects of secondary compaction on the fatigue performance of a hot-rolled asphalt." TRRL-LR 471, Crowthorne, England.

Salam, Y.M. (1971). "Characteristics of Deformation and Fracture of Asphalt Concrete." Ph.D. Dissertation, University of California, Berkeley.

Shell (1978). "Shell Pavement Design Manual-Asphalt Pavement and Overlays for Road Traffic." Shell International Petroleum, London.

Sherwood, J.A., X. Qi, P. Romero, K.D. Stuart, S. Naga, N.L. Thomas, and W. Mogawer. (1999). “Full-scale pavement fatigue testing from FHWA superpave validation study.” Proceedings, International conference on Accelerated Pavement Testing, Reno, Nevada.

Sousa, J.B. (1986). “Dynamic Properties of Pavement Materials.” Ph.D. thesis, University of California, Berkeley.

Strategic Highway Research Program (1994). “SHRP-LTPP General Pavement Studies: Five-Year Report.” SHRP, National Research Council, Washington, D.C.

Stuart, K. D., W. S. Mogawer, and P. Romero (2002). "Validation of the superpave asphalt binder fatigue cracking parameter using an Accelerated Loading Facility." Rep. No. FHWA-RD-01-093, Federal Highway Administration, McLean, Va.

Sun, L. and W.R. Hudson (2005). “Probabilistic approaches for pavement fatigue cracking prediction based on cumulative damage using Miner's law.” Journal of Engineering Mechanics, Vol. 131, No 5.

Tangella, R., J. A. Deacon, and C. L. Monismith (1990). “Summary report of fatigue response of asphalt mixtures.” Technical Memorandum No. M-UCB-A-003A-89-3M, prepared for SHRP Project A-003A. Institute of Transportation Studies, University of California, Berkeley.

Tayebali, A. A., G. M. Rowe, and J. B. Sousa (1992). "Fatigue response of asphalt–aggregate mixtures." Journal of the Association of Asphalt Paving Technologists, Vol. 61.

Tayebali, A. A., J. S. Coplantz, J.A. Deacon, F. N. Finn, and C. L. Monismith. (1994), “Fatigue Response of Asphalt-Aggregate Mixtures.” Report No. SHRP-A-404, Strategic Highway Research Program, National Research Council, Washington, D.C.

Theyse, H. L., M. De Beer, and F. C. Rust (1996). "Overviews of South African Mechanistic Pavement Design Method." Transportation Research Record 1539, Transportation Research Board, National Research Council, Washington, D.C.

Thompson, M. R.(1996). "Mechanistic-Empirical Flexible Pavement Design: An Overview." Transportation Research Record 1539, Transportation Research Board, National Research Council, Washington, D.C.

Tsai, B. W., Harvey, J. T., and Monismith, C. L. (2003). “The application of weibull theory in asphalt concrete fatigue performance prediction.” Transportation Research Board Annual Meeting Presentation, Washington, D.C.

Van Der Poel, C. (1954)."A General System Describing the Viscoelastic Properties of Bitumens and its Relations to Routine Test Data." Journal of Applied Chemistry, Vol. 4.

Van Dijk, W., H. Moreaud, A. Quedeville and P.Uge (1972). “The Fatigue of Bitumen and Bituminous Mixes.” Journal of the Association of Asphalt Paving Technologists, Vol. 38.

Van Dijk, W. (1975). “Practical Fatigue Characterization of Bituminous Mixes.” Journal of the Association of Asphalt Paving Technologists, Vol. 44.

Van Dijk, W. and W. Vesser (1977). ”The Energy Approach to Fatigue for. Pavement Design.” Journal of the Association of Asphalt Paving Technologists, Vol.46.

Wang, F., R. F. Inman, R. B. Machemehl, Z. Zhang and C. M. Walton (2000). “Study of Current Truck Configurations.” Tx-00/1862-2. Texas Department of Transportation, Austin.

VITA

Runhua Guo was born in Jianshi, Hubei, China on November 5, 1975, the son of Zhonghe Guo and Shifeng Yang. After completing his study at Enshi Senior High School in 1993, he entered Tongji University in Shanghai. He earned the degree of Bachelor of Engineering and Master of Engineering in civil engineering from Tongji University in July 1997 and March 2000 respectively. In January 2002 he entered the transportation group of the University of Texas at Austin. During the following years, he worked as a graduate research assistant at the Center for Transportation Research of the University. His primary research interests include Accelerated Pavement Testing (APT), pavement performance modeling, integrated transportation infrastructure management and pavement management systems, applications of probability and statistics in transportation engineering, pavement materials and testing, and applications of Geographic information system (GIS) in transportation engineering.

Permanent Address: #1 Guangrun road, Jianshi jibing kongzhi zhongxin, Hubei Province, P.R.China 445300

This dissertation was typed by the author.